INVESTIGATIONS ON THE DYNAMICS OF COMBINATION MAPS AND THE ANALYSIS OF BIFURCATIONS IN A DISCONTINUOUS LOGISTIC MAP.

Thesis submitted

in partial fulfilment of the requirements

for the degree of

DOCTOR OF PHILOSOPHY

P.R. KRISHNAN NAIR

International School of Photonics

Cochin University of Science and Technology

Cochin - 682 022, INDIA

October 1999

Cochin University of Science & Technology
International School of Photonics
A centre of higher learning dedicated to the Science & Technology of Photonics
Cochin 682 022, INDIA

Dr V M Nandakumaran
Professor

October 23, 1999

CERTIFICATE

This is to certify that the work presented in the thesis entitled ***Investigations on the Dynamics of Combination Maps and the Analysis of Bifurcations in a Discontinuous Logistic Map*** is based on the bonafide research work carried out by Mr. P R Krishnan Nair under my guidance at the International School of Photonics, Cochin University of Science & Technology, Cochin 682 022 and that no part thereof has been included in any other thesis submitted previously for the award of any degree.

V. M. Nandakumaran

V M Nandakumaran

(Supervising guide)

Phone: (off) +91-484-5328+8, (res) +91-484-425132 E-mail: photonix@md2.vsnl.net.in

Preface

Most of the systems in nature are nonlinear. Many of them show irregular temporal behaviour as the system parameters are varied. The term 'chaos' has been used to denote this irregular behavior in a completely deterministic system without any external stochastic source. Extreme sensitivity to initial conditions makes it impossible to predict the longtime behaviour of such a chaotic system. A great deal of research activity has been centered on the understanding of chaos in nonlinear dynamical systems. Chaos and Nonlinear dynamics have applications in many areas of knowledge like turbulence, electronic circuits, laser systems, astronomy and also in many interdisciplinary fields like biology, ecology, population dynamics etc.

Chaos is generally studied under two categories: (1) Continuous dynamical systems represented by differential equations of the form $\frac{dX_t}{dt} = F(X_t, \mu)$ and (2) Discrete dynamical systems described by mappings of the form $X_{t+1} = F(X_t, \mu)$ where X_t denotes the state of the system at time t, μ is the set of control parameters and F is some nonlinear function of X. In this thesis we confine to the study of discrete nonlinear systems represented by one dimensional mappings. As one dimensional iterative maps represent Poincarrè sections of higher dimensional flows, they offer a convenient means to understand the dynamical evolution of many physical systems.

The work presented in the thesis is the result of the investigations made by the author for studying the dynamics of combination maps, scaling relations of Lyapunov characteristic exponents and the nature of bifurcations in discontinuous systems. This was done under the guidance of Prof. Dr. V. M. Nandakumaran in the International School of Photonics, Cochin University of Science and Technology. The thesis is divided into five chapters. The chapterwise description of the contents of the thesis is given below.

Chapter 1 is a general introduction to chaos, highlighting the basic ideas of deterministic chaos. Qualitative and quantitative measures for the detection and characterization of chaos in nonlinear systems are discussed. Some simple mathematical models exhibiting chaos are presented. The bifurcation scenario and the possible routes to chaos are explained, taking the logistic map as a specific example. The dynamics of one dimensional maps are briefly discussed. The relevance of the scaling relations of the Lyapunov characteristic exponent in control of chaos is specified.

Chapter 2 deals with the numerical and analytical investigations on combination maps. A combination map is obtained by combining two one dimensional maps. The constituent maps may or may not belong to the same universality class. The dynamics of combination maps are significantly different from those of simple maps. We consider two combination maps in detail. The first one is formed by combining two maps belonging to the same universality class and the second is got by combining two maps from two different universality classes.

In the third chapter, we present the results of the numerical computations of the Lyapunov exponents (λ) of one dimensional maps. The Lyapunov characteristic exponent acts as a kind of order parameter in the transition from regular to chaotic state of a nonlinear system. A theoretical relationship for the scaling of Lyapunov exponents had already been obtained by Huberman and Rudnick. We have established numerically that the Hubermann-Rudnick relationship is valid for all one dimensional maps of different orders of maxima. However, the scaling law for the Lyapunov exponent of a combination map is significantly different from those of the individual maps.

Chapter 4 deals with the nature of bifurcations in a discontinuous logistic map. A different type of bifurcation other than the usual period doubling one had already been reported for discontinuous maps. Most of the studies in discontinuous systems have been numerical. We provide an analytical explanation for the bifurcations in a discontinuous logistic map. We have observed that the map possesses multiple attractors. The basins of attraction of the fixed points are identified and an expression for the basin boundary is deduced. We establish that whenever the elements of an $n-$cycle ($n > 1$) approach the discontinuities of the n^{th} iterate of the map, a bifurcation takes place. The periods of the cycles are shown to decrease in an arithmetic progression. It is also shown that the periods depend on the precision with which the computations are done. Direct and inverse cascades of bifurcation are possible. Our results are verified by

numerical experiments as well. Bifurcation diagrams, time plots of the iterates, tables showing the basin boundaries and bifurcation points, parameter space plots etc. are included.

The last chapter gives a summary of the whole work done. Our main conclusions are the following:

1. The Hubermann-Rudnick scaling relation for the Lyapunov exponents is valid for simple one dimensional maps of different orders of maxima.

2. The scaling relations of the Lyapunov characteristic exponents of combination maps are entirely different from those of the individual maps.

3. The discontinuous logistic map possesses multiple attractors; Every periodic cycle of the system undergoes a bifurcation whenever a cycle element collides with the discontinuity of the map. The periods are precision dependent and show an arithmetic convergence.

The possibilities for future research are also included.

CONTENTS

1. Deterministic chaos

The discovery that even simple nonlinear systems governed by perfectly known equations of motion can evolve into a completely erratic, complex behaviour is of far-reaching consequences in many areas of knowledge. It goes against one of the basic tenets of science that deterministic systems are predictable. The historic observation of H.Poincaré in 1892 that certain Hamiltonian systems can display chaotic motion was left unnoticed for a considerably long time. E.N.Lorenz in 1963 made a truncation of the Navier-Stoke's equation in hydrodynamics and obtained a set of three ordinary, nonlinear differential equations. The Lorenz model shows, for certain parameter ranges, extreme sensitivity to initial conditions. i.e., it exhibits chaotic behaviour for certain ranges of the system parameters[1]. Since then, a lot of research work have been done in the field of chaos and nonlinear dynamics. At present, there is hardly any branch of science where the concept of chaos has not been used. Nonlinearity is a neccessary (but, not sufficient) ingredient for chaos. Generally speaking, the higher the dimensionality of the system, the less severe the nonlinearity required to produce chaos. Many natural systems are replete with nonlinearities. Chaos is thus a rule, rather than an exception, in the real world. The phenomenon of turbulence, i.e., fully devoloped chaos in space and time, is an unsolved problem of classical physics. The developments in chaotic dynamics during the last few decades have greatly increased the understanding of the phenomenon of turbulence. The study of

deterministic chaos has given new concepts and modes of thought that have far-reaching repercussions in many different fields, such as Solid state physics, Plasma physics, Chemistry, Cosmology, Biology etc. Future developments in the field may help to solve the age-old problem of turbulence.

The deterministic nature of the system implies that there exists a law, either in the form of a differential equation or in terms of a difference equation, for determining the future state from the given initial conditions. The observed irregular behaviour is neither due to any external noise nor due to any intrinsic uncertainty as in the case of quantum mechanics. The chaotic behaviour arises from the property of the nonlinear system of exponentially separating initially close trajectories in phase space. Consequently, the long-time behaviour of a chaotic system becomes unpredictable. Various routes for the transition of a nonlinear system from regular to chaotic state have been identified. This chapter provides a review of the basic mathematical tools to detect and characterize chaotic motion. Certain model systems and the possible routes to chaos are discussed.

1.1 Dynamical Systems

A dynamical system is described by an evolution equation that determines the successive states from a knowledge of the initial state of the system. They are usually divided into two categories: (a) Continuous-time dynamical systems and (b) Discrete-time dynamical systems.

a) A continuous-time dynamical system is represented by a set of ordinary differential equations (ODE) of the form,

$$\frac{dX}{dt} = F(X, t, \mu); X(t_0) = X_0 \tag{1.1}$$

where, $X(t) \in R^n$ is the state at time t, μ is the set of control parameters and $F: R^n \rightarrow R^n$ is called the vector field. The dynamical system is linear if F is linear and nonlinear if F is nonlinear. The system is said to be *autonomous* if F does not contain time explicitly. Now, an n^{th} order non-autonomous ODE can be converted to an $(n+1)^{th}$ order autonomous ODE. Furthermore, an m^{th} order autonomous ODE can be reduced to a system of m first order ODE. Thus, any continuous-time dynamical system can be brought to the form given by equation(1.1). A solution to equation(1.1) with the initial condition X_0 at $t = 0$, $\{X_1(t), X_2(t), ..., X_n(t)\}$ is called a trajectory in the n -dimensional phase space of the system and is denoted by $\phi_t(X_0)$. The mapping $\phi_t : R^n \rightarrow R^n$ defines a flow of the system.

b) A discrete-time dynamical system is represented by a difference equation or mapping as

$$X_{k+1} = f(X_k, \mu) \tag{1.2}$$

where $X_k \in R^n$, μ is the set of control parameters and $f: R^n \rightarrow R^n$ maps the state X_k to the next state X_{k+1}. The sequence of points $\{X_k\}_{k=0}^{\infty}$ obtained by the repeated iterations of the initial state X_0 defines an orbit of the system in the n-dimensional phase space. If f is nonlinear, the system is nonlinear.

1.2 Poincaré map.

The flow of a continuous-time dynamical system can be conveniently replaced by a discrete mapping by a technique due to Poincaré[2,3]. Consider, for example, a set of three first order differential equations,

$$\frac{dx}{dt} = f(x, y, z); \frac{dy}{dt} = \phi(x, y, z); \frac{dz}{dt} = \psi(x, y, z).$$

Let us plot the points $(x_n, y_n) \equiv [x(t_n), y(t_n)]$ for values of time $t = t_n$ at which $z = 0$ and $\frac{dz}{dt} > 0$. Then the mapping $(x_n, y_n) \rightarrow (x_{n+1}, y_{n+1})$ defines a Poincaré map. In general, the Poincaré section of an n-dimensional system is the intersection of the trajectories with an $(n-1)$ dimensional hypersurface, from one side of the surface. The entire sequence of crossing points taken without regard for crossing direction defines a two sided Poincaré map. The Poincaré section gives a stroboscopic picture of the underlying continuous-time dynamical system. There is a one-to-one correspondence between the different types of steady state behaviour of the system and the steady state behaviour in the Poincaré section. Since iterations are much easier to perform than integration, the Poincaré construction technique will be of immense help in analyzing the dynamics of continuous-time dynamical systems.

1.3 Detection of chaos.

In an experimental situation involving a nonlinear system, one will be dealing with a set of values of the system variable(s) at various instants of time. i.e., the data consists of a time series. It is therefore neccessary to inspect whether the time series correspouds to a periodic behaviour or chaotic state

of the system. Usually it is not an easy task to differentiate between multiply periodic behaviour and a chaotic state. Various qualitative and quantitative measures are adopted for this. In this section, we shall review some of the qualitative measures that are usually employed to detect the presence of chaos in a system.

Consider, for example, the case of a periodically driven pendulum, represented by $\frac{d^2\theta}{dt^2} + \gamma\frac{d\theta}{dt} + g\sin\theta = f\sin\omega t$ where θ is the angular displacement at time t, g is the acceleration due to gravity, γ is the damping constant, f is the amplitude of the driving force and ω is the angular frequency of the driving force. For each set of parameters (γ, f, ω), the equation can be integrated numerically. A plot of θ against t will be a smooth curve, if the system is periodic. When the system enters the chaotic regime, the time dependence of θ shows an irregular pattern. For example, when f exceeds some threshold value, the pendulum shows a chaotic behaviour.

Another method to detect chaos is to consider the power spectrum $P(\omega) = |x(\omega)|^2$, where $x(\omega)$ is the Fourier transform of the signal $x(t)$. i.e.,

$$x(\omega) = \lim_{T\to\infty} \int_0^T x_t e^{i\omega t} dt \tag{1.3}$$

For periodic motion, the power spectrum shows only discrete lines at the corresponding frequencies. But when the system becomes chaotic, the power spectrum appears as a broad continuous pattern.

A third criterion for chaos is to observe the autocorrelation function. This function measures the correlation between subsequent signals. A constant or an oscillatory behaviour of the correlation function implies that the system is periodic. Chaotic behaviour manifests itself through a rapidly decaying correlation function.

Another check for the presence of chaos is to investigate the Poincaré return map. This map represents the intersection of the orbits in phase space with a given plane. For chaotic motion, the Poincaré section shows space filling points. But, periodic motion produces only a finite number of points in the Poincaré section.

1.4 Quantitative Measures of Chaos.

Lyapunov characteristic exponents, Invariant measure, Autocorrelation function, etc. are the major mathematical measures adopted to determine how chaotic a system is. For completeness, we give a brief definition of each of these quantities.

1.4.1 Lyapunov characteristic exponent

The Lyapunov characteristic exponent (L.C.E) is a measure of the sensitivity to initial conditions [4]. It gives the exponential rate of divergence of the separation between two nearby points, as the system evolves in time. A formal expression for it can be obtained as follows.

Consider a one dimensional mapping $x_{n+1} = f(x_n)$ on an interval of the real axis. Let ϵ_0 be a small change in the initial value x_0 and ϵ_n be the corresponding change in the n^{th} iterate. Thus, $x_n = f^n(x_0)$ and $x_n + \epsilon_n = f^n(x_0+\epsilon_0)$. A Taylor series expansion gives, $x_n+\epsilon_n = f^n(x_0)+\epsilon_0 f^{n'}(x_0)+O(\epsilon_0^2)$, where the prime denotes differentiation w.r.t x. Neglecting higher powers of ϵ_0, $x_n + \epsilon_n = x_n + \epsilon_0\ f^{n'}(x_0)$. Using the chain rule of differentiation, we have,

$$f^{n'}(x_0) = f'(x_0)f'(x_1)f'(x_2).....f'(x_{n-1})$$

$$i.e., f^{n'}(x_0) = \prod_{i=0}^{n-1} f'(x_i)$$

$$or, |\epsilon_n| = |\epsilon_0| \prod_{i=0}^{n-1} |f'(x_i)| = |\epsilon_0|\, e^{n\lambda_n},$$

where,

$$\lambda_n = \frac{1}{n} \log \prod_{i=0}^{n-1} \left|f'(x_i)\right| = \frac{1}{n} \sum_{i=0}^{n-1} log \left|f'(x_i)\right|$$

The limiting value of λ_n as n tends to ∞ gives the Lyapunov Characteristic Exponent, λ. i.e.,

$$\lambda = \lim_{n\to\infty} \frac{1}{n} \sum_{i=0}^{n-1} log \left|f'(x_i)\right| \tag{1.4}$$

Thus, e^{λ} represents the average factor by which the separation between nearby points gets stretched after one iteration. Clearly, λ measures the rate of exponential separation of nearby orbits in phase space. If λ is negative, the system is periodic. A positive value of λ implies that the system is chaotic. Thus, in a sense, it acts as an order parameter in the transition of a nonlinear system from regular to chaotic state. A higher dimensional system has a spectrum of

Lyapunov exponents, one for each dimension. If at least one of the L.C.E's is positive, the system is chaotic. For quasiperiodic motion, all the L.C.E's are negative or zero. If the spectrum of Lyapunov exponents can be determined, the Kolmogorov entropy[5] can be computed by summing all of the positive Lyapunov exponents and the fractal dimension may be estimated using the Kaplan-Yorke conjecture[6]. The Lyapunov exponent defined above is the first order Lyapunov exponent. Higher order Lyapunov exponents can be defined by generalizing this definition[7,8].

1.4.2 Invariant measure

The invariant measure, $\rho(x)$, associated with a one-dimensional map, say, $x_{n+1} = f(x_n)$, $x_n \in (0,1)$, $n = 0,1,2,..$, is the probability distribution of the iterates over the interval of mapping. Thus, $\rho(x)dx$ is the fraction of the iterates in the interval $(x, x+dx)$ and as such, $\rho(x)$ can be defined as

$$\rho(x) = \lim_{N\to\infty} \frac{1}{N} \sum_{j=0}^{N} \delta(x - x_j) = \lim_{N\to\infty} \frac{1}{N} \sum_{j=0}^{N} \delta[x - f^j(x_0)] \qquad (1.5)$$

This quantity represents the density of the iterates of the map $f(x)$. The time average of a function $\phi(x)$ can be converted to an average over the invariant measure as,

$$\lim_{N\to\infty} \frac{1}{N} \sum_{i=0}^{N} \phi(x_i) = \lim_{N\to\infty} \frac{1}{N} \sum_{i=0}^{N} \phi[f^i(x_0)] = \int_0^1 dx \rho(x)\phi(x)$$

The invariant density $\rho(x)$ satisfies the Frobenius-Perron integral equation,

$$\rho(y) = \int dx \rho(x) \delta[y - f(x)]. \qquad (1.6)$$

This equation can be used to find the value of $\rho(x)$ for various values of x, if the map function $f(x)$ is known[2]. It can be solved exactly only for certain special cases.

1.4.3 Autocorrelation function

Consider the mapping, $x_{n+1} = f(x_n)$, $x_n \in (0,1)$. Starting with a seed value x_0, the map generates a sequence of iterates,
$\{x_0, x_1 = f(x_0), x_2 = f(x_1) = f^2(x_0), x_3 = f^3(x_0), ..., x_n = f^n(x_0), ...\}$. The mean or average value of the iterates is given by

$$\overline{x} = \lim_{N\to\infty} \frac{1}{N} \sum_{i=0}^{N} x_i$$

Then the correlation function $C(m)$ is defined as

$$C(m) = \lim_{N\to\infty} \frac{1}{N} \sum_{n=0}^{N} x_n x_{n+m} - (\overline{x})^2 \qquad (1.7)$$

Thus, $C(m)$ gives a measure of the extent to which the iterates m steps apart (i.e., x_n and x_{n+m}) are correlated. The correlation function can be expressed in terms of the invariant density $\rho(x)$ of the map as

$$C(m) = \int_0^1 dx \rho(x) x f^m(x) - [\int_0^1 dx \rho(x) x\ ]^2 \qquad (1.8)$$

1.5 Mathematical models exhibiting chaos

In this section, we discuss some of the typical one dimensional maps that display chaotic behaviour.

1.5.1 Bernoulli shift map

The map is expressed by $x_{i+1} = \sigma(x_i) = 2x_i mod 1,\ i = 0, 1, 2, 3, \ldots$ (1.9)

Figure 1.1 is a plot of $\sigma(x)$ versus x.

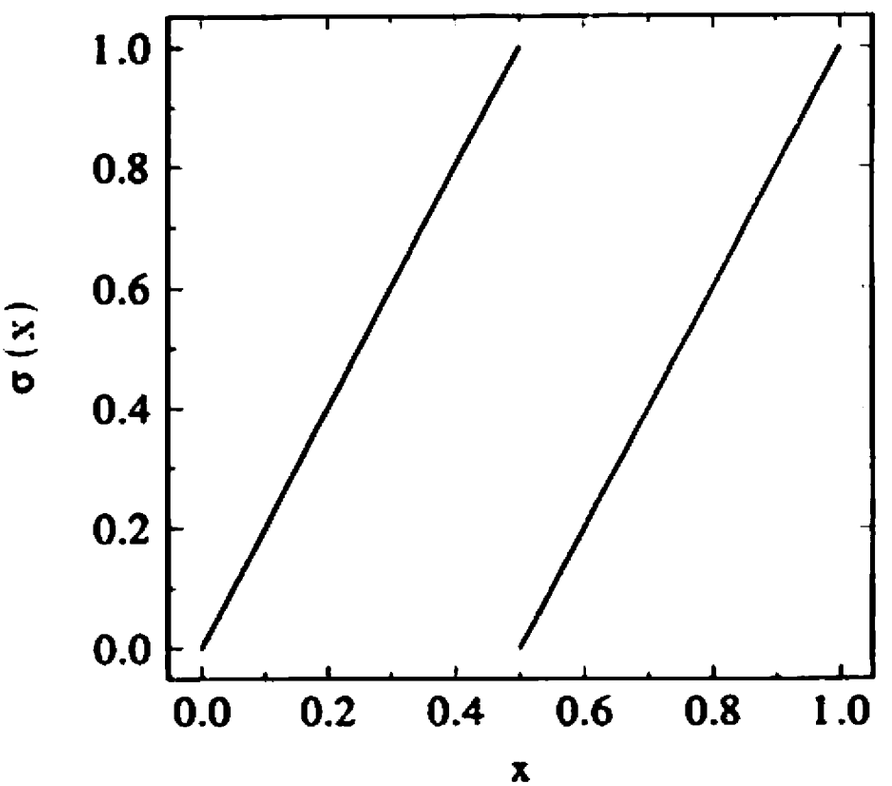

Fig. 1.1 A plot of the Bernoulli shift map, given by equation (1.9)

Repeated iterations of an initial value x_0 generates the sequence, $\{x_1 = \sigma(x_0),\ x_2 = \sigma^2(x_0),\ x_3 = \sigma^3(x_0),\ ....,\ x_r = \sigma^r(x_0),\ ...\}$. The modular arithmetic involved will confine all the iterates into the unit interval. Therefore we need consider only $x < 1$. Many important features of one dimensional chaotic maps can be deduced from the properties of this map. Some of them are given below :

(1). ***Stretching and back folding property.***

Any point $x_0 < 1/2$ becomes stretched by a factor 2 after each iteration. i.e., $\sigma(x_0) = 2x_0$. Now for $r > k$ where $2^k x_0 \geq 1$, the iterate x_r is folded back to (0,1). (since, $\sigma(x) = 2x - 1$ for $x > 1/2$). This stretching and back-folding property gives rise to a double valued inverse for points on the map. The complex behaviour of the iterates is a consequence of this property.

(2). ***Sensitive dependence on initial conditions.***

The Bernoulli shift map can be used to illustrate the sensitive dependence of a chaotic system on the initial conditions. Let us use the binary representation for points x in $(0, 1)$. Thus, $x = 0.a_1 a_2 a_3 .....$ where each $a_r = 0$ or 1. Then $\sigma(x) = 2x$ if $a_1 = 0$ and $\sigma(x) = 2x - 1$ if $a_1 = 1$. Therefore, $\sigma(x) = 0.a_2 a_3 a_4 .....$ Thus the action of σ on the binary number x is to delete the first digit and shift the sequence to the left. The map is therefore known as Bernoulli shift map.

Consider two points x and x' very close to each other so that they differ only in the n^{th} and higher digits in their binary representation. Let $x = 0.a_1\,a_2\,a_3.....a_n,...$ where each digit a_i is either zero or unity. Then, $x' = 0.a_1\,a_2\,a_3.....a_n'...$ Also $a_n \neq a_n'$. During each iteration, the first digit is deleted and the sequence is shifted to the left by one digit. Repeating the process n times, we get, $\sigma^n(x) = 0.a_n\,a_{n+1}\,a_{n+2}.....$and $\sigma^n(x') = 0.a_n'\,a_{n+1}'\,a_{n+2}'.....$ Thus, the n^{th} iterate differs in the first digit itself. Hence, the longtime behaviour of the iterates depend very sensitively on the initial value. A very small error in specifying the initial value can lead to an entirely different final state. This extreme sensitivity of chaotic systems to initial conditions leads to a completely unpredictable asymptotic state.

(3). *Ergodic behaviour*

Any point x in $(0,1)$ can be approximated arbitrarily well by a finite sequence of binary digits 0 and 1 as $(0.a_1\,a_2\,a_3....a_r)$ upto a difference of $\epsilon = (1/2)^r$. Now, the action of σ on x is to delete the first digit and shift the 'decimal' point to the right by one digit. Thus it follows that $\sigma^i(x_0)$ { for $i = 1, 2, 3, ...\}$ of an arbitrary irrational number $x_0 \in (0,1)$ approach x upto an accuracy ϵ infinitely many times. i.e., the iterates are distributed ergodically in $(0,1)$. This resembles the ergodic theorem in statistical mechanics; i.e., given enough time, any point in the phase space is visited by infinitely many phase points in course of time. The ergodic theory says that time averages can be replaced by space averages, when the motion is ergodic [9].

1.5.2 Triangular map

This is a one dimensional map defined by

$$T(x) = a\{1 - 2|1/2 - x|\};\ 0 < x < 1. \tag{1.10}$$

The map function is sketched in figure 1.2.

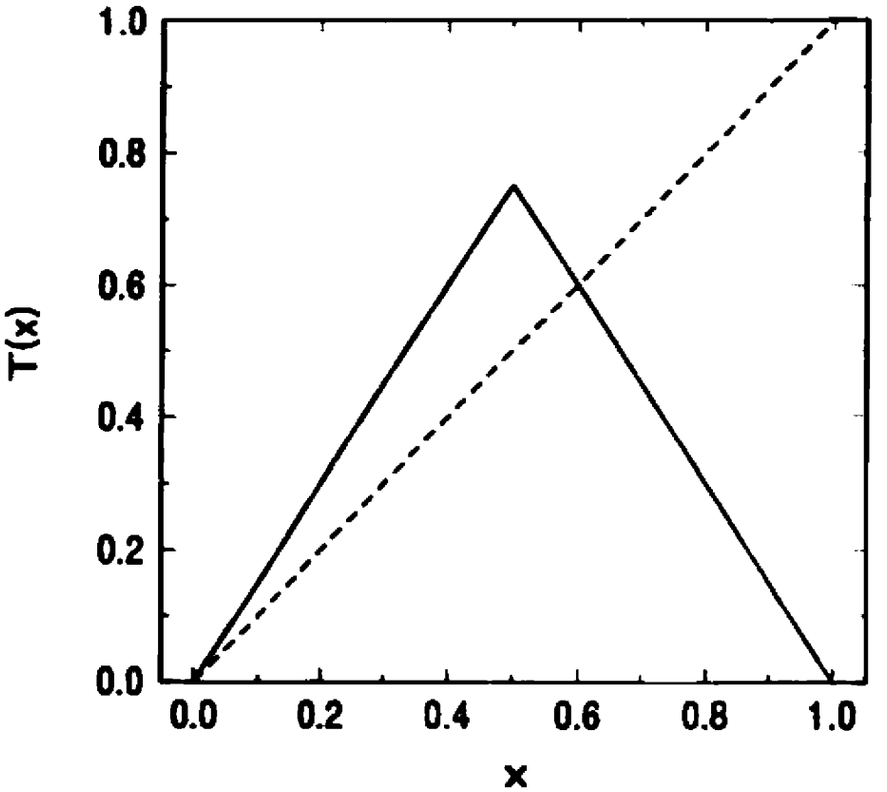

Fig. 1.2 The map defined in equation (1.10), for $a = 0.75$

The control parameter a can be varied from 0 to 1 so as to keep the iterates within$(0, 1)$. For $a < 1/2$, the iterates will eventually settle down at the origin; i.e., the origin is a stable fixed point of the map. For $a > 1/2$, the map generates a chaotic sequence of iterates.

1.5.3 Logistic map.

A one dimensional quadratic map that has been studied extensively is the logistic map[1,10,11]:

$$x_{n+1} \equiv f(x_n) = \mu x_n(1 - x_n);\ x_n \in (0,1);\ 0 < \mu < 4. \tag{1.11}$$

The map function is plotted in figure 1.3.

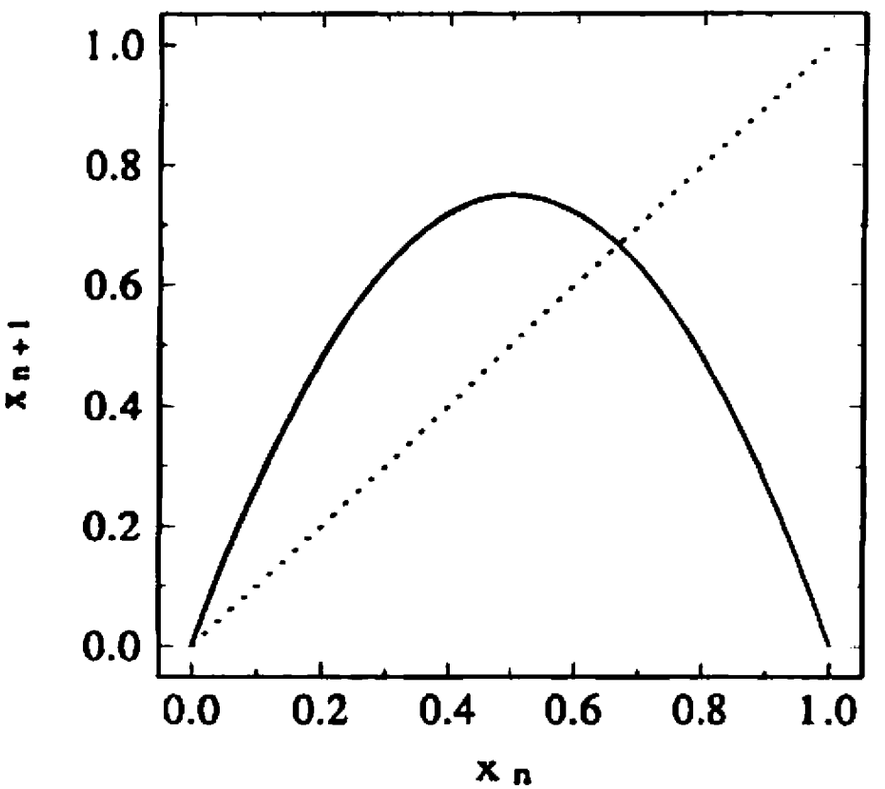

Fig. 1.3 The logistic map defined in equation (1.11). The control parameter μ is taken as 3.

In the investigations of the qualitative properties of dynamical systems, whether they are mechanical devices, electrical circuits, chemical reactions or any other kind, the asymptotic behaviour plays a central role. By asymptotic behaviour, we mean the properties that prevail when time $t \to \infty$, or, for all practical purposes, when t is sufficiently large. Asymptotically, the system may converge to an equilibrium point, a periodic motion, a quasi-periodic motion, or it may have a completely erratic behaviour, commonly designated by the term chaotic motion. The asymptotic behaviour of the iterates of the map depends crucially on the value of the control parameter μ. For small values of μ, the iterates show a periodic behaviour. When μ exceeds a threshold value, the system exhibits a chaotic behaviour. At $\mu = 4$, the map shows fully chaotic behaviour. The logistic map can be written in another form as

$$y_{n+1} = 1 - a y_n^2;\ y_n \in (-1, 1);\ 0 < a < 2. \tag{1.12}$$

These two representations are equivalent and one can switch over from one form to the other by means of the following transformation:

$$x_n = (\mu/4 - 1/2) y_n + 1/2;\ a = \mu(\mu/4 - 1/2) \tag{1.13}$$

The reverse transformation is:

$$y_n = \frac{1-k}{a} x_n + \frac{k-1}{2a};\ \mu = 1 - k;\ k = \pm\sqrt{1+4a} \tag{1.14}$$

Throughout this thesis, we shall adhere to the representation of the logistic map on the unit interval. If x_n somehow falls outside the interval $(0, 1)$, subsequent iterations diverge towards $-\infty$. As is clear from fig 1.3, the map

has an extremum at $x = 1/2$ which is a second order of maximum. (Order of maximum is the order of the highest non vanishing derivative at the point of maximum. In other words, it is the order of the leading term in the Taylor series expansion of the function around the maximum.) The maximum value of the function $= \mu/4$. Hence the maximum permissible value for μ is 4 and the minimum value for $\mu = 0$. The map is a unimodal map. An important feature of the map is that it is non-invertible. Thus, given x_n, the next iterate x_{n+1} is uniquely determined by x_n. But the reverse is not true. A given point x can have two pre-images.

In order to illustrate the sensitive dependence of a chaotic system on initial conditions, let us consider the logistic map at $\mu = 4$. The transformation $x_n = \sin^2(\pi\theta_n)$ gives an explicit solution $\theta_n = 2^n\theta_0 mod 1$. Let the initial value θ_0 be changed by a very small amount ϵ. Then θ_n is changed by an amount $2^n\epsilon = \epsilon \exp(n \log 2)$. Thus the separation between two initial values gets amplified by a factor $\exp(n \log 2)$, after a 'time' n. The rate of exponential separation = log2 (which is the Lyapunov characteristic exponent) is positive. Thus there is chaos. Let us, for the sake of convenience, express θ_0 in binary notation. Let $\theta_0 = 0.10100011....$ Then $\theta_1 = 0.0100011...$, $\theta_2 = 0.100011...$, $\theta_3 = 0.00011...$etc. Thus, the iteration scheme is to delete the first digit and shift the remaining sequence to the left. Hence, the value of θ_n depends on the n^{th} and higher digits of θ_0. When n is very large, θ_n depends very sensitively on the precise value of θ_0.

Now, there are a number of situations in which one dimensional iterative maps, such as the logistic map, provide a convenient model for the system behaviour [12,43]. The simplest example comes from ecological models. Consider the case of a seasonally breeding insect population in which generations do not overlap. The population x_{n+1} in the $(n+1)^{th}$ generation is a function of the population x_n in the n^{th} generation. i.e., $x_{n+1} = f(x_n, \mu)$ where μ represents some control parameter (availability of food, fraction of area available etc). The logistic map can be used to represent a strongly damped kicked rotator[1]. Again, such one dimensional non-invertible maps can also arise as the Poincaré map of a highly dissipative flow. The Poincaré section of a 3-dimensional flow is in general, a 2-dimensional surface. Now, if the dissipation is very large, leading to a rapid contraction of areas, then the Poincaré section can practically be approximated by a set of points along a curve. Defining a point X for every point on this curve, the time evolution of X can be reduced to a one dimensional non-invertible map of the form $X_{n+1} = F(X_n)$. The logistic map is only a particular form of this one dimensional difference equation. It is usually taken as a representative of the quadratic family of maps. The logistic map serves an example to study the bifurcation phenomenon and the routes to chaos in one dimensional unimodal maps.

1.6 Routes to chaos in one dimensional maps.

One dimensional endomorphisms defined on an interval of the real axis have been used in modelling a wide variety of nonlinear systems[13,14]. They are usually simple enough for analytical treatment and at the same time not very time consuming for numerical studies. They provide a convenient model to explore the dynamics of many practical systems like laser cavities[1], electronic circuits, neural networks etc. Many important features like the scaling behaviour and the universality properties of higher dimensional flows are shared by these mappings as well. Various routes to chaos have been observed in dissipative deterministic systems. These routes differ in the way in which the signal behaves before becoming chaotic. In this section, we shall give a brief review of the possible routes to chaos in one dimensional unimodal maps; viz., period doubling, intermittency, crises etc. In particular, the Feigenbaum scenario and the universal properties of one dimensional quadratic maps are discussed in some detail. We choose the logistic map given by equation 1.11 as a specific example.

1.6.1 Period doubling phenomena.

Given the nonlinear dynamical system $x_{n+1} = f(x_n, \mu)$, our interest is in the asymptotic solutions. Starting with an initial value x_0, the map function is iterated a large number of times. The longtime behaviour of the system is determined by the iterates x_n, after the initial transients have died

out. These transients, in general, depend on the seed value x_0. The iterates may converge to a fixed point, a periodic cycle or a chaotic attractor, depending on the value of μ. As the 'knob' μ is varied, the nature of the solution changes. The system undergoes a transition from regular, periodic cycles to a state of erratic behaviour or vice versa. Different routes to chaos have been identified, the most prominent among them being the period doubling route. In the period doubling process, a fixed point undergoes a bifurcation and a 2-cycle is formed, when the control parameter crosses a particular value, say, μ_1. The 2-cycle behaviour continues for some range of values of μ and then it bifurcates to a 4-cycle at $\mu = \mu_2$. When μ is continuously varied, the 4-cycle bifurcates to an 8-cycle at $\mu = \mu_3$; and so on. The period of every cycle gets doubled at definite values of μ. These period doublings accumulate at a critical value of the system parameter. Beyond this critical value, the system exhibits chaotic behaviour.

For the mapping $x_{n+1} = f(x_n)$, a fixed point x^* is defined by $f(x^*) = x^*$. A fixed point x^* is stable, if small perturbations on it eventually die out. The necessary condition for this is $| f'(x^*) | < 1$. If $| f'(x^*) | > 1$, the fixed point is unstable. If $| f'(x^*) | = 1$, the fixed point is said to be "marginally stable". Fixed points and their stability properties play a vital role in the theory of mappings, as they contribute a definite structure for the trajectories in their neighbourhood. The stable fixed points $(x_1^*, x_2^*, x_3^*, ..., x_n^*)$ of the n^{th} iterate of $f(x)$ constitute an n-periodic cycle of $f(x)$. The elements of the n-cycle are

such that $x_2^* = f(x_1^*)$; $x_3^* = f(x_2^*)$; $x_4^* = f(x_3^*)$; ..., $x_n^* = f(x_{n-1}^*)$; $x_1^* = f(x_n^*)$. Thus every element x_i^* of an n-cycle of f satisfies $f^n(x_i^*) = x_i^*$. An n-cycle is stable if the magnitude of the slope of the n^{th} iterate at the cycle elements is less than unity. A given cycle $\{x_j^*\}$ of period n is said to be superstable if the slope of the n^{th} iterate of the map at the cycle elements vanishes. Thus, by the chain rule of differentiation, the condition for superstable cycles is

$$\prod_j f'(x_j^*) = 0;\ j = 1, 2, 3, \ldots\ldots\ldots n. \tag{1.15}$$

This implies that the cycle contains the critical point, because it is the only point where $f'(x) = 0$.

For the logistic map defined in equation 1.11, the fixed points are $x^* = 0$ and $x^* = 1 - 1/\mu$. Clearly, $x^* = 0$ is a trivial fixed point whereas the second fixed point makes sense only if $\mu > 1$. Since $f'(x) = \mu(1 - 2x)$, we observe that $x^* = 0$ is stable for values of μ ranging from 0 to 1. Beyond $\mu = 1, x^* = 0$ becomes unstable. The fixed point $x^* = (1 - 1/\mu)$ is stable for $1 < \mu < 3$. Thus we see that the iterates of the logistic map settles down to the zero fixed point for all values of $\mu < 1$ and to a non-zero fixed point for $1 < \mu < 3$. These fixed points are also known as *attractors*, since the sequence of iterates $\{x_n\}$ generated from any initial point $x_0 \in (0, 1)$ converges to these points. Note that the slope of $f(x)$ at the first fixed point is μ and that at the second fixed point is $(2 - \mu)$. Thus, when the control parameter is varied from 0 to 3, the magnitude of the slope is always less than unity. This ensures the stability of these fixed points. When $\mu = 3$, the slope becomes equal to -1.

If μ is slightly greater than $\mu_1 = 3$, we get a 2-cycle $\{x_1^*, x_2^*\}$. The system is said to undergo the first period doubling. This 2-cycle is independent of x_0, but depends only on μ. In other words, it is an attractor of period 2. The stability properties of the 2-cycle are determined by the slope of the second iterate, $f^2(x)$ at x_1^* and x_2^*. Clearly, $x_2^* = f(x_1^*)$ and $x_1^* = f(x_2^*)$. Thus, $f^2(x_1^*) = x_1^*$ and $f^2(x_2^*) = x_2^*$. Again, $f^{2'}(x_1^*) = f'(x_1^*)f'(x_2^*)$, by the chain rule of differentiation. Likewise, $f^{2'}(x_2^*) = f'(x_1^*)f'(x_2^*)$. Therefore, the second iterate has equal slopes at both the cycle elements. (This is true for all n-cycles). The 2-cycle behaviour continues for some range of values of μ. At $\mu = \mu_2$, the slope of $f^2(x)$ at the cycle elements also becomes -1. The 2-cycle then bifurcates into a 4-cycle whose elements are the stable fixed points of $f^4(x)$. This process of period doublings repeats ad infinitum. The parameter values for successive period doublings accumulate to μ_∞. Beyond this critical value, the system exhibits chaotic behaviour. The value of μ_∞ for the logistic map has been found to be 3.56994555... The mechanism of period doubling bifurcation can easily be assimilated by a graphical analysis[18]. At this stage, a fundamental feature of all unimodal maps on an interval may be noted. Guckenheimer *et al.*,[4] has shown explicitly that maps with one critical point can have at most one stable attractor, to which all initial points in the interval (excepting a set of measure zero) are attracted asymptotically. Thus, if there exists a stable attractor of period k for the logistic map, almost all points in (0,1) will eventually be attracted towards it. The transient time depends, of course, on the initial value chosen. A plot of the asymptotic values $\{x_n\}$ against the control parameter

is known as a bifurcation diagram of the map. Bifurcation diagrams are very useful in analyzing the dynamics of nonlinear systems. It gives an overall view of the behaviour of the system, as the control parameter is varied. One such diagram is given in figure 1.4.

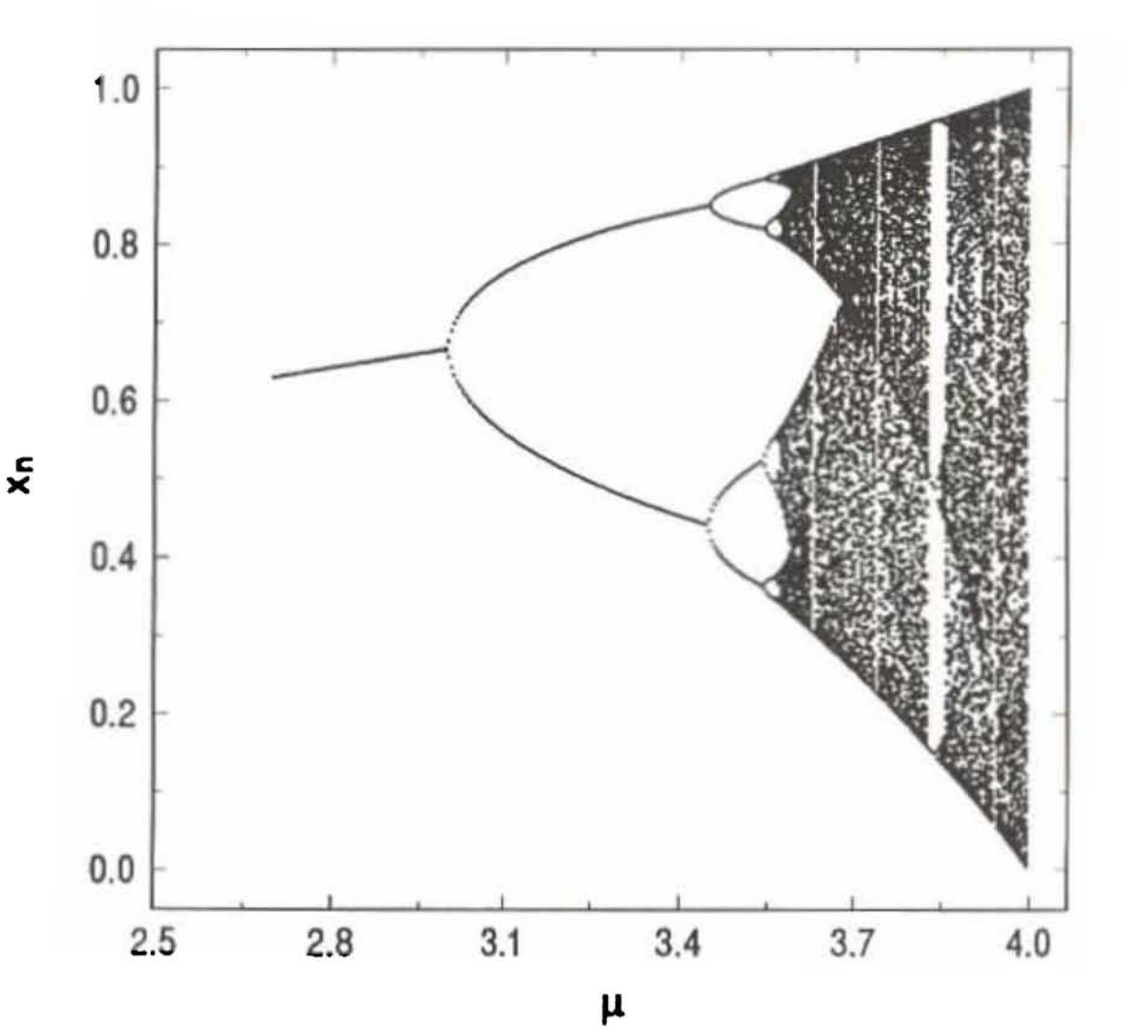

Fig. 1.4 A bifurcation diagram of the logistic map. A seed value of 0.6 was used for iteration. For each value of μ, the first 1000 iterates were left for transients and the next 500 points were plotted against μ

It has been shown by Feigenbaum[15] that certain universality properties are associated with the period doubling phenomenon. Applying the renormalization group analysis, he has shown that this route to chaos via an infinite sequence of pitchfork bifurcations is characterized by two constants α and δ which are independent of the particular form of the map function. To understand the universality theory, we note the following facts:

1). There exists discrete values of the parameter, say, $\mu_1, \mu_2, \mu_3, ..., \mu_k, \mu_{k+1}, \cdots$ at which the periods of the cycles get doubled. For $\mu_k < \mu < \mu_{k+1}$, there exists a stable 2^k-cycle $\{x_1^*, x_2^*, x_3^*, ..., x_{2^k}^*\}$ such that

$$|\frac{d}{dx}f^{2^k}(x)|_{x=x_i^*} \equiv \prod_i |f'(x_i^*)| < 1;\ k = 1, 2, 3, ... \tag{1.16}$$

2). At $\mu = \mu_{k+1}$, all points of the 2^k-cycle lose stability and a pitchfork bifurcation takes place leading to an attracting cycle of period 2^{k+1}. These cycle elements are the equilibrium points of $f^{2^{k+1}}(x)$; i.e.,

$$f^{2^{k+1}}(x) = f^{2^k} \circ f^{2^k}(x);\ k = 0, 1, 2, 3, ... \tag{1.17}$$

The main ingredient of the theory is that the mechanism by which f^{2^k} undergoes period doubling at μ_{k+1} is the same as the one that $f^{2^{k+1}}$ uses to double the period at μ_{k+2}. This observation is of paramount importance in that it connects the mechanism of subsequent bifurcations to a general law of functional composition. The elements of every periodic cycle are the stable fixed points of the corresponding iterate, with identical slopes. At every bifurcation point μ_{k+1}, the slope of f^{2^k} at its cycle elements becomes equal to -1.

Consider a superstable cycle of period 2^n. Clearly, the cycle contains $x = 1/2$ as one element. Let d_n denote the separation between $x = 1/2$ and its nearest element. But the element nearest to $x = 1/2$ is the $(2^{n-1})^{th}$ iterate of $x = 1/2$ (These two points were coincident, before the n^{th} period doubling separated them out). Thus,

$$d_n = f^{2^n - 1}(1/2) - 1/2 \tag{1.18}$$

Applying a co-ordinate translation from $x = 1/2$ to $x = 0$, we get

$$d_n = f^{2^{n-1}}(0) \tag{1.19}$$

It can be seen that the distance d_n is reduced by a constant factor during successive bifurcations. Also the nearest element alternates from one side of the critical point to the other. (The bifurcation diagrams can be used to verify these). Thus the distances d_n scales down as,

$$\frac{d_n}{d_{n+1}} = -\alpha \tag{1.20}$$

Repeated application of this result gives,

$$d_1 = \lim_{n \to \infty} (-\alpha)^n d_{n+1} \tag{1.21}$$

Using equation (1.19), we get,

$$\lim_{n \to \infty} (-\alpha)^n f^{2^n}(0) = d_1 \tag{1.22}$$

This implies that the sequence of rescaled iterates converges to a limiting function, say, $g_1(x)$. i.e.,

$$g_1(x) = \lim_{n \to \infty} (-\alpha)^n f^{2^n}(\frac{x}{(-\alpha)^n}) \tag{1.23}$$

Likewise, we can form a whole set of functions $g_i(x)$ corresponding to each of the superstable cycles. These functions obey the recurrence relation,

$$g_{i+1}(x) = -\alpha g_i[g_i(\frac{-x}{\alpha})] \equiv Tg_i(x) \tag{1.24}$$

where T is called the doubling transformation. The set of functions $g_i(x)$ converges to a function $g(x)$, as i tends to ∞. Clearly, $g(x)$ is a fixed point of the doubling operator T in the function space. Thus,

$$g(x) = Tg(x) = -\alpha g[g(\frac{-x}{\alpha})] \tag{1.25}$$

It can be seen that this equation holds equally well for $cg(x/c)$. Thus, the renormalization theory does not deal with absolut scales. We can, therefore, arbitrarily fix $g(0) = 1$. Thus, $g(0) = -\alpha g[g(0)] = 1$. There exists a unique smooth solution for this equation, depending on the nature of the maximum of $g(x)$ at $x = 0$, which gives, $\alpha = 2.502907875...$ for all quadratic maps.

We now consider the scaling relations for μ. From the bifurcation diagram, it is obvious that the parameter values μ_i for successive bifurcations converge geometrically to a finite value μ_∞ at which the iterates become aperiodic. The value of μ_∞ for the logistic map works out to 3.56994555.... The parameter values for successive superstable cycles also converge at the same rate. Denoting these values by Λ_1, Λ_2, Λ_3, ...Λ_i, ... the scaling relation can be written as

$$\Lambda_i - \Lambda_\infty \propto \delta^{-i} \tag{1.26}$$

Since $x = 1/2$ is an element of every superstable cycle,

$$f_{\Lambda_k}^{2^k}(1/2) = 1/2;\ k = 1, 2, 3, \ldots \tag{1.27}$$

Under a co-ordinate translation to $x = 1/2$, one obtains

$$f_{\Lambda_k}^{2^k}(0) = 0. \tag{1.28}$$

A Taylor expansion of $f_\Lambda(x)$ around $f_{\Lambda_\infty}(x)$ gives

$$f_\Lambda(x) = f_{\Lambda_\infty}(x) + (\Lambda - \Lambda_\infty)|\frac{\partial f_\Lambda(x)}{\partial \Lambda}|_{\Lambda=\Lambda_\infty}. \tag{1.29}$$

Repeated applications of the operator T to this equation show that δ is the only relevant (> 1) eigen value of the linearised doubling operator T and is therefore universal. The convergence rate δ for the quadratic family has been estimated as 4.6692016.

The main results of the universality theory for the period doubling route to chaos can be summarised as follows:

1) The distances d_n of a point in a 2^n-cycle closest to the critical point, scale down in successive bifurcations as

$$\lim_{n\to\infty} \frac{d_n}{d_{n+1}} = -\alpha \tag{1.20}$$

2) Existence of a geometric convergence for the parameter values for successive bifurcations. i.e.,

$$\lim_{n\to\infty} \frac{\mu_n - \mu_{n-1}}{\mu_{n+1} - \mu_n} = \delta \tag{1.30}$$

Thus we have,

$$\mu_n = \mu_\infty \text{ - a constant } \delta^{-n} \text{ for } n \gg 1. \tag{1.31}$$

The universality theory developed by Feigenbaum suggests that maps can be grouped into various universality classes; Each class is characterized by definite values for α and δ (depending on z, the order of the maximum). The high convergence rate ($\delta \approx 4.669$) gives serious predictive power to the universality theory. Thus, if a period doubling system is investigated upto four or five bifurcations, its behaviour throughout and even beyond the period doubling region can be predicted with a high degree of accuracy. The scaling constants associated with the quadratic maps appear to be observed and measured in relatively complicated dynamical systems[19,20]. Related scaling constants corresponding to the circle map have also been observed experimentally[21]. Studies related to phase transitions and critical phenomena have given a new meaning to the concept of universality. Many mathematical models and natural phenomena can be categorized into classes characterized by similar behaviour in their parameter dependence. The sudden change of the system at a certain transition point can be characterized by only a few variables. Each class will be characterized by certain set of universality constants.

1.6.2 Intermittency

The phenomenon of Intermittency[16] offers another route to chaos in nonlinear systems. In this case, the signal alternates randomly between long periodic phases and relatively short irregular bursts. The number of chaotic bursts increases with an external parameter, until finally, the system shows a completely chaotic behaviour. This has been observed, for example, in the Lorenz model[1], when the control parameter r exceeds some critical value r_c. For $r < r_c$, the Poincaré map has got a stable fixed point. For $r > r_c$, the map has no fixed points and the iterates wander around erratically. But near the original fixed point, the trajectory slows down and a large number of iterations are needed to escape the channel of regular motion. This type of intermittency is known as Type-1 Intermittency. The mechanism responsible for this is an *inverse tangent bifurcation* in which a stable and an unstable fixed point collide and disappear at $r = r_c$. Other prominent types of intermittency are Type-2 and Type-3 intermittencies. Experimental observations of the intermittency route to chaos have been found in a variety of experments including Rayleigh-Benard convection[23,24], nonlinear oscillators[25,26], and Belousov-Zabotinsky reactions[27,28]. As in the case of period doubling bifurcations, there exists universality relations for the Intermittency route as well. Exact solutions for the functional renormalization group equation for intermittency have been obtained[22].

1.6.3 Crises.

The phenomenon of crises arises out of the collisions between a chaotic attractor and a coexisting unstable fixed point or periodic orbit[17]. These collisions produce sudden changes in the chaotic attractor. For example, it occurs in the period-3 window of the logistic map, where three stable and three unstable fixed points are genertated by tangent bifurcations[1]. Almost all sudden changes in chaotic attractors are due to crises. Similar crises occur in two and three dimensional systems and also for higher dimensional flows.

1.7 Scaling relations and control of chaos

Recently, a lot of interesting research activities are centered around controlling the chaos in a nonlinear system[29-38]. That chaos can be suppressed is of course a highly desirable feature in many practical situations like lasers, plasma confinement, particle accelerators and electronic systems. Various techniques like adaptive control [33,34], feedback control[38], parametric perturbations[32,35], addition of external noise[30], external harmonic perturbation[36] etc. have been adopted for the control of chaos. Most of these methods presupposes a detailed knowledge about the dynamics of the system. A knowledge of the behaviour of the system near the transition point to chaos as well as the scaling behaviour of the characteristic constants near the onset of chaos are quite useful in this context. The spectrum of Lyapunov exponents

provides a quantitative measure of the sensitivity to initial conditions and is the most useful dynamical diagnostic for chaotic systems. As such, the scaling relations of the Lyapunov characteristic exponent near the transition point to chaos are very useful in developing suitable control algorithms. Huberman and Rudnick[39] have shown analytically that the Lyapunov characteristic exponent (λ) for maps undergoing the Feigenbaum scenario of bifurcations follow the scaling relation, $\lambda = \lambda_0(a - a_\infty)^\nu$, where λ_0 is a constant of the order of unity, a_∞ is the value of the control parameter a at the period doubling accumulation point and $\nu = (\ln 2/\ln \delta)$, δ being the Feigenbaum constant. This relation suggests that the scaling index ν is different for maps belonging to different universality classes. However, a detailed investigation of the scaling behaviour of λ near the onset of chaos for one dimensional maps of different order of maxima has not been made. We have established numerically that the Huberman-Rudnick relation is true for all one dimensional maps that exhibit the Feigenbaum route to chaos. The dynamics of one dimensional maps can be controlled by changing the value of an extra parameter introduced into the system[40-42]. In this context, it will be worthwhile to investigate the dynamics of a combination map obtained by combining two one dimensional maps. Such combination maps possess two control parameters. Hence it would be possible to have a desired dynamics for the system, by proper choice of one of the parameters for each value of the other parameter. A study of the bifurcation phenomena and the scaling relations of combination maps can provide

certain important and interesting results that can be used advantageously for controlling the dynamics of the system. Again, the presence of a discontinuity at the extremum of a map produces severe changes to the bifurcation phenomenon. Most of the studies reported for discontinuous maps are numerical in nature. An analytical study of the bifurcation phenomenon of a discontinuous logistic map will therefore be useful in understanding the dynamics of discontinuous maps.

We present the results of a combined analytical and numerical investigation on combination maps in chapter 2. The scaling relations of the Lyapunov exponents of one dimensional maps as well as those of combination maps are discussed in chapter 3. The bifurcation phenomena of a discontinuous logistic map is dealt with in chapter 4. Chapter 5 summarizes the major results obtained by our investigations on one dimensional nonlinear maps.

2. Combination Map.

In this chapter, we study the dynamics of combination maps. A combination map is obtained by combining two one-dimensional maps. These maps have two control parameters that determine the dynamics of the system. This leads to a possibility of controlling the behaviour of the system by a suitable choice of the parameters. An analysis of the dynamics of combination maps will therefore be relevant in the context of control of chaos. Another motivation for studying the combination map is to see whether the map still has all the characteristics of the constituent maps. The scaling behaviour of the Lyapunov characteristic exponent of the combination map is of particular interest, as we want to check whether the combination map follows the same scaling behaviour as that of simple one dimensional maps or not. The structure of the chaotic band and its bifurcations have got a vital role in determining the scaling relations. A detailed analysis of combination maps can give certain important informations that are useful for taming the dynamical behaviour of many nonlinear systems. We have found that the band bifurcations inside the chaotic regime of the combination map is quite different from that of simple maps. The behaviour of the Lyapunov characteristic exponent of the system near the transition point to chaos is significantly different from those of the constituent maps. The bifurcation phenomenon of a combination map depends on the parameters of both of the individual maps. By suitably tuning these

parameters, one can have any desired periodicity for the system. Likewise, it is possible to have a chaotic behaviour or periodic behaviour by proper choice of the system parameters.

The combination map can be formed from two maps chosen either from the same universality class or from different universality classes. These two types of combination maps show remarkable differences in their bifurcation structure. We consider these two cases separately. Both numerical and analytical investigations were carried out to analyse the bifurcation phenomena of the combination maps. A linear stability analysis of the fixed points and the parameter space plot of the system are presented. The variation of the Lyapunov characteristic exponent of combination maps with the control parameters is included in the next chapter.

2.1 Combination of two maps belonging to the same universality class.

The sinusoidal map is combined with the well known logistic map to get a combination map in the form,

$$x_{n+1} = f(x_n, \mu, A) = \mu x_n(1 - x_n) - A\sin(\pi x_n) \tag{2.1}$$

This map is a two parameter one-dimensional map. The control parameters μ and A are so chosen as to confine the iterates $\{x_n\}$ within the unit interval (0,1) of the real line.

The constituent maps $f_1(x_n, \mu) = \mu x_n(1 - x_n)$ and $f_2(x_n, A) = A\sin(\pi x_n)$ belong to the quadratic family (order of maximum, $z = 2$). Both f_1 and f_2 exhibit the Feigenbaum's period doubling route to chaos and are characterized by the same values of α and δ. The chaotic regimes of the individual maps also look alike. On approaching the period doubling accumulation point (μ_∞ or A_∞) from the fully chaotic limit, the chaotic bands undergo an infinite sequence of band splittings. The band bifurcations in the chaotic regime looks like a mirror sequence of the pitch-fork bifurcations in the periodic regime, and has the same convergence rate δ. In short, both the constituent maps have similar qualitative and quantitaive behaviour. The scaling properties of the individual maps are also the same. But, it is seen that the structure of the chaotic bands of the combination map is entirely different from those of the individual maps.

2.1.1 Analysis of the combination map.

The combination map is shown in figure 2.1, for different values of A, keeping $\mu = 4$. The map function has an extremum at $x = 1/2$ which is a second order maximum for A varying from $(\mu/4 - 1)$ to $(2\mu/\pi^2)$ while it is a minimum for $(2\mu/\pi^2) < A < (\mu/4)$. Clearly, $x = 1/2$ is a point of inflection when $A = 2\mu/\pi^2$. Consequently, the map is one-humped for $(\mu/4 - 1) < A < (2\mu/\pi^2)$ and two humped for $(2\mu/\pi^2) < A < (\mu/4)$.

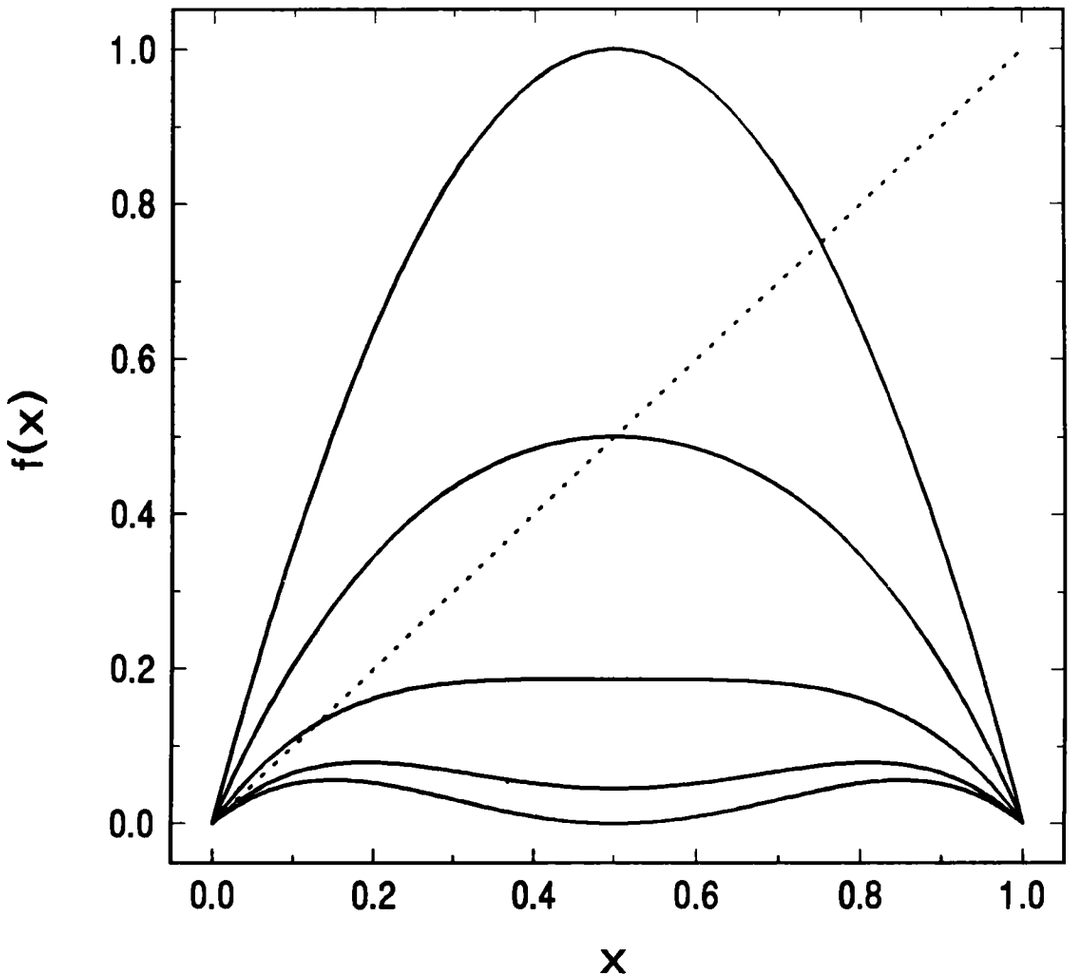

Figure 2.1. The combination map defined in eqn.(2.1) for $\mu = 4$. The curves correspond to $A = (\mu/4-1)$, $(\mu/4-1/2)$, $(2\mu/\pi^2)$, $(\mu-1)/\pi$ and $(\mu/4)$ in that order from top to bottom.

This map possesses the property that it goes over from single humped to double humped nature, by continuously varying one of the parameters (A in this case). Most of the interesting phenomena like universal indices and sequences can be traced back to the one humped nature of one-dimensional maps[13]. The dynamics of two humped maps is entirely different from that of one humped maps. A period doubling bifurcation with a convergence rate different from the Feigenbaum rate has already been reported for certain one dimensional transformations with two extrema[57]. The bifurcation scenario and the scaling behaviour of two humped maps are, in general, quite different from those of the Feigenbaum maps. Hence, it would be stimulating to investigate what happens if the combination map has a double hump. Such double humped maps can arise in the Poincaré sections of higher dimensional flows. For any chosen value of μ, the minimum value for A is $(\mu/4 - 1)$ at which $f(x_n, \mu, A)$ becomes equal to 1. The maximum possible value for A for a given value of μ is $\mu/4$ and this occurs when the ordinate of $f(x_n, \mu, A)$ at $x = 1/2$ becomes equal to zero. Thus the parameter A must lie between $(\mu/4 - 1)$ to $(\mu/4)$ so as to keep the iterates within the unit interval (0,1).

2.1.2 Fixed points of the map.

The fixed points of the map are the solutions of $f(x^*) = x^*$. i.e., $\mu x^*(1 - x^*) - Asin(\pi x^*) = x^*$. Obviously, one of the fixed points is $x_1^* = 0$.

The second fixed point is given by

$$\mu(1 - x_2^*) - \frac{Asin\pi x_2^*}{x_2^*} = 1. \tag{2.2}$$

The slope of the map function is given by $f'(x) = \mu(1-2x) - A\pi \cos \pi x$. Thus, the zero fixed point will be stable for all values of A ranging from $(\mu - 1)/\pi$ to $(\mu + 1)/\pi$. But, A is varied only upto $(\mu/4)$. Thus the zero fixed point will be stable for all values of $A > (\mu - 1)/\pi$. The non-zero fixed point, x_2^* will be stable or not, according as $f'(x_2^*)$ is numerically less than unity or not. As the parameter A increases from $(\mu/4 - 1)$ onwards, the map function $f(x)$ gets lowered and as a result, $x_2^* \to x_1^* = 0$. In the limiting case,

$$\lim_{x_2^* \to 0} A = (\mu - 1)/\pi \tag{2.3}$$

Thus, $A = (\mu - 1)/\pi$ gives the equation of the line representing the zero fixed point in the (μ, A) plane. Hence, the slope of the line representing the zero fixed point on the parameter space (μ, A) should be equal to $(1/\pi)$.

2.1.3 Numerical investigations.

Numerical analysis of the system were carried out by keeping μ at various fixed values. To start with, μ is kept at a value =4, corresponding to the fully chaotic state of the logistic map. The parameter A is increased in steps of 0.001 and the bifurcation structure is analyzed. Fig.2.2 shows a bifurcation diagram of the combination map, in which the asymptotic values x_n of the iterates are plotted against the parameter A, keeping μ at a value equal to 4.

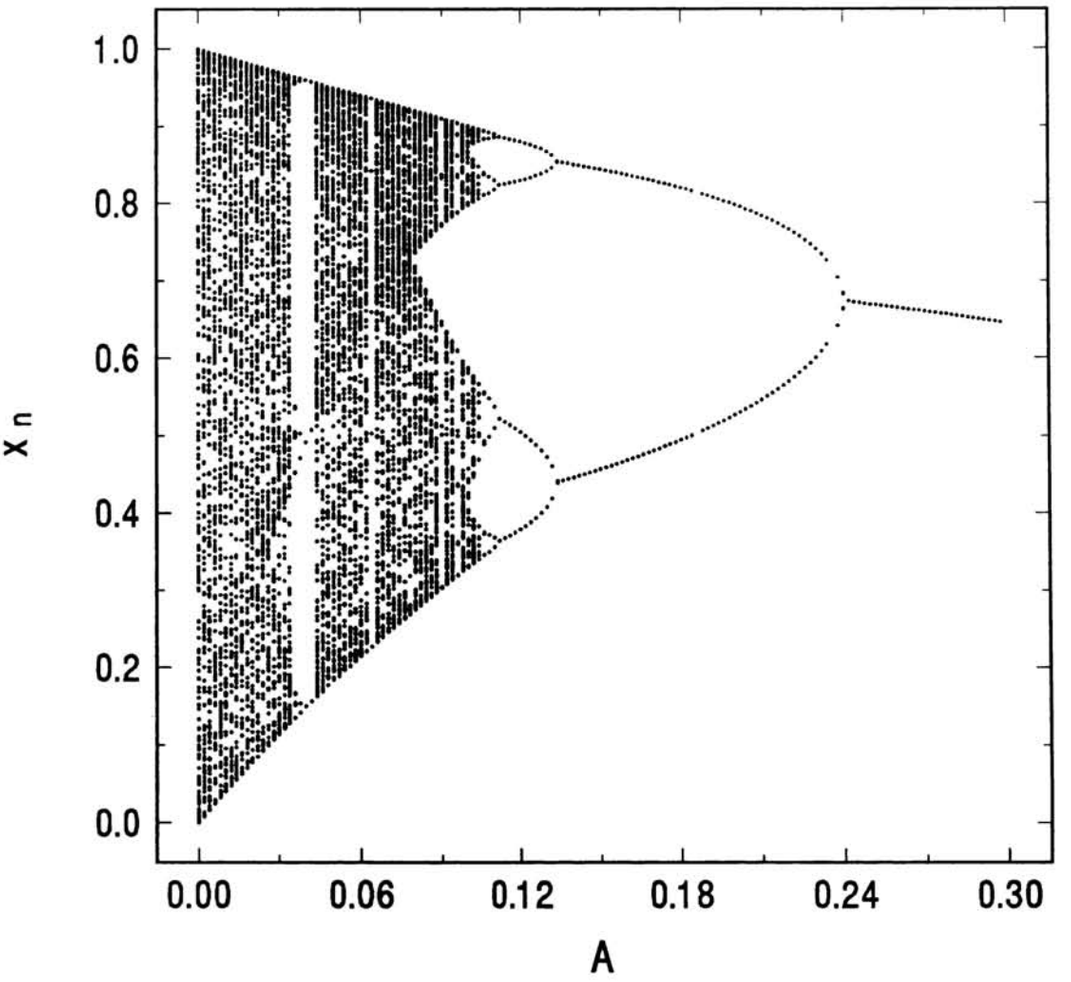

Figure 2.2 Bifurcation diagram of the map in eqn.(2.1). With $\mu = 4$ and $A = 0$, the system is fully chaotic. As A is slowly increasesd, periodic cycles are traced in the reverse direction.

The system retraces the entire period doubling route to chaos in the reverse order, as A slowly increased. Finally, it settles down to a stable fixed point (1-cycle) for $A > 0.2435$. This is not quite surprising, since the effect of the sinusoidal term is to reduce the height of the extremum at $x = 1/2$. However, this is in contrast with the behaviour in certain continuous systems which are reported to go back to periodicity only through intermittency[32].

In the one-humped region of the combination map, the Schwarzian derivative of $f(x_n, \mu, A)$ is negative throughout the interval (0,1). This implies that period doubling is generic in the system[1]. The bifurcation diagram gives the approximate values of the parameter A for successive bifurcations. From further blow-ups of the bifurcation diagrams near these values, the parameter values corresponding to successive period halvings can be obtained more accurately. We now compute the periods numerically, near these points. In this way, the bifurcation points are obtained to a high degree of precision(of the order of $10^{-}6$). This procedure is repeated for various fixed values of μ ranging from 3 to 4. The parameter A is varied from $(\mu/4 - 1)$ to $\mu/4$ in steps of 0.001 in each case, and a series of bifurcation diagrams are drawn. In all these cases, reverse period doubling is observed, when the parameter A is increased. If μ is kept in the chaotic regime of the logistic map (i.e., $\mu > \mu_\infty$), the system can be brought to a periodic state of any desired periodicity by applying suitable positive values for A. Likewise, if μ lies already in the periodic regime of the logistic map, the system can be taken to chaos by applying suitable negative

values for A. Thus the sinusoidal term offers an opportunity to have a control over the dynamics of the logistic map. Detailed numerical investigations are carried out by slowly and carefully varying the parameters A and μ and a full parameter space representation is obtained. Table 2.1 shows the values of A for successive bifurcations corresponding to various chosen values of μ. Fig.2.3 is the parameter space plot for the system. The bifurcations of the various periodic attractors to the corresponding half periodic ones occur along parallel lines. (Only, a few of them are shown in the figure). For each value of μ, the Lyapunov characteristic exponent is calculated by increasing A in small steps. The L.C.E (λ) is given by the formula,

$$\lambda = \lim_{N\to\infty} \frac{1}{N} \sum_{i=0}^{N-1} ln\,|f'(x_i)| \tag{2.4}$$

This can be used as such for computing λ[12]. Since round off errors may possibly build up in a computer, an upper bound for N is to be fixed. (This will lead to some truncation error, of course.) In our computations, N is taken as 10000. The value of A_∞ at which transition from chaos to order occurs is spotted out as that value of A at which λ becomes zero and after which it remains negative throughout. The transition from chaos to order and vice versa occurs along a straight line, parallel to the bifurcation lines. The thick line shown in fig.2.3 represents A_∞ for different values of μ. The chaotic regime is indicated by the shaded portion.

Table 2.1 Parameter values for successive bifurcations, for various μ values.

μ	A min	A ∞	A 16	A 8	A 4	A 2	A 1	A 0
3.0	-.2500	-.1385	-.1380	-.1370	-.1315	-.1075	.0035	.6366
3.1	-.2250	-.1150	-.1140	-.1125	-.1075	-.0835	.0275	.6685
3.2	-.2000	-.0900	-.0895	-.0885	-.0830	-.0590	.0515	.7003
3.3	-.1750	-.0655	-.0650	-.0640	-.0590	-.0350	.0755	.7321
3.4	-.1500	-.0420	-.0410	-.0395	-.0345	-.0105	.0995	.7639
3.5	-.1250	-.0170	-.0165	-.0155	-.0100	.0135	.1235	.7958
3.6	-.1000	.0075	.0080	.0090	.0140	.0380	.1475	.8276
3.7	-.0750	.0315	.0320	.0335	.0385	.0620	.1710	.8594
3.8	-.0500	.0560	.0565	.0575	.0630	.0865	.1955	.8913
3.9	-.0250	.0805	.0810	.0820	.0870	.1105	.2195	.9231
4.0	0	.1050	.1055	.1065	.1115	.1350	.2435	.9549

Table 2.1 The parameter values (A) for successive reverse bifurcations of the combination map, for different values of μ. At each value A_n, a bifurcation takes place from an $n+1$-cycle to an n-cycle

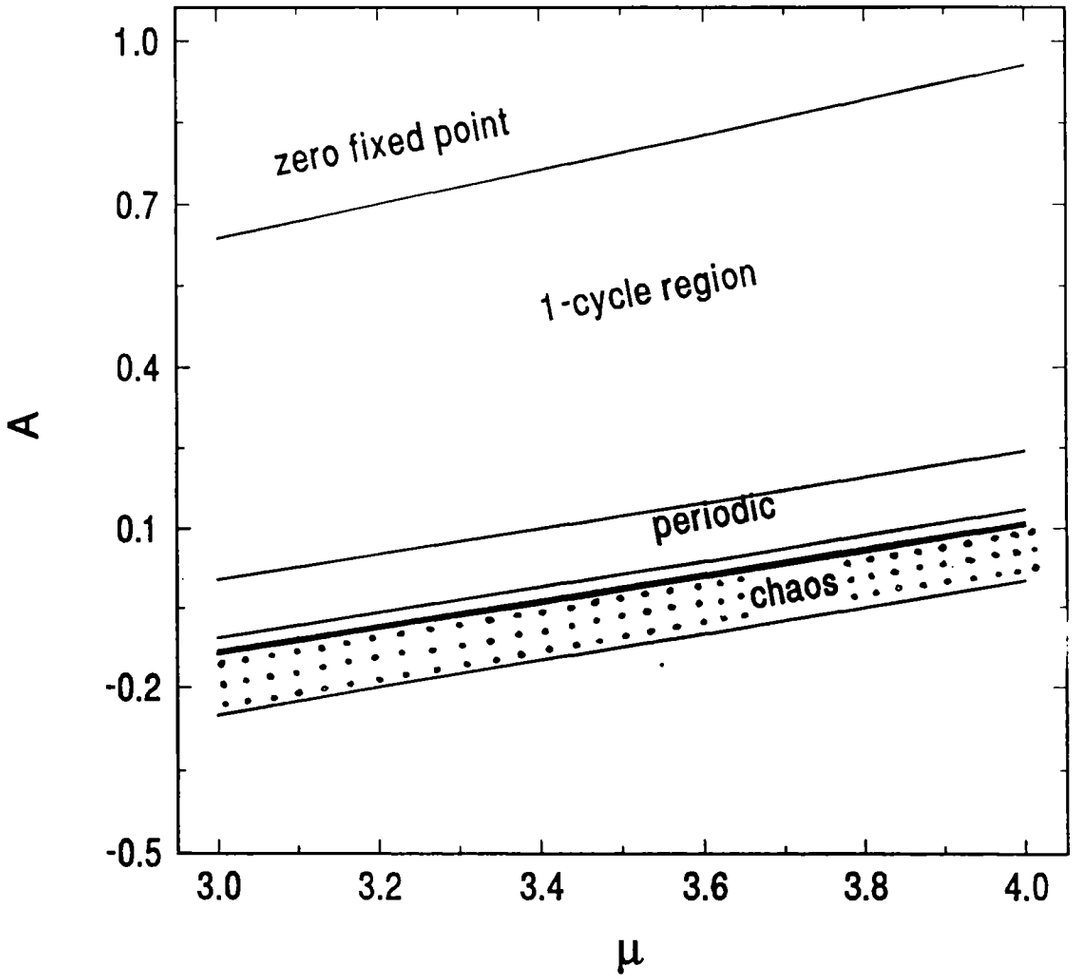

Figure 2.3 The parameter space (μ, A) of the two parameter map in eqn.(2.1). The thick line represents the transition from order to chaos while the lines parallel to it are the bifurcation lines. The shaded region corresponds to the chaotic regime.

The lowermost line represents $A = (\mu/4 - 1)$. By extending this line upwards, one can increase the value of μ beyond 4 by taking suitable high values for A. The sinusoidal term therefore provides an extension in the range of the control parameter of the logistic map. From the bifurcation diagram for each value of μ, the value of A at which the system returns to the zero fixed point is obtained as A_0. These values are then computed more accurately, by numerical iterations. The values of A_0 for different μ are also plotted in the parameter space. These points also lie along a straight line, but its slope is different from those of the bifurcation lines. The slope of the line representing the zero fixed point is found to be 0.318. This value agrees well with the theoretical value $(1/\pi)$, given by equation 2.3. The bifurcation lines have a slope equal to 0.25.

Since the bifurcation lines in the (μ, A) space are parallel to each other, it is obvious that the Feigenbaum index δ defined in terms of the bifurcation values A_n for fixed μ must be the same as the δ for the logistic map alone.

The chaotic region of the combination map is then compared with the chaotic regime of the logistic map (or, sine map). To observe the fine structure of the chaotic region ($A < A_\infty$), a series of bifurcation diagrams of x_n against A for various fixed values of μ are drawn on enlarged scales. Each time, a portion of the bifurcation diagram is blown up. The periodic windows are found to be less in number as compared with the logistic map. The presence of the sine term washes out the fine structure of the chaotic bands. On approaching the accumulation point A_∞ from the fully chaotic

state ($A = 0$), we observe a number of band splittings and mergings. This is quite contrary to the behaviour of the logistic map. In the latter case, at $\mu = 4$, the chaotic attractor exists as a single band. On approaching μ_∞, this band undergoes an infinite cascade of bifurcations. No recombination of bands can be seen in that case. The incomplete nature of the cascade of bifurcations of the combination map indicates that the scaling behaviour of the system near the onset of chaos can be different from those of simple one-dimensional maps. This point is explained in the next chapter, while discussing the scaling law for the Lyapunov exponents.

Investigations on the system were then carried out for certain high values of μ, like $\mu = 32, 36, 40$ etc. Such high values for μ are not possible for the usual logistic map, due to the constraint that the iterates are to be confined in the unit interval (0,1). As the combination map is a two parameter map, μ can be increased to any high value, by giving suitable high values for A as well. In this way, the iterates can still be confined to the unit interval. Note that the combination map in this case is two humped throughout the range of variation of A. Since A varies from $(\mu/4 - 1)$ to $(\mu/4)$ and since the map becomes two humped for all $A > (2\mu/\pi^2)$, the combination map is two humped from the very begining, if $(\mu/4 - 1) > (2\mu/\pi^2)$. [i.e., $\mu > (4\pi^2/\pi^2 - 8)$].
Fig 2.4 shows the map function for $\mu = 32$, for different values of A. A bifurcation diagram for the two humped state is given in fig 2.5

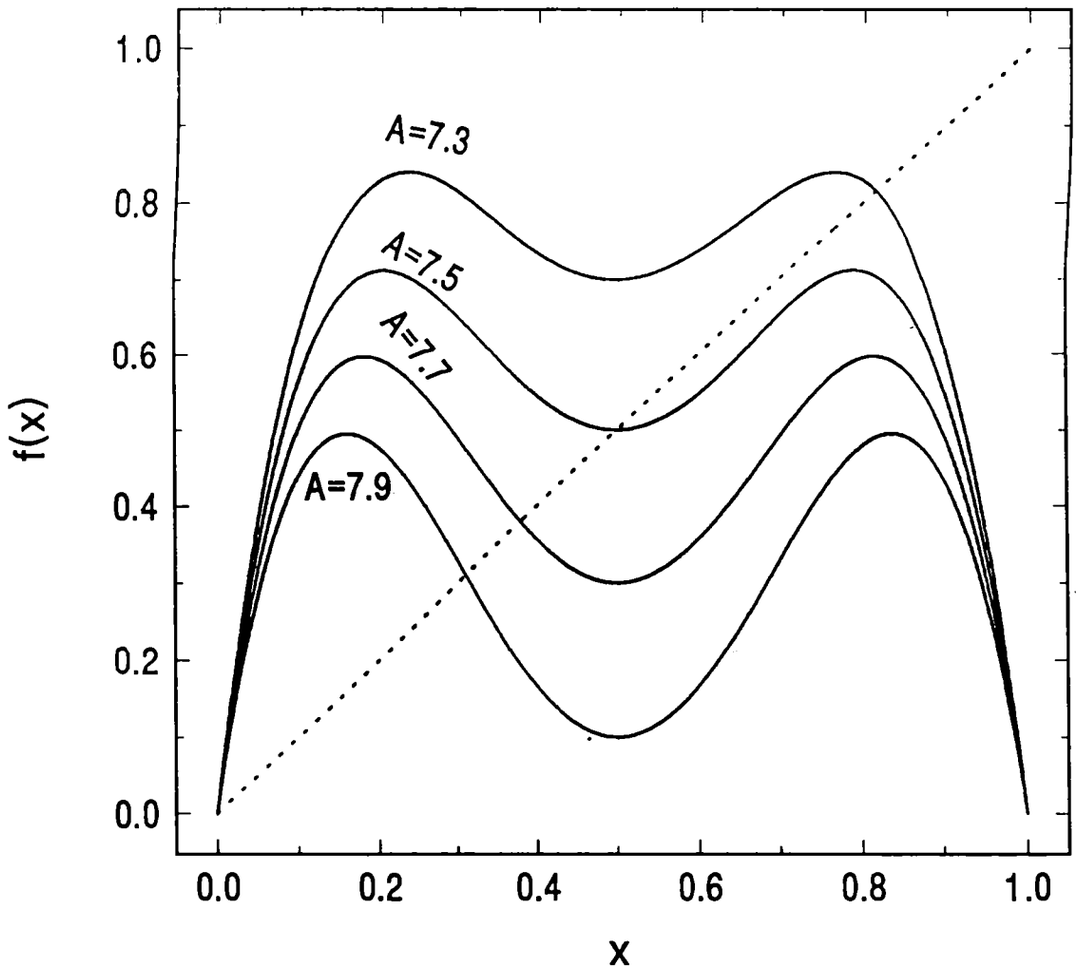

Figure 2.4 The combination map in eqn.(2.1) for $\mu = 32$. The values of A are indicated near the curves.

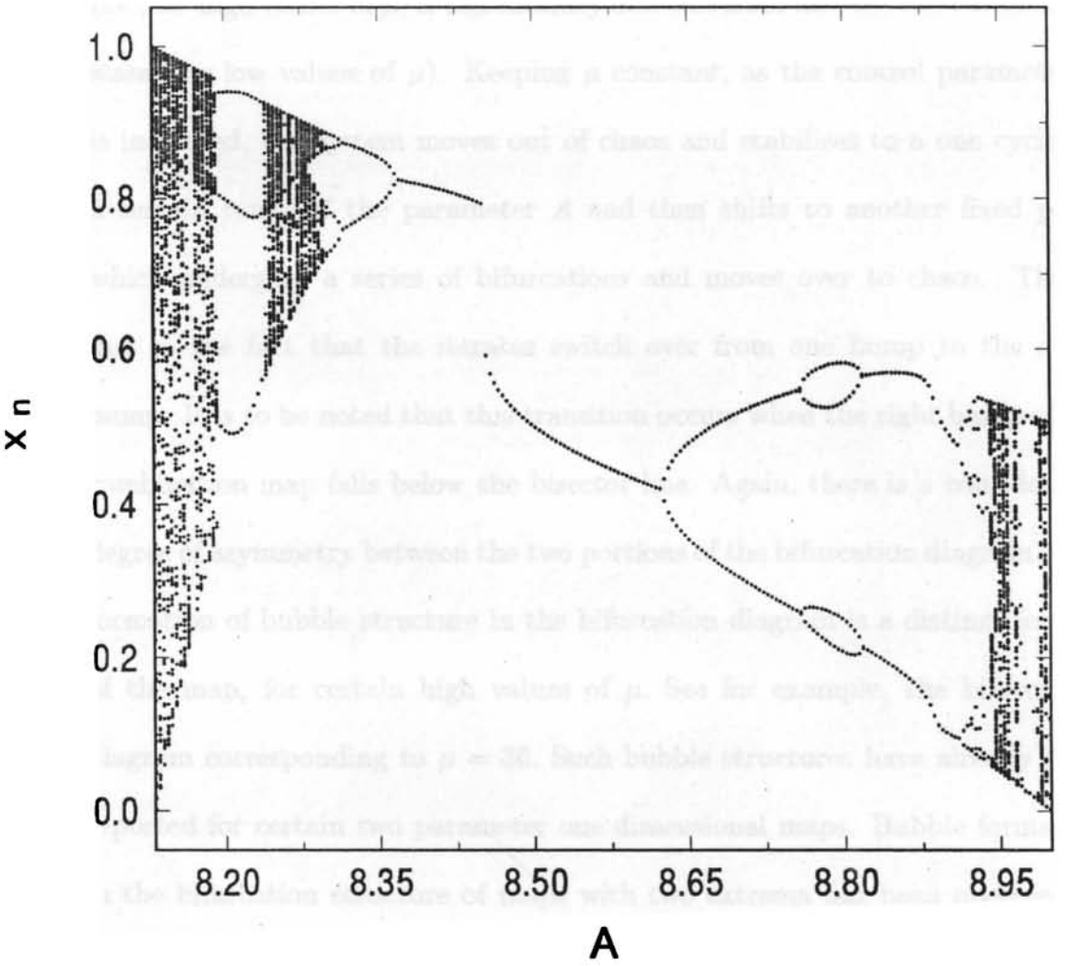

Fig.2.5 The bifurcation diagram of the map in equation (2.1) corresponding to the two humped state. Here, the value of $\mu = 36$. The bubble structure can be clearly seen, in this case.

The bifurcation structure for the two humped state of the combination map (i.e., for high values of μ) is significantly different from that for the one humped state (for low values of μ). Keeping μ constant, as the control parameter A is increased, the system moves out of chaos and stabilizes to a one cycle for a certain range of the parameter A and then shifts to another fixed point which undergoes a series of bifurcations and moves over to chaos. This is due to the fact that the iterates switch over from one hump to the other hump. It is to be noted that this transition occurs when the right hump of the combination map falls below the bisector line. Again, there is a considerable degree of asymmetry between the two portions of the bifurcation diagram. The formation of bubble structure in the bifurcation diagram is a distinct feature of the map, for certain high values of μ. See for example, the bifurcation diagram corresponding to $\mu = 36$. Such bubble structures have already been reported for certain two parameter one dimensional maps. Bubble formation in the bifurcation structure of maps with two extrema has been observed in certain laser systems, when the cavity losses are sinusoidally modulated[44]. The period 'bubbling' phenomenon has been observed in many other systems and seems characteristic of low dimensional dynamics[45-47].

2.2 Combination of two maps from different universality classes.

A combination map can also be formed by combining two maps chosen from two different universality classes. For this, we combine the Hemmer's map (order of maximum, $z = 1/2$) with the logistic map ($z = 2$). The Hemmers map is of the form, $x_{n+1} = 1 - a_1|x_n|^{1/2}$ defined in the interval (-1, 1) with the control parameter $a_1 \in (0, 2)$. For convenience, we convert this map into one on the unit interval (0,1) by a nonlinear transformation[48] as,

$$x_{n+1} = (a/4) - 2^{-1.5}a|x_n - 1/2|^{1/2};\ 0 < a < 4 \tag{2.5}$$

The logistic map is taken in the form, $x_{n+1} = \mu x_n(1 - x_n); 0 < x_n < 1;$ $\mu \in (0, 4)$. The combination map is given by,

$$x_{n+1} \equiv f(x_n, \mu, a) = \mu x_n(1 - x_n) - [(a/4) - 2^{-1.5}a|x_n - 1/2|^{1/2}] \tag{2.6}$$

The logistic map displays the period doubling route to chaos whereas the dynamics of Hemmer's map is quite different.

2.2.1 Analysis of Hemmer's map.

The Hemmer's map has got a cusp at the centre. The bifurcation structure of this map is entirely different from that of the quadratic family. Figure 2.6 gives a plot of the Hemmer's map for different values of a.

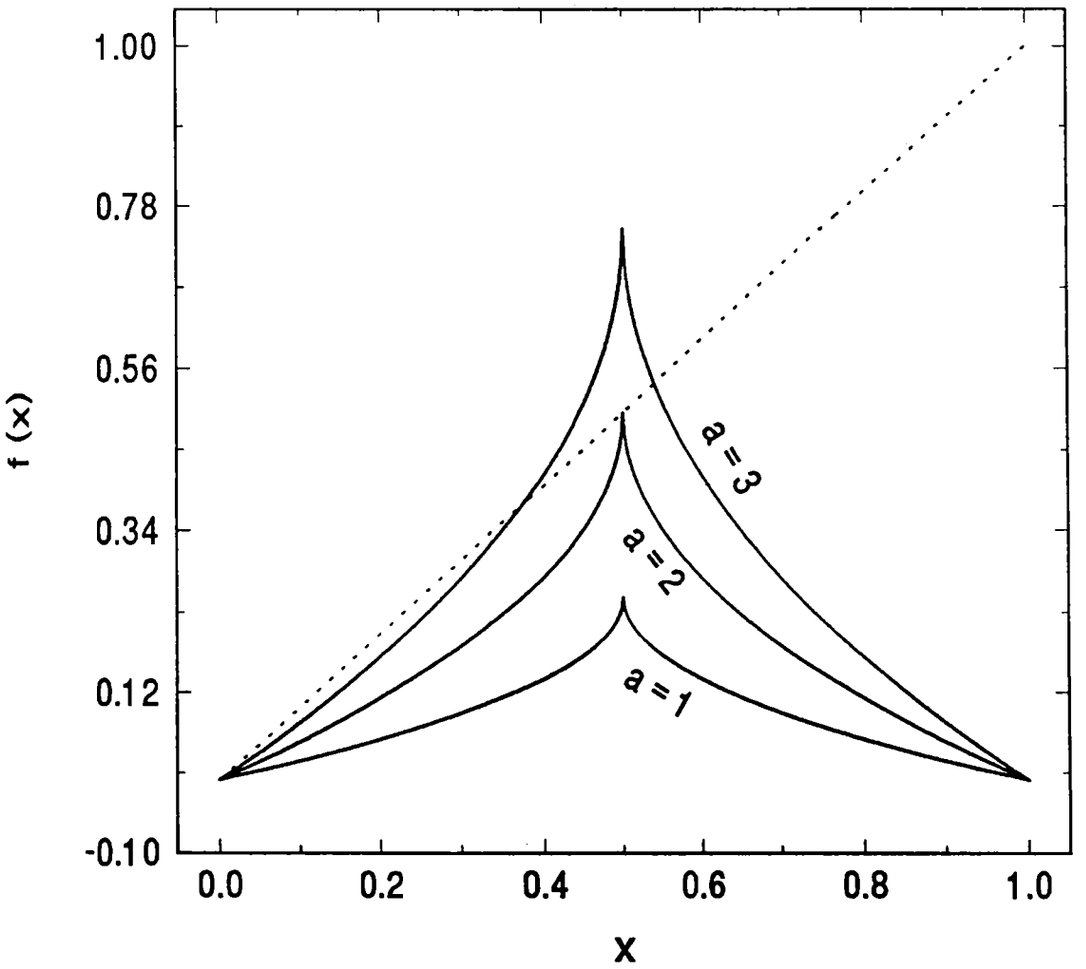

Fig 2.6 A plot of the Hemmers map, defined in eqn. 2.5. The values of a are indicated near the curves.

The map function is symmetric about $x = 1/2$. For any value of a, the function attains a maximum $= a/4$ when $x = 1/2$. The slope of the tangent to this curve is positive for $x < 1/2$ and negative for $x > 1/2$. The slope increases continuously from $(a/4)$ to ∞ as x varies from 0 to $1/2$. At $x = 1/2$, the slope has got an infinite discontinuity. As x varies from $1/2$ to 1, the slope increases from $(-\infty)$ to $(-a/4)$. For a varying from 0 to 2, the map has got only one fixed point, $x^* = 0$. When a varies from 2 to 4, there are two more fixed points; x_l^* from the left half and x_r^* from the right half of the interval of mapping. A linear stability analysis shows that the two fixed points x_l^* and x_r^* are unstable and the the fixed point $x^* = 0$ is stable for all values of $a < 4$. When $a = 4$, the origin becomes marginally stable. The slope at the origin becomes equal to $+1$, when $a = 4$. Thus, when the control parameter a is continuously varied from 0 to 4, the iterates are attracted to the origin.

2.2.2 Analysis of the combination map.

The combination map is a two parameter one dimensional map. Figure 2.7 gives the plot of the combination map for a typical choice of $\mu = 4$ and $a = 3$. The combination map is two humped in nature for all values of a in $(0, 4)$. To begin with, the parameter μ is kept fixed at a value $= 4$ and the parameter a is varied from 0 to 4 in steps of 0.001. Figure 2.8 represents a bifurcation diagram for the system.

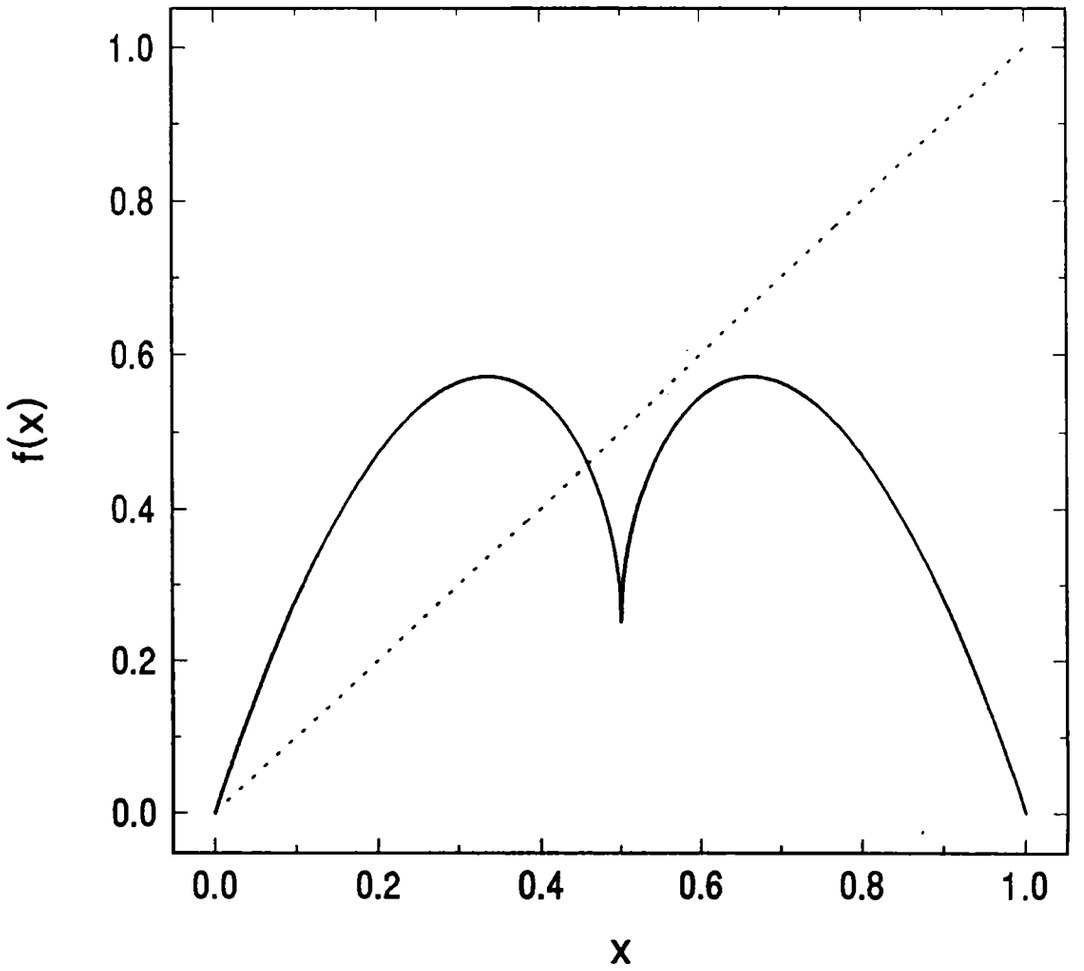

Fig. 2.7 The combination map given by eqn. 2.6, corresponding to $\mu = 4$ and $a = 3$

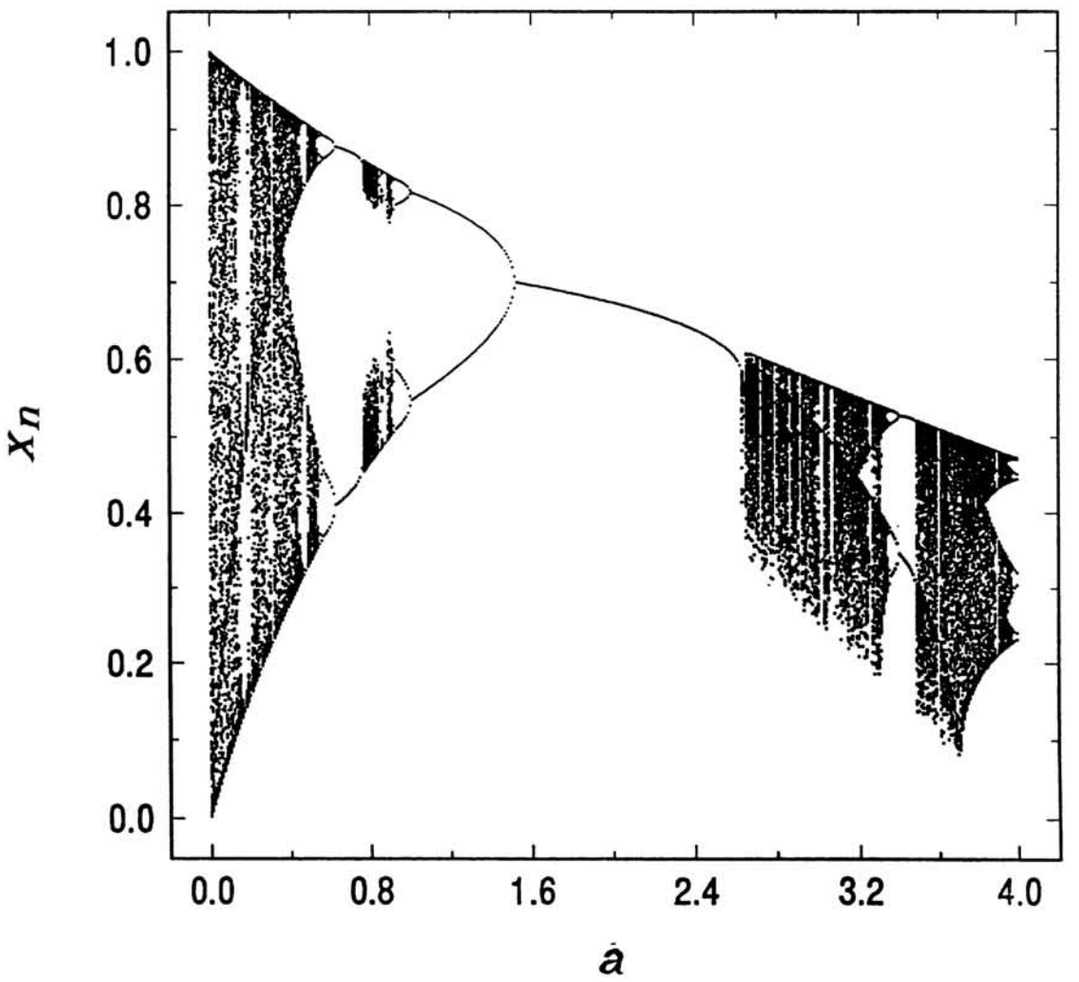

Fig 2.8 A bifurcation diagram of the map in eqn 2.6

The bifurcation diagram reveals the following aspects. The system undergoes a transition from chaos to order and also from order to chaos. The transition from chaos to order occurs by reverse period doubling. But the transition from order to chaos takes place by tangent bifurcations. The system first switches over from an aperiodic state to a periodic behaviour when the parameter a is increased beyond 0.546373. With further increase of a, the periods get halved at subsequent bifurcations until a 2-cycle is attained. The elements of this two cycle belong to the two humps of the map. When a increases beyond 0.760476, the system again shows an erratic behaviour. In this case, both the two cycle elements undergo tangent bifurcations. This can be easily understood from figure 2.9, where the second iterates are plotted for a value of a very near the transition point. Periodic behaviour again sets in when a becomes > 0.916421. Subsequent bifurcations (reverse period doublings) take the system to a 1-cycle, which remains stable for a considerably long interval of the parameter a. When a becomes > 2.629335, the 1-cycle suffers a tangent bifurcation and the system becomes chaotic. This is evident from figure 2.10 . Again there is a transition from regular to chaotic nature and vice versa. When $a > 3.974561$, the iterates become periodic. The transition from chaotic to periodic state and vice versa are confirmed by computations of the L.C.E of the system for various values of a. A plot of λ versus a is presented as figure 2.11. It can be seen that reverse period doublings occur in the periodic regime. Also, the transition from order to chaos takes place whenever one of the cycle elements approaches the cusp (at $x = 1/2$) of the the map.

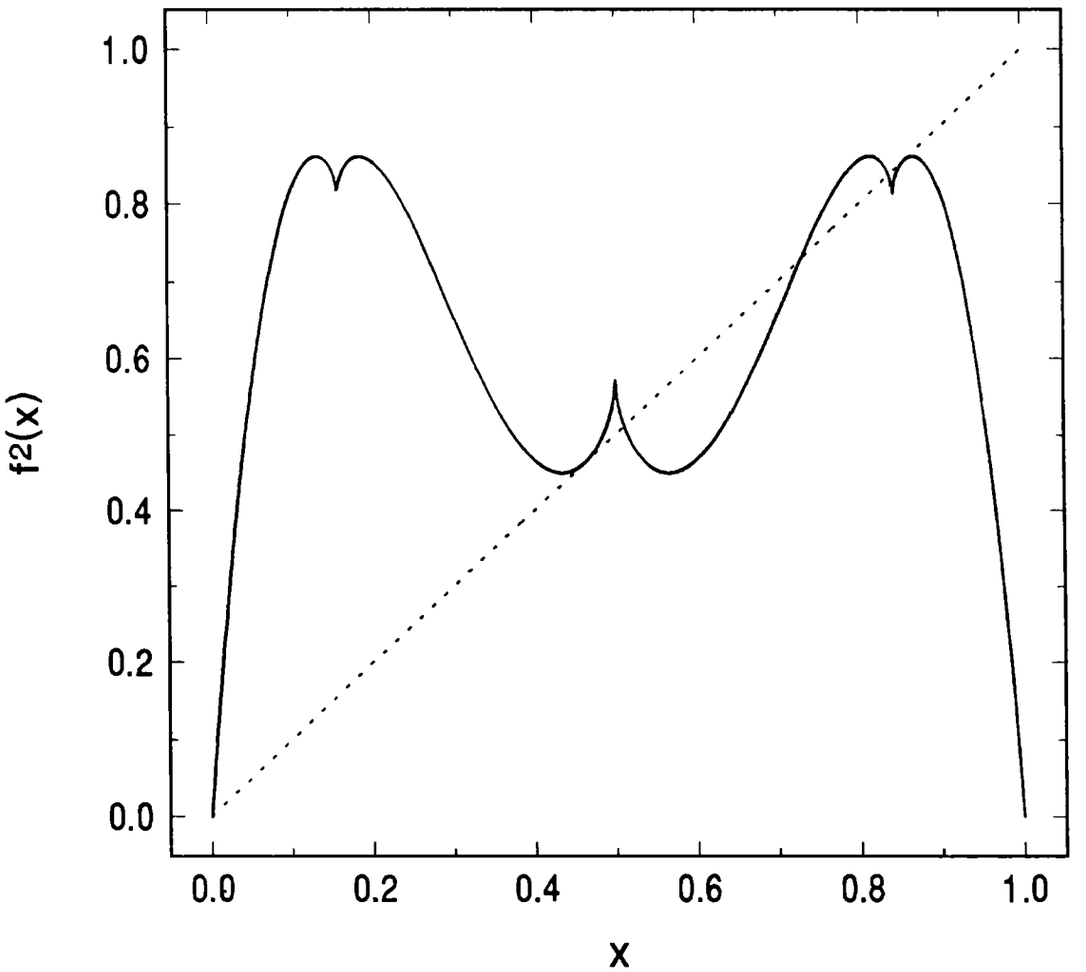

Fig. 2.9 A plot of the second iterate of the map in eqn 2.6. The value of $\mu = 4$ and $a = 0.761$. Note that the slope of the second iterate becomes equal to $+1$ and a tangent bifurcation occurs.

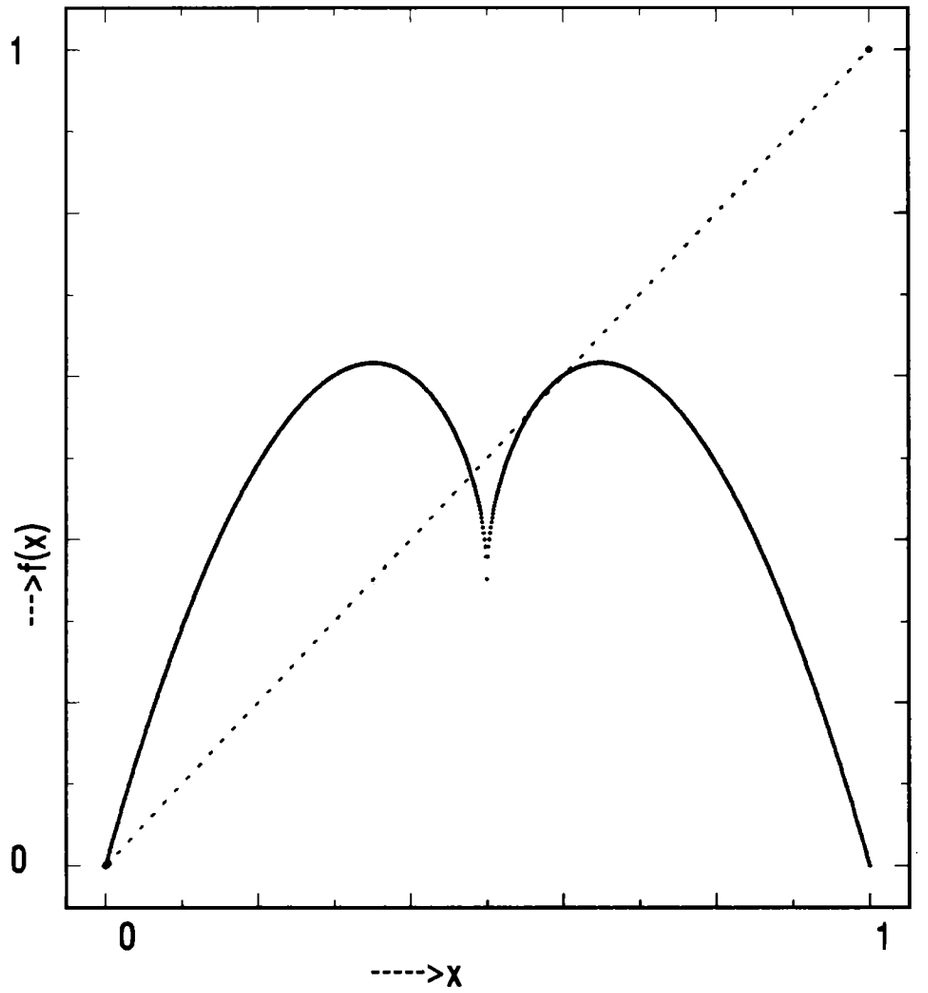

Fig.2.10 A plot of the map function in eqn 2.6.The value of $\mu = 4$ and $a = 2.6$ in this case.

A tangent bifurcation occurs for this (μ , a)

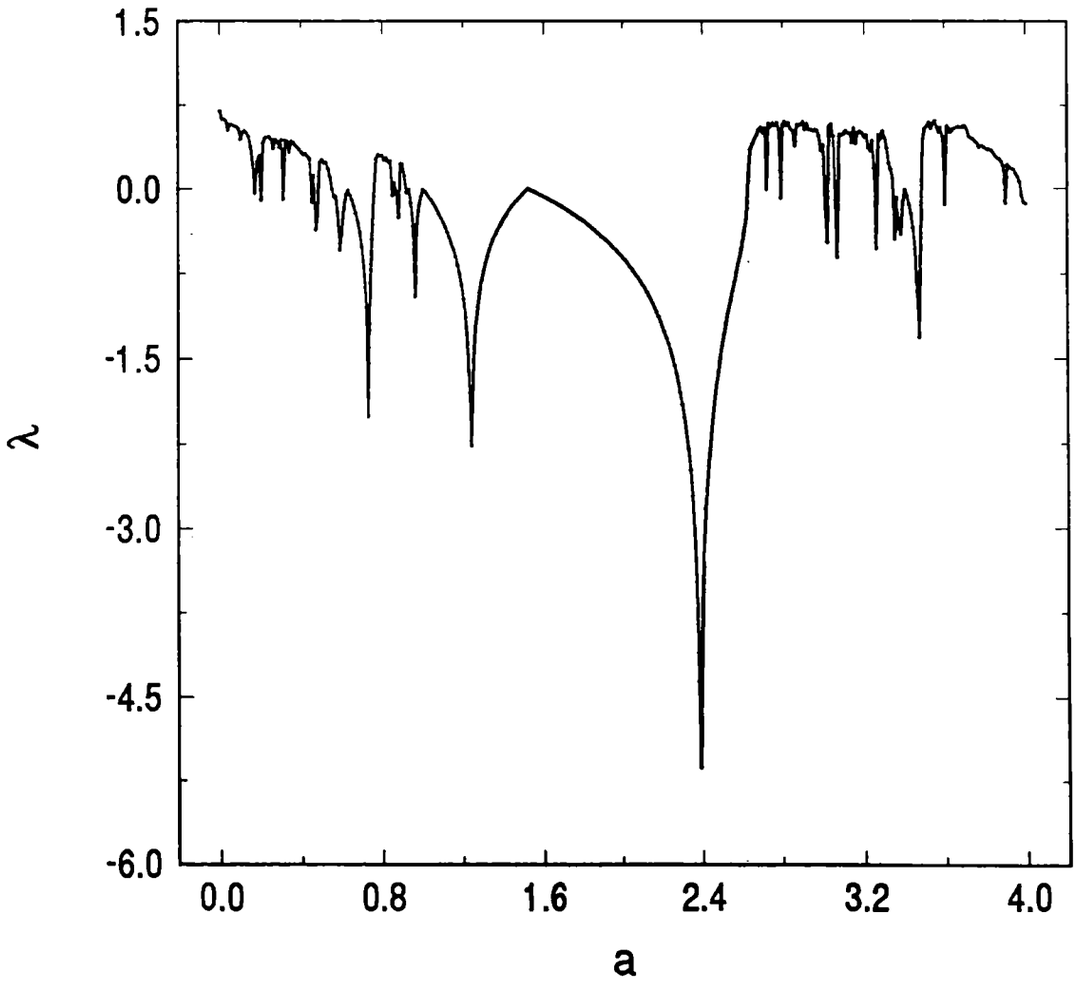

Fig 2.11 A plot of the L.C.E of the map in eqn 2.6, against the control parameter a.The value of μ is kept at 4.

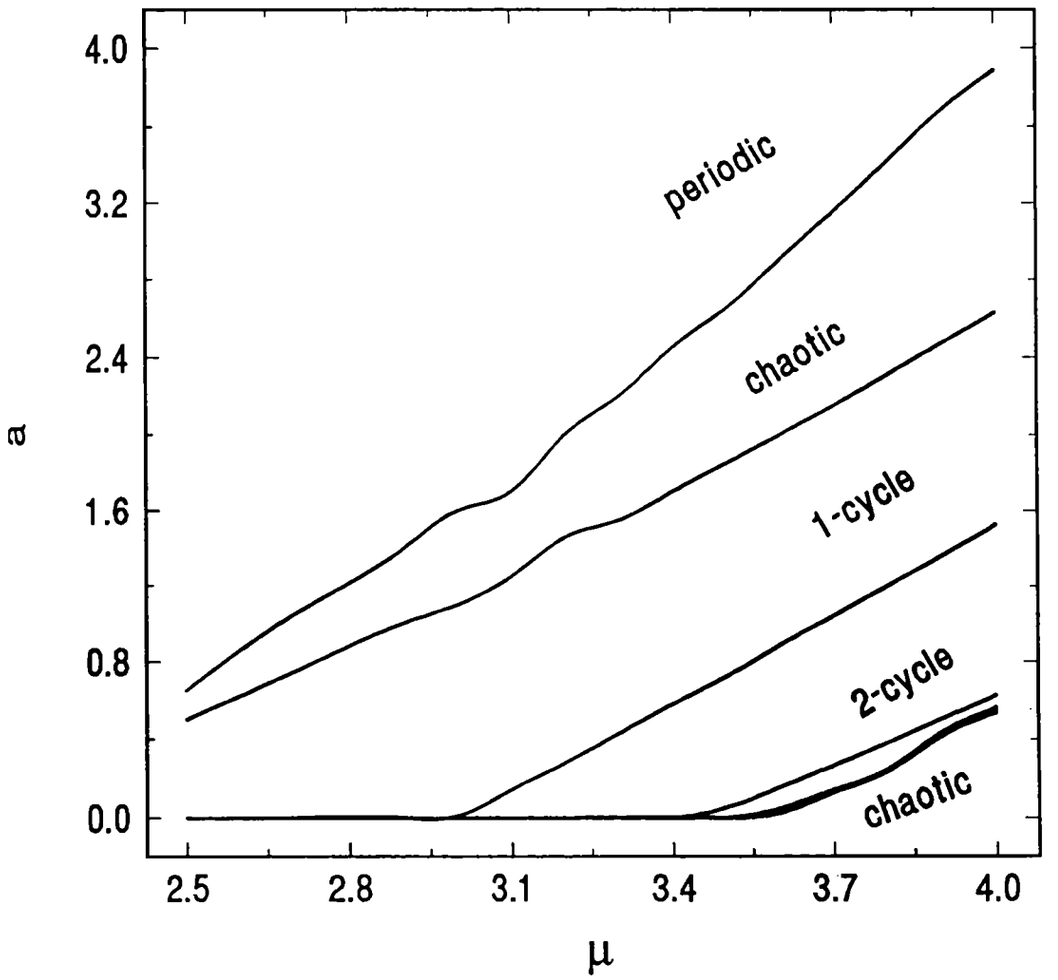

Fig 2.12 The parameter space (μ, a) for the system, defined in eqn 2.6

The bifurcation analysis is then repeated for various fixed values of μ both in the chaotic and in the periodic region of the logistic map. A parameter space plot (μ, a) of the system is thus obtained. Figure 2.12 represents the parameter space of this combination map. Unlike in the case of the combination map discussed in the previous section, the bifurcation lines are curved lines. This indicates that the dynamical behaviour of this system is very much different from that of the previous combination map.

2.3 Conclusion.

We conclude this chapter, with a summary of the main results of the investigations on the dynamics of combination maps:

The bifurcation structure of combination maps are, in general, different from those of the individual maps. In the case of a combination map got by combining the logistic map with the sine map, a transition from chaos to order by reverse period doubling is observed. For every value μ of the logistic map, a value A for the control parameter of the sine map can be found for any desired periodicity of the system. The parameter values A for successive period doublings converge at the Feigenbaum rate δ. Although the periodic region of the combination map is similar to that of the quadratic family, the chaotic regime behaves in a different way. The periodic windows are less in number compared with that of the pure logistic map. The chaotic bands undergo a sequence of band splittings and recombinations. This suggests that the scaling

behaviour of the characteristic constants in the immediate vicinity of the transition to chaos can be different from that of the individual maps. That it is so is established in the next chapter. For very high values of μ, the combination is always two humped in nature. In this case, transition from chaos to order and vice versa occur as the other parameter is continuously varied. Bubble structure in the bifurcation diagram is observed for certain high vales of μ. In the case of a combination of maps from two different universality classes, both the periodic and chaotic regimes are significantly different from those of the constituent maps. In both the cases, the combination map is a two parameter one dimensional map. The system can be brought to the desired periodicity or chaos, by proper choice of the parameters. The parameter space plot will be quite useful in this context. The bifurcation lines in the parameter space plot are parallel straight lines in the case of the first combination map. But, these lines are smooth curves for the second combination. Again, the intermittency phenomenon is more pronounced for the second combination. The presence of a sharp cusp at the extremum produces severe changes to the bifurcation phenomenon of a map. Similarly, the occurence of two humps in a map causes considerable changes to the behaviour of the system, as compared to that of simple one dimensional smooth maps.

3. Scaling Behaviour of the Lyapunov Characteristic Exponents

A hallmark of ergodic and mixing behaviour of nonlinear systems is their extreme sensitivity to initial conditions. The separation of two trajectories in phase space will either remain constant or decrease in course of time, if the system is periodic or quasiperiodic. But in chaotic systems, the orbits in phase space diverge out. A very small error in specifying the initial conditions grows rapidly and after some time it becomes almost impossible to predict the phase space trajectory. The rate of divergence of the orbits in phase space is usually measured by the Lyapunov characteristic exponent (λ). A positive value of λ implies that the system is chaotic. If λ is negative, the system is periodic or quasiperiodic. Thus λ can be considered as an order parameter in the transition from regular to chaotic state. In this context, the scaling behaviour of λ during the transition from order to chaos is important and interesting in understanding the onset of chaos in the system. A knowledge of the variation of λ near the onset of chaos is particularly useful in developing suitable algorithms for control of chaos. The nature of this scaling for one dimensional maps exhibiting the period doubling route to chaos have been theoretically worked out by Huberman and Rudnick[39]. It has been established that an infinite cascade of band mergings takes place in the chaotic regime, in a mirror sequence of the cascading bifurcations in the periodic regime[49]. For such systems, the envelope of positive Lyapunov exponent λ varies in a steep and

continuous manner. Huberman and Rudnick have shown analytically that the Lyapunov characteristic exponent behaves as

$$\lambda = \lambda_0 (a - a_\infty)^\nu \tag{3.1}$$

where λ_0 is a constant of the order of unity, a_∞ is the value of the control parameter a at the period doubling accumulation point and

$$\nu = \frac{\ln 2}{\ln \delta}, \tag{3.2}$$

δ being the Feigenbaum constant. This power law behaviour of the L.C.E for quadratic maps has been experimentally verified using a sinusoidally driven diode circuit[50]. Shraiman *et al.*,[51] has developed a scaling theory for noisy period doubling route to chaos, in which it is shown that in the limit of the noise amplitude tending to zero, the Huberman-Rudnick relation (H-R relation) is recovered. The H-R relation suggests that the scaling index ν depends on the order of maximum z through the value of δ which is different for different universality classes. However, it is not clear whether ν depends on z in some other way. No detailed numerical investigations have been reported for z values other than 2. We prove numerically the validity of the H-R relation for general one-dimensional maps. We also extend our studies to a combination map got by combining the logistic map with the sinusoidal map. This combination map has the same value of δ as the logistic map. Hence one would expect that the combination map also has the same value for ν. But we have found that the scaling index for the combination map is different. Thus, the Huberman-Rudnick relationship is not true for combination maps.

3.1 Scaling Law for General One Dimensional maps.

Consider the one-dimensional map on the interval (-1,1),

$x_{n+1} = 1 - a_1|x_n|^z$ where the control parameter a_1 varies from 0 to 2. This is a unimodal map with the *critical point* $x_c = 0$; Critical points play a fundamental role in determining and classifying global bifurcations[13]. The so called *critical curves* for two dimensional endomorphisms are generalizations of the critical points of one-dimensional mappings[53], and can be used as a basic analytical tool in characterizing the bifurcations in two dimensional systems[54]. z is the order of the maximum. Using a nonlinear transformation[48], this map can be converted to one on the unit interval (0,1). The transformed mapping is $x_{n+1} \equiv f(x_n) = (a/4) - 2^{(z-2)}a|x_n - 1/2|^z$ where $a \in (0,4)$ and the critical point $x_c = 1/2$. These maps exhibit the Feigenbaum scenario of period doublings. The values of α and δ are characteristic of the value of z. The Lyapunov characteristic exponent of the map can be computed by the formula[52],

$$\lambda = \lim_{N\to\infty} \frac{1}{N} \sum_{i=0}^{N-1} \ln \left| f'(x_i) \right|. \tag{3.3}$$

The upper bound for N is kept as 10^3, for computational purposes. To start with, the value of z is taken as 1.2. The L.C.E. values are determined by increasing a in small steps. The period doubling accumulation point, a_∞ is roughly estimated as that value of a at which λ changes from negative to positive for the first time. The parameter is then varied by further small steps around this rough value and the L.C.E's are computed. Thus, a better estimate

for a_∞ is obtained. This process is repeated again and again until the value of a_∞ is found upto an accuracy of 10^{-6} to 10^{-8}. The Lyapunov exponents (λ) are then calculated for a number of values of $a > a_\infty$ and very near to a_∞. This procedure is repeated for maps of various order of maxima, z. The presence of a large number of periodic windows in the chaotic regime near the accumulation point reduces the number of useful values of λ, especially for large values of z. The L.C.E's in the chaotic side near a_∞ changes to negative values at the periodic windows. The variation of a_∞ with z is shown in fig 3.1

As z increases, a_∞ approaches (asymptotically) the fully chaotic limit $a = 4$. Consequently, the entire chaotic regime shrinks to a narrow region in the parameter space. Since the chaotic regime has to accommodate all the periodic windows, the density of periodic windows near a_∞ will be greater for higher values of z. The addition of a small noise term can wash out the fine structure of the periodic windows and smoothen the curve for λ against a[55]. Thus, we added a Gaussian noise of zero mean and variance 0.2 for values of $z > 2$. The amplitude of noise added was of the order of 10^{-15}. Such a very low noise can not seriously affect the scaling behaviour of the system. Even with noise, the difficulty due to periodic windows near a_∞ can not be completely overcome. For z-values ≥ 4, we consider only an envelope scaling for λ with the periodic windows avoided. In fact, the Huberman-Rudnick scaling relation itself has been derived for the envelope of positive Lyapunov exponents.

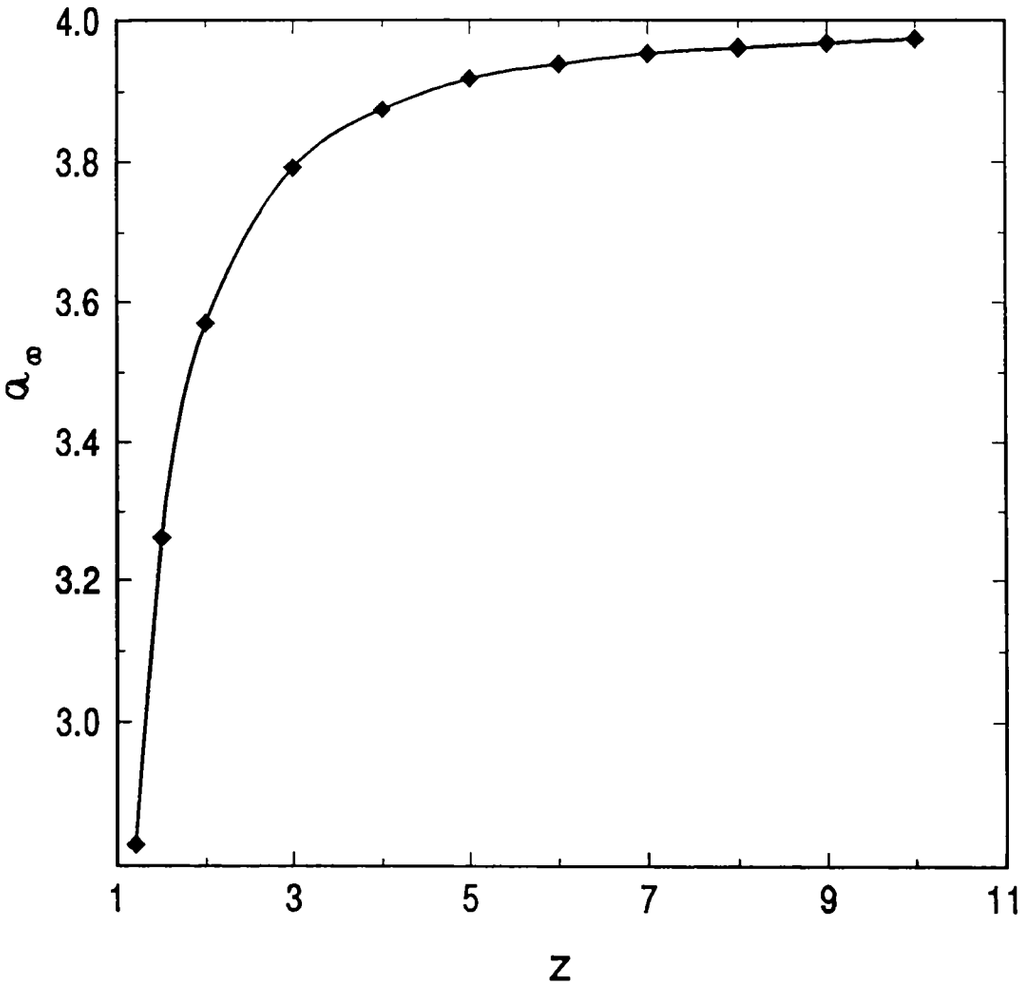

Fig 3.1 The variation of a_∞ with z, the order of maximum of the map. Note that as z increases, the chaotic regime, $a_\infty < a < 4$, shrinks and becomes very narrow for $z > 10$.

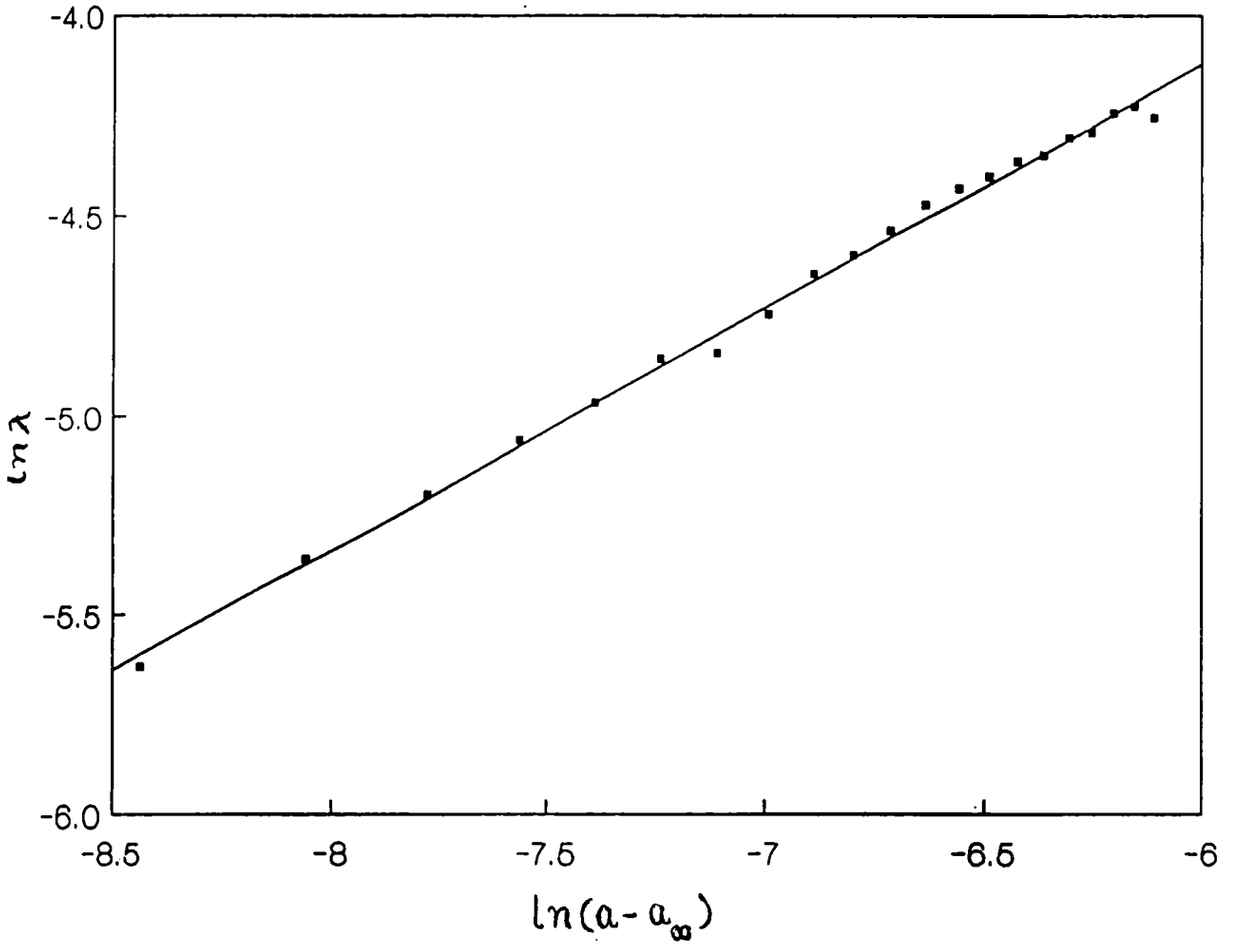

Fig 3.2 A typical log-log plot of λ vs $(a - a_\infty)$ for $z = 1.2$. The slope of this line gives the scaling exponent ν.

Table 3.1 The scaling index ν for various values of z

Order of maximum, z	ν (numerical)	ν = ln 2 / ln δ, using H-R law
1.2	0.60171	0.605779
1.5	0.52281	0.519209
2.0	0.42117	0.449820
3.0	0.40711	0.383449
4.0	0.30117	0.348928
5.0	0.29953	0.326608

Table 3.1 The scaling index ν for different values of z, calculated numerically and using H-R relation.

For each value of z, a plot of $\ln|\lambda|$ against $\ln|a - a_\infty|$ is obtained. The line of best fit is then drawn. The slope of the line gives the value of ν. Figure 3.2 gives such a log-log plot. The theoretical values for ν are calculated using the H-R law and also from the known values of δ for various z[56]. Table 3.1 gives the scaling indices (ν) for the various values of z. Within the possible computational errors, there is excellent agreement with the H-R relation. Thus we have established that the Huberman-Rudnick relationship for the scaling of Lyapunov exponents is true not only for the quadratic maps, but also for all one dimensional one-extremum maps exhibiting the Feigenbaum's route to chaos.

3.2 Scaling of Lyapunov Characteristic Exponents of a Combination Map.

In order to investigate the scaling behaviour of a combination map, we consider the first of the combination maps discussed in chapter 2. viz., $x_{n+1} = f(x_n, \mu, A) = \mu x_n(1 - x_n) - A\sin(\pi x_n)$; $0 \leq x_n \leq 1$; $0 \leq \mu \leq 4$; $(\mu/4 - 1) < A < \mu/4$. Keeping the value of $\mu = 4$, the parameter A is increased from 0 to 1 slowly in steps of 0.001. The L.C.E (λ) for each value of A is computed by the same algorithm discussed in the previous section. In this case, the system moves out of chaos and becomes periodic on increasing A. The Lyapunov exponent (λ) is positive for almost all values of A in the chaotic regime, except for certain windows of periodicity. But, in the periodic region, λ is always negative. The value of A_∞ is determined as that value of a at which

λ becomes zero and after which λ remains negative throughout. Repeated computations of λ by changing A on finer and finer scales give the value of A_∞ upto an accuracy of the order of 10^{-8}. The parameter A is then varied in steps of 10^{-8} around A_∞ and the corresponding λ values are found. As before, the line of best fit to the plot of $\ln|\lambda|$ against $\ln|A - A_\infty|$ is drawn. The slope gives the scaling index, ν. The computations are then repeated for other values of μ namely, $\mu = 3.5$ and $\mu = 3$. We have also extended the investigations for a very high value of μ. i.e., $\mu = 32$. In the latter case, the parameter A can vary from 7 to 8. Here, the combination map is two humped from the very beginning. As is clear from the discussions in chapter 2, the two humped nature sets in whenever the parameters are so tuned as to make the value of $A > (2\mu/\pi^2)$. But, the range of variation of A is from $(\mu/4 - 1)$ to $(\mu/4)$. Thus, if $(\mu/4 - 1) > (2\mu/\pi^2)$ i.e., $\mu > 4\pi^2/(\pi^2 - 8)$, the map will be two humped throughout the range of variation of A. A typical log-log plot for the combination map is presented in figure 3.3. The scaling index ν and the accumulation point A_∞ for the combination map for various values of μ are presented in table 3.2. From the log-log plot of the combination map, it can be noted that a power law behaviour for the Lyapunov exponents is more accurate for the combination map than for simple maps (For, the points lie more exactly on a straight line). Moreover, the proximity of the periodic windows does not hinder the numerical computations in this case. The periodic windows are less in number or they have been smeared out by the sinusoidal term.

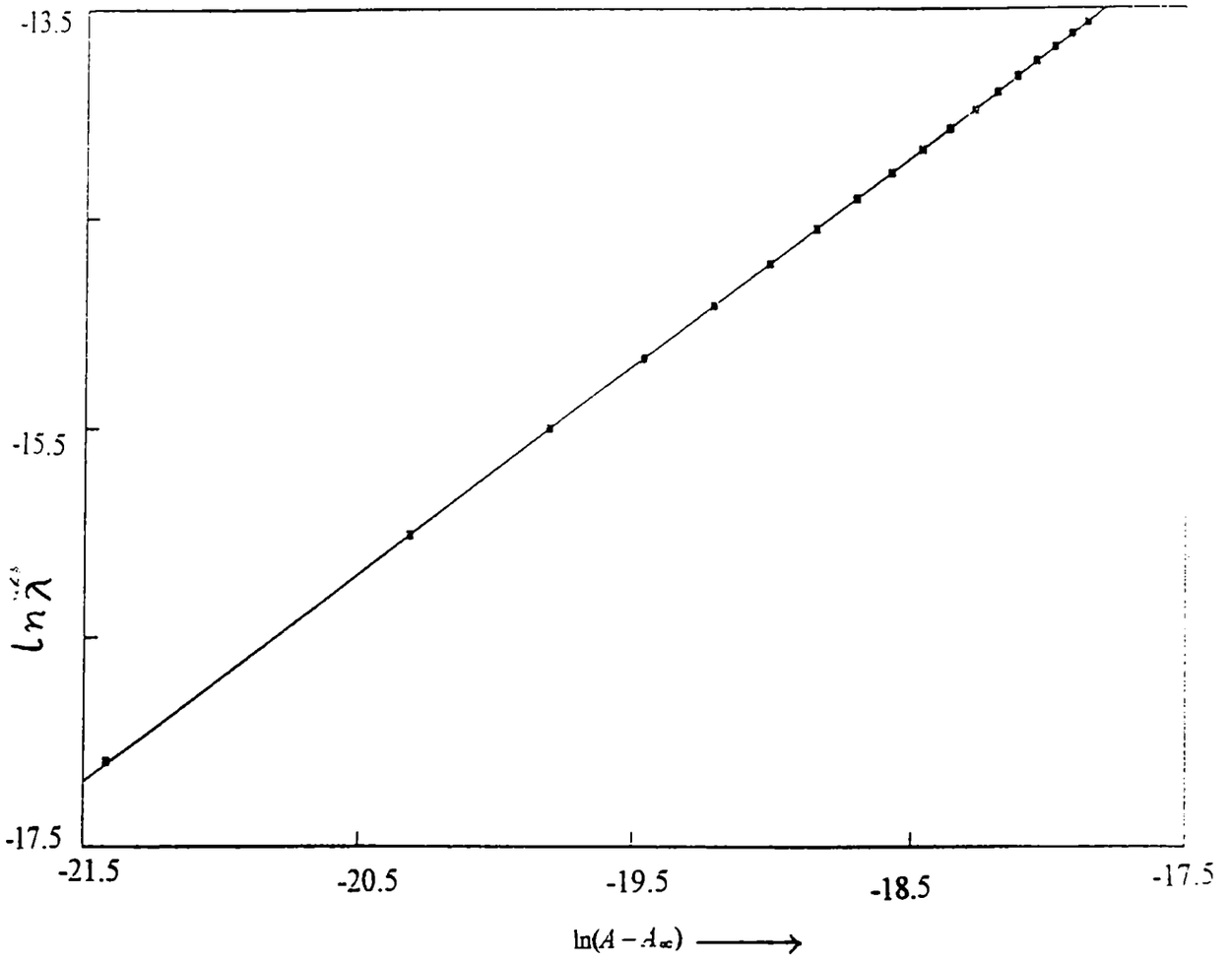

Fig 3.3 The L.C.E scaling for the combination map. $\ln|A - A_\infty|$ is plotted against $\ln|\lambda|$. Here, the value of $\mu = 32$. The scaling index ν in this case is found to be $\simeq 1$.

Table 3.2 The scaling index ν for and the accumulation point for various values of μ

μ	Accumulation point A ∞	Scaling index ν
3.0	-.1382968	0.9989838
3.5	-.0170178	0.9677731
4.0	0.1046909	0.9936844
32	7.22126758	0.9996790

Table 3.2 The scaling index ν and the accumulation point A_∞ for various values of μ.

In all the cases considered for the combination map, the scaling index is entirely different from that of the quadratic family. The value of ν for the combination map is nearly unity. i.e., it is almost double the value for the quadratic family as predicted by Huberman and Rudnick and also computed numerically for the logistic map. The combination map has the same value of δ as the quadratic map. This implies that the combination map does not follow the H-R scaling law. To see why the combination map has a different scaling behaviour for λ, we have carried out a detailed numerical analysis of the chaotic regime of the map. The parameter μ is fixed at 4. With $A = 0$, the system is fully chaotic. The parameter A is then slowly varied and a series of bifurcation diagrams are drawn. Each time, a portion of the previous bifurcation diagram is taken and a blow-up is formed. By this technique, we are able to observe the fine structure of the chaotic bands. When A is increased towards A_∞, the chaotic attractor exhibits a sequence of bifurcations. After each bifurcation, one of the branches of the bifurcation diagram is taken and the structure is analyzed on an enlarged scale. By carefully varying A , the next bifurcation point of the band is determined. Continuing like this, the values of A for successive band bifurcations are obtained. We could trace out the values of A upto the 8^{th} stage of band bifurcation. These values A_n and the convergence rate δ_n are provided in table 3.3. When A is increased further, recombination of bands is observed. The band bifurcation structure of the combination map is shown in figure 3.4. The merging of bands for the combination map is evident from this figure.

Table 3.3 Parameter values for successive band bifurcations and the convergence rate δ.

Parameter value A(n)	Convergence rate δ (n)
0.07909091	----------
0.09954546	----------
0.10360000	5.0449130
0.10440000	4.8267857
0.10463500	4.3076923
0.10467600	4.7560975
0.10468445	4.8235300
0.10468625	4.7222222

Table 3.3 The parameter values for successive bifurcations of the chaotic band of the combination map and its convergence rate δ_n.

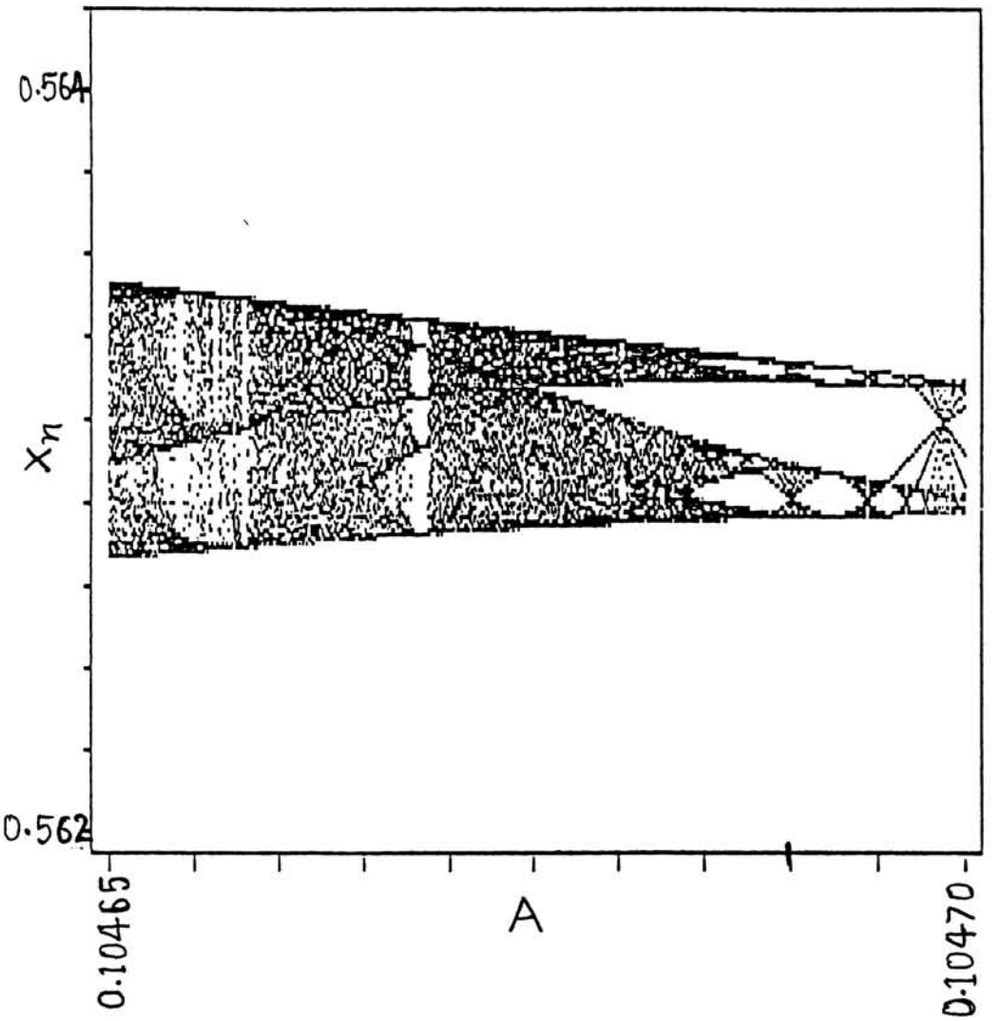

Fig 3.4 The band structure of the combination map on an enlarged scale. As A increases towards A_∞, merging of bands take place.

In the case of the combination map considered, the band bifurcations do not take place ad infinitum. This is not the case with simple one-dimensional one humped maps. In the case of the logistic map, for example, the iterates form a single band at $\mu = 4$. But, as μ is decreased towards μ_∞, the chaotic band undergoes an infinite cascade of bifurcations. On approaching μ_∞ from the periodic region, every periodic cycle of period 2^n bifurcates to a cycle of period 2^{n+1} at a distinct value μ_n and the sequence $\{\mu_n\}$ converges to a finite value μ_∞ as $n \rightarrow \infty$. Likewise, in the chaotic regime, the chaotic bands undergo a mirror sequence of band bifurcations. i.e., a chaotic attractor with 2^{k+1} bands bifurcates to a chaotic attractor with 2^k bands, as μ is increased. Thus, when μ_∞ is approached from the periodic region, we get an attractor with infinite period. But, when μ_∞ is approached from the chaotic region, we get a chaotic attractor with infinite bands. The rate of convergence of the parameter values for the chaotic band bifurcations is the same as the rate of convergence of the parameter values for period doublings, namely $= \delta$. This property has been made use of by Huberman and Rudnick for deriving the scaling law for one dimensional one humped maps. For the combination map, the chaotic bands merge together after a few bifurcations. This incomplete nature of the cascade of band bifurcations is the reason for a different scaling behaviour of the combination map.

3.3 Conclusion

In conclusion of this chapter, we summarize the main results obtained from the numerical computations of the Lyapunov characteristic exponents of a number of one dimensional maps. For all one dimensional one humped maps following the period doubling route to chaos, the envelope of positive λ scales according to the Huberman-Rudnick law. Thus, $\lambda \propto (a - a_\infty)^\nu$ where $\nu = \ln 2 / \ln \delta$, δ being the Feigenbaum convergence rate. The existence of an infinite cascade of band bifurcations in the chaotic regime is an essential requirement for the validity of the Huberman-Rudnick scaling law. The Huberman-Rudnick relation is true for one dimensional one humped maps of different order of maxima. But it is not true for combination maps. In the latter case, the cascade of band bifurcations does not take place ad infinitum. After a few splittings, recombination of chaotic bands is seen. This results in a different scaling behaviour for the Lyapunov exponents of combination maps.

4. Discontinuous Logistic Map

One dimensional iterative maps on an interval of the real axis have been used in modelling a wide variety of nonlinear systems. The most prominent route to chaos in these maps is through the Feigenbaum period doubling bifurcations. The transition from periodic to chaotic state through an infinite sequence of pitch fork bifurcations has been found to be a common feature of all unimodal functions having negative Schwarzian derivative [1]. One of the most extensively analyzed maps in this context is the logistic map [1,10,15,48]. The evolution of the system from regular to chaotic state has been investigated not only with the control parameter in its pure form, but also in some or other modified forms leading to a class of modulated logistic maps [58-64,75]. A remarkable property of the Feigenbaum scenario of bifurcations is the geometric convergence of the parameter values for successive bifurcations. This is found to be a universal property of almost all one dimensional continuous maps with a single hump. The presence of a discontinuity or asymmetry in the map, however, produces a considerable change in the bifurcation structure of the system. A 'new road to chaos' has been identified by de Souza Vieira *et al.*, based on the numerical investigations on a discontinuous logistic map [65,66]. The existence of inverse cascades of bifurcations in which the periods change arithmetically is a novel aspect in these systems. Certain empirical rules for

the existence of inverse and direct cascades have also been reported [67]. The number of inverse cascades and the type of route to chaos depend on the location of the discontinuity as well [68]. The periods of the cycles depend highly on the precision of the computations [69]. The phenomenon of border-collision bifurcations and the formation of inverse and direct cascades in one-dimensional piecewise smooth maps have also been investigated [70-72]. A possibility for having a discontinuous bifurcation from any selected orbit of the period-doubling cascade to an orbit of the inverse or direct cascade has also been reported [72]. A bifurcation phenomenon different from the standard period-doubling one has been observed for a piecewise cubic map [74] and also in an experimental situation in a He-Ne laser system [73]. Similar bifurcations have been observed for other piecewise continuous quadratic maps like the circle map [76] and the logistic-like *sawtooth map* [77]. Inverse cascades of bifurcations together with direct cascades had been reported for certain Hamiltonian systems [78]. Such Hamiltonian systems exhibit only a few continuous bifurcations in which the periods change geometrically. But, the discontinuous logistic map shows a number of discontinuous bifurcations in which the periods decrease in an arithmetic progression. The whole set of bifurcations can be viewed as an alternate route to chaos, with scaling laws different from that of Feigenbaum's [66]. Most of the studies in these systems are numerical. We provide an analytical explanation for the bifurcation phenomenon of a discontinuous logistic map. Numerical findings in support of the results are also included.

4.1 Analysis of the Discontinuous Logistic Map; Coexistence of Multiple Attractors and their Basins of Attraction

We consider the logistic map with a discontinuity at the centre. The map is defined as,

$$\begin{aligned} x_{n+1} &= 4\mu x_n(1-x_n); \textit{for } 0 < x_n \leq 1/2. \\ x_{n+1} &= 4\mu x_n(1-x_n) + C; \textit{for } 1/2 < x_n < 1. \end{aligned} \tag{4.1}$$

where μ is the control parameter and C is a constant representing the strength of the discontinuity. This map corresponds to a special case of the more general asymmetric map that has been numerically investigated by De Sousa Vieira *et al.*, [65] given by

$$\begin{aligned} x_{t+1} &= 1 - \epsilon_1 - a_1|x_t|^{z_1}; \quad x_t > 0. \\ x_{t+1} &= 1 - \frac{1}{2}(\epsilon_1 + \epsilon_2); \quad x_t = 0 \\ x_{t+1} &= 1 - \epsilon_2 - a_2|x_t|^{z_2}; \quad x_t < 0. \end{aligned} \tag{4.2}$$

The map given by equation 4.1 differs slightly from the one referred to above in that the value of the function at the point of discontinuity is also included in the left half of the interval of the mapping. Also, the interval of the mapping is (0,1) instead of (-1,1) in equation 4.2. Again it differs from the discontinuous map analyzed by Chia & Tan [67] in that the discontinuity parameter C is introduced in the right half of the interval in our case instead of in the left

part as in the case of Chia & Tan. De souza Vieira *et al.*, numerically investigated the effect of three type of asymmetries:

a) $\epsilon_1 = \epsilon_2 = 0,\ z_1 = z_2 \equiv z,\ a_1 \neq a_2$; b) $\epsilon_1 = \epsilon_2 = 0,\ a_1 = a_2 \equiv a,\ z_1 \neq z_2$ and c) $a_1 = a_2 \equiv a,\ z_1 = z_2 \equiv z,\ \epsilon_1 \neq \epsilon_2$. They have verified that the Feigenbaum scenario for one-dimensional one-extremum maps gets strongly modified if asymmetry is introduced in the extremum. Amplitude asymmetry ($a_1 \neq a_2$) and exponent asymmetry ($z_1 \neq z_2$) have relatively minor influence on the bifurcation pattern whereas the discontinuity in the extremum drastically alters the bifurcation phenomenon. With typical choices of $(\epsilon_1, \epsilon_2) = (0, 0.1)$ and $(0.1, 0)$, they have observed various inverse cascades of bifurcations. The periods of the cycles were found to decrease in arithmetic progressions, as a is increased. In the case of $(\epsilon_1, \epsilon_2) = (0, 0.1)$ for example, the first cascade of bifurcations occur immediately above $a = 1$, with periods like $16 \rightarrow 14 \rightarrow 12 \rightarrow 10 \rightarrow 8 \rightarrow 6 \rightarrow 4$. Just above this cascade, some standard pitch-fork bifurcations are observed. Again inverse cascades with periods $...76 \rightarrow 58 \rightarrow 40 \rightarrow 22$; $...92 \rightarrow 70 \rightarrow 48 \rightarrow 26$; $...134 \rightarrow 108 \rightarrow 82 \rightarrow 56$ ..., etc. are observed. Tan & Chia [67] have given certain empirical rules for the existence of inverse and direct cascades. Note that in all the cases considered for the discontinuous logistic map, the common difference of the progressions are even numbers. This observation is of much significance in our analytical investigations.

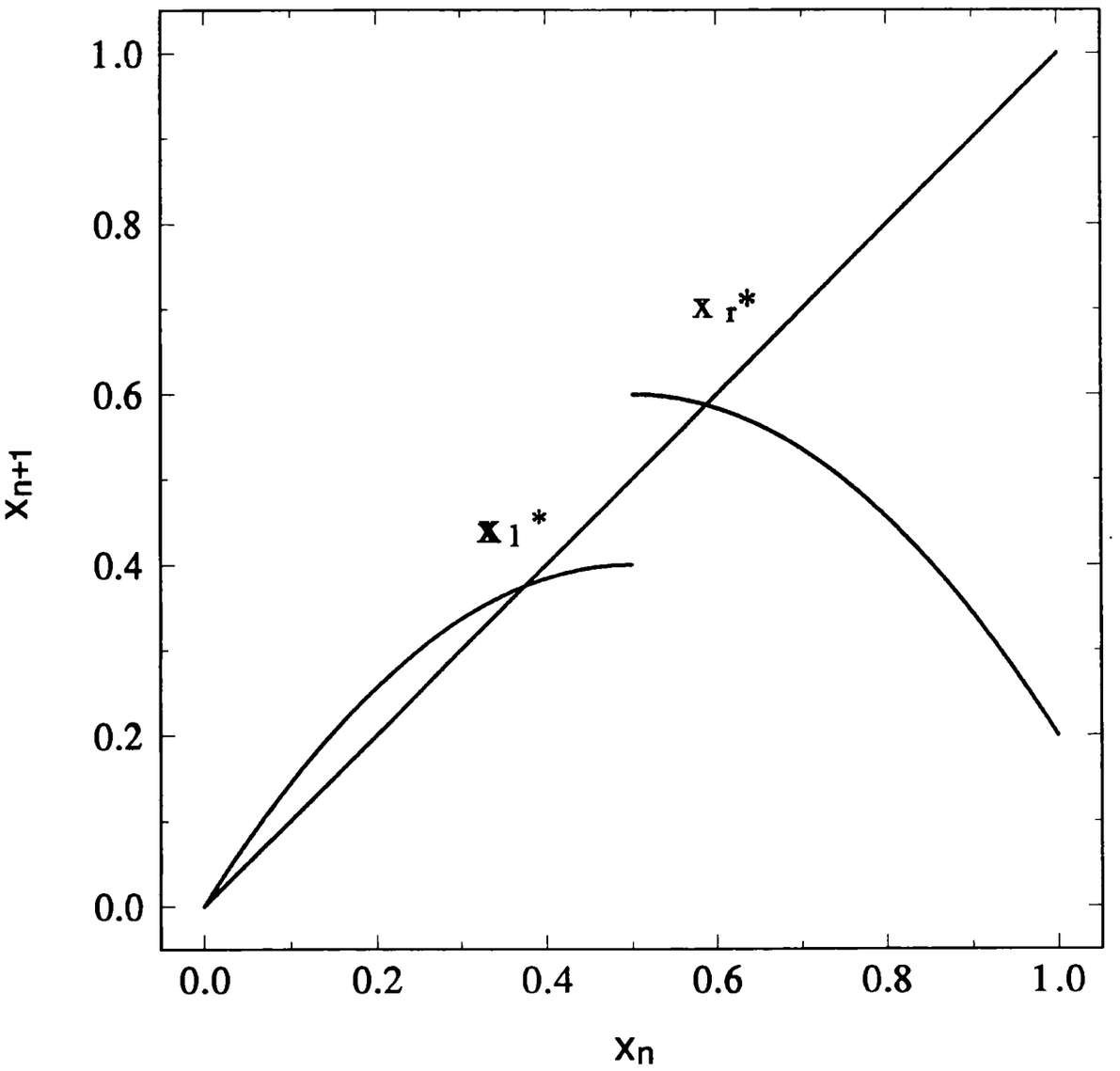

Fig 4.1 The discontinuous map defined in eqn 4.1. The discontinuity parameter $C = 0.2$ and the control parameter $\mu = 0.4$. Note that the two fixed points x_l^* and x_r^* coexist in this case.

For convenience, we write equation 4.1 in the form, $x_{n+1} = T(x_n)$, where the mapping T is such that $T(x) = f(x) = 4\mu x(1-x)$ for $0 < x \leq 1/2$ and $T(x) = \phi(x) = 4\mu x(1-x) + C$ for $1/2 < x < 1$. The qualitative shape of the map function is shown in figure 4.1. In the left half of the interval (0,1), the curve is logistic in nature and the function increases from 0 to μ as x increases from 0 to 1/2. As x increases from 1/2 to 1, the map function $\phi(x)$ decreases monotonically from $(\mu + C)$ to C. The presence of such discontinuities (i.e., different $x \rightarrow (\frac{1}{2})_+$ and $x \rightarrow (1/2)_-$ behaviour) in physical systems [10,79] perturbs the dynamics of them considerably. For every value of C, the control parameter μ is varied from 0 to $(1-C)$ so as to confine the iterates within the unit interval. The fixed points of the system are determined by $T(x^*) = x^*$. Depending on the relative values of μ and C, there will be one or more fixed points. The fixed point of the left part is $x^* = 0$ for values of μ ranging from 0 to 1/4. When $\mu > 1/4$, the fixed point from the left part is

$$x_l^* = 1 - \frac{1}{4\mu} \tag{4.3}$$

The fixed point arising from the right part is given by $\phi(x^*) = x^*$. i.e., 4 $\mu x^*(1-x^*) + C = x^*$. This quadratic equation gives the solution,

$$x^* = \{(4\mu - 1) \pm [(4\mu - 1)^2 + 16\mu C]^{1/2}\}/8\mu \tag{4.4}$$

Since the negative root for x^* is inadmissible, we have the fixed point to the right of $x = 1/2$ as

$$x_r^* = \frac{1}{2} + \frac{\sqrt{(4\mu-1)^2 + 16\mu C} - 1}{8\mu} \tag{4.5}$$

Thus we have simultaneous occurrence of attractors x_l^* and x_r^*. In the limit of $C \to 0$, we get $x_r^* \to x_l^* = 1 - (1/4\mu)$. This is understandable since the pure logistic map has only one attractor. The fixed point (x_r^*) and its stability properties depend on the two parameters μ and C so that one can have a desired dynamics for the system by proper choice of μ and C as in the case of combination maps [80,81]. The asymptotic state of the system is determined by either x_l^* or x_r^* or both, depending on the values of μ and C. Keeping C fixed, let μ be varied from 0 to $(1 - C)$. The fixed point of the system is $x^* = 0$ for values of μ ranging from 0 to 1/4. When μ increases beyond 1/4, the zero fixed point loses its stability and becomes a repellent while the only attracting fixed point on the left part is x_l^*. As μ increases from 1/4 to 1/2, x_l^* moves from 0 to 1/2. When the control parameter exceeds the value $\mu = 1/2$, the left half of the map lies above the bisector line. Thus the left attractor (x_l^*) ceases to exist beyond $\mu = 1/2$. To the right of $x = 1/2$, the map is of the nature of a combination map, obtained by combining the logistic map with an additive constant. The fixed point (x_r^*) manifests itself whenever the parameter μ is so tuned as to make $x_r^* > (1/2)$. For this we have from eqn.4.5, $[\{(4\mu-1)^2 + 16\mu C\}^{1/2} - 1] > 0$. This necessitates $\mu + C > 1/2$. i.e., $\mu > (1/2 - C)$. This criterion for the appearance of x_r^* can also be inferred from figure 4.1, as the condition for the height of the extremum when approached

from the right of $x = 1/2$ to be greater than $1/2$. If $\mu + C < 1/2$, then the right branch $\phi(x)$ of the curve lies wholly below the $y = x$ line. Thus we see that the x_r^* exists for all $\mu > (1/2 - C)$ and x_l^* appears for $1/4 < \mu \leq 1/2$. Hence the two attractors co-exist in the parameter range $(1/2 - C) < \mu \leq 1/2$. For values of $\mu < (1/2 - C)$, only x_l^* exists and for $\mu > 1/2$ only x_r^* exists. When the two attractors co-exist, there are two different basins of attraction. The bifurcation structure will therefore depend on the initial value used for iteration. Multiple basins of attraction for one dimensional maps of a single hump are usually uncommon. That it is seen in our case is a consequence of the fact that the map is represented by two different functions (f and ϕ) on either side of $x = 1/2$.

The basin of attraction for a fixed point is the set of initial points (x_0) that converge asymptotically to that fixed point. The basins of attraction of the attractors of the map can be obtained as follows. The mapping T is such that the left half $f(x)$ increases monotonically with x , while the right part $\phi(x)$ decreases monotonically with x. Let x_r be the pre-image of $1/2$ on the right. i.e., $x_r = \phi^{-1}(1/2)$. Or, $4\mu x_r(1 - x_r) + C = 1/2$. This gives,

$$x_r = 1/2 + \frac{\sqrt{16\mu(\mu + C - 1/2)}}{8\mu} \tag{4.6}$$

The pre-image of 1/2 on the left is

$$x_l = 1/2 - \sqrt{\frac{1}{4} - \frac{1}{8\mu}} \quad . \tag{4.7}$$

For the logistic map $x_{n+1} = 4\mu x_n(1 - x_n)$, the two pre-images of 1/2 are $1/2 \pm \sqrt{\frac{1}{4} - \frac{1}{8\mu}}$ which are symmetric w.r.t $x = 1/2$. But, for the discontinuous map, the pre-image of 1/2 on the right of $x = 1/2$ is shifted further to the right (for positive C). This asymmetry in the two pre-images play a vital role in the nature of bifurcations of the map, as the iterates approach the point of discontinuity. For values of x in $(1/2, x_r)$, the function $\phi(x)$ decreases from $(\mu+C)$ to 1/2. For all initial values x_0 greater than x_r, the first iterate $T(x_0) = \phi(x_0)$ is less than 1/2 so that the second iterate, $T^2(x_0) = T[\phi(x_0)] = f[\phi(x_0)]$; third iterate, $T^3(x_0) = f^2[\phi(x_0)]$ and so on. Thus the second and higher iterates fall on the left branch and the asymptotic state is x_l^*. If we start from an initial value $x_0 \in (0, 1/2)$, the iterates are $f(x_0), f^2(x_0), f^3(x_0), f^4(x_0) \ldots$ which converge to x_l^*. For x_0 lying in the interval $(1/2, x_r)$, the successive iterates form the sequence $\{\phi(x_0), \phi^2(x_0), \phi^3(x_0), \ldots \phi^n(x_0), \ldots\}$ which converges to x_r^*. Hence, the basin of attraction (R) for the attractor x_r^* is the set of points $R = \{x_0 \mid x_0 \in (1/2, x_r)\}$ where x_r is given by eqn. 4.6. Obviously, the basin of attraction (L) for the attractor x_l^* is the set of points on the unit interval, complimentary to the set R. i.e., $L = (0, 1/2)\ U\ (x_r, 1)$. The 'width' of the basin of attraction (R) is $W = x_r - 1/2 = 1/8\mu\{[16\mu(\mu + C - 1/2)]^{1/2}\}$. From the expression for x_r, it is clear that the basin R will be real only if $(\mu+C) > 1/2$. This should be so since the condition $(\mu+C) > 1/2$ is an essential requirement

for the existence of the attractor x_r^* itself. Keeping C fixed, as μ increases from $(1/2-C)$ onwards , the width of the basin R increases and that of L decreases. At $\mu = 1/2$, the value of W becomes a maximum $= \sqrt{(C/2)}$. When μ increases beyond 1/2, there exists only one attractor (x_r^*) for the system and all points in (0,1) constitute its basin of attraction. Similarly for values of $\mu < (1/2-C)$, there will be x_l^* only and the entire (0,1) interval forms its basin of attraction. It is also possible for the right attractor x_r^* to co-exist with the zero fixed point, if $\mu < 1/4$ and $\mu + C > 1/2$. For this, C must be $> 1/4$. Since the stability conditions for the zero fixed point and x_l^* are mutually exclusive ($\mu < 1/4$ and $\mu > 1/4$ respectively), the possibility of coexistence of all the three attractors is ruled out. It is obvious that when x_r^* coexists with the zero fixed point, the basin of attraction of x_r^* is $R = (1/2, x_r)$ and that of the zero fixed point is $(0, 1/2)\ U\ (x_r, 1)$ where x_r is the same as the one given by equation 4.6. When only one attractor exists, the basin of attraction is (0,1).

4.2 Bifurcation Scenario for the Discontinuous Map

We now consider the stability of the fixed points, as the system parameters are varied. A fixed point x^* will be stable, if the slope of the tangent to $T(x)$ at $x = x^*$ is less than unity, in magnitude. Keeping C fixed, let the control parameter μ be varied from 0 to $(1 - C)$. For $0 < \mu < 1/4$, the fixed point $x^* = 0$ is stable. For $1/4 < \mu < 1/2$, we have x_l^* as the fixed point from the left part. This fixed point remains stable upto $\mu = 1/2$ and after that it

vanishes. For $\mu > 1/2$, the asymptotic state of the system is solely determined by x_r^*. This attractor is not stable throughout the range of variation of μ. The slope of the map function $= T'(x) = f'(x) = \phi'(x) = 4\mu(1-2x)$. Therefore, $T'(x_r^*) = 1 - \sqrt{(4\mu-1)^2 + 16\mu C}$, where equation 4.5 has been used. At $\mu = (1/2 - C)$, this slope = 0. As μ increases, the slope becomes negative and its magnitude increases. When the slope becomes = -1, the first period doubling occurs and a 2-cycle is formed. The corresponding value of μ is given by,

$$\mu_1 = \frac{(1-2C) + \sqrt{(2C-1)^2 + 3}}{4} \tag{4.8}$$

Upto this value of μ, the system exhibits one cycle behaviour. Thus there will be two attractors (x_l^* and x_r^*) for μ in the region $(1/2 - C) < \mu < 1/2$. Beyond $\mu = 1/2$, only x_r^* exists and it remains stable upto the parameter value $\mu = \mu_1$. The attractor x_r^* exhibits period doubling at $\mu = \mu_1$ and then the system shows a two cycle behaviour. In the limit, $C \to 0, \mu_1 \to 0.75$, the value for the logistic map.

In the usual Feigenbaum route to chaos, the 2-cycle bifurcates to a 4-cycle at a parameter value $\mu = \mu_2$ and it remains stable for a range of μ and then the 4-cycle bifurcates to an 8-cycle at $\mu = \mu_3$ and so on and these period doublings take place ad infinitum. The system then enters the chaotic region at a parameter value $\mu = \mu_\infty$, the period doubling accumulation point. But in the case of discontinuous maps, another type of bifurcation (a 'discontinuous bifurcation') takes place, when μ is increased. A different route to chaos is

thus possible. In the 2-cycle region of the map, the slope of $\phi^{2}(x)$ at the cycle elements $= \phi'(x_1^*)\phi'(x_2^*) = 64\mu^2(x_1^* - 1/2)(x_2^* - 1/2)$, where x_1^* and x_2^* are the elements of the two cycle. It remains positive as long as both the cycle elements fall to the right of $x = 1/2$. For $\mu = \mu_1$, the slope of $\phi(x)$ at $x = x_r^*$ becomes equal to -1, so that the slope of $\phi^{2}(x) = +1$ at this point. With increase of μ above μ_1, we have a two cycle and the slope of $\phi^2(x)$ at the cycle elements decreases from 1. Both the cycle elements x_1^* and x_2^* lie within the interval $R = (1/2, x_r)$. As μ increases, the cycle elements move out. The lower element x_1^* moves towards $1/2$ and the upper element x_2^* approaches x_r. Let $x_1^* = (1/2 + \epsilon)$. Then $x_2^* = \phi(x_1^*) = (\mu + C - 4\mu\epsilon^2)$. In the limit $\epsilon \to 0$, $x_1^* \to (1/2)_+$ and $x_2^* \to (\mu + C)_-$. In this limiting case, the slope of $\phi^{2}(x) \to 0$. Thus the limiting 2-cycle $\{(1/2)_+, (\mu + C)_-\}$ is a stable one. This 2-cycle behavior continues upto $\mu = \mu_r$, at which the right element $(\mu_r + C) = x_r$, the pre-image of $1/2$ on the right part. Using equation 4.6,

$$\mu_r = \frac{(\frac{1}{2} - C) + \sqrt{1 + (\frac{1}{2} - C)^2}}{2} \tag{4.9}$$

For $\mu_1 < \mu < \mu_r$, a two cycle (x_1^*, x_2^*) is obtained. $\phi(x_1^*) = x_2^*$ and $\phi(x_2^*) = x_1^*$. Thus, x_1^* and x_2^* are solutions of $\phi^2(x) = x$. Now, for $\mu = \mu_r$, the right element $x_2^* = x_r$. The next iterate of x_r, say, $x_1 = T(x_r) = \phi(x_r) = 1/2$, falls on the left branch. Consequently, the second iterate of x_r is decided not by the function $\phi(x)$, but by $f(x)$. i.e., $x_2 = T^{2}(x_r) = T(1/2) = f(1/2) = \mu_r$. Now, since μ_r is greater than $1/2$, (for $C < 1/2$, as is usually the case), the second iterate of x_r comes back to the interval $(1/2, x_r)$. The third and

higher iterates are decided by the function ϕ. Thus, we get the sequence of iterates, $\{ x_2, \phi(x_2), \phi^2(x_2), \ldots, \phi^r(x_2), \ldots\}$ and the two cycle behaviour is lost. Clearly, all these iterates lie in the interval $(1/2, x_r)$. These iterates are attracted towards the 'virtual' 2-cycle $(1/2, x_r)$ [i.e., the two cycle that the system would have, if the mapping were $\phi(x)$ on both sides of $x = 1/2$]. Once x_r is attained, the sequence is repeated. In this sequence of iterates, the odd iterates $\phi(x_2), \phi^3(x_2), \phi^5(x_2), \ldots$ approach one end of the interval $(1/2, x_r)$ and the even iterates $\phi^2(x_2), \phi^4(x_2), \phi^6(x_2), \ldots$ approach the other boundary. The system thus exhibits a large periodicity n, which is highly dependent on the precision of the computer. The period n will be even or odd depending on whether $x_2 > x_r^*$ or $x_2 < x_r^*$, where x_r^* is the fixed point (unstable) of $\phi(x)$ and x_2 is the second iterate of x_r. We consider the two cases separately.

Case (1). Second iterate of x_r is greater than the unstable fixed point x_r^*. i.e., $x_2 > x_r^*$.

The function $\phi(x)$ decreases monotonically for all $x > 1/2$. Therefore, since x_2 lies to the right of x_r^*, its iterate, $\phi(x_2) < \phi(x_r^*)$. But, $\phi(x_r^*) = x_r^*$, as it is a fixed point (though unstable). Hence, $\phi(x_2) < x_r^*$. Now, since $\phi(x_2) < x_r^*$, under the next iteration, $\phi^2(x_2) > \phi(x_r^*)$. i.e., $\phi^2(x_2) > x_r^*$. Continuing like this, after each stage of iteration, the inequality gets reversed. Thus, the odd iterates $\phi(x_2), \phi^3(x_2), \phi^5(x_2), \ldots$ lie to the left of x_r^* and the even iterates $\phi^2(x_2), \phi^4(x_2), \phi^6(x_2), \ldots$ lie to the right of x_r^*.

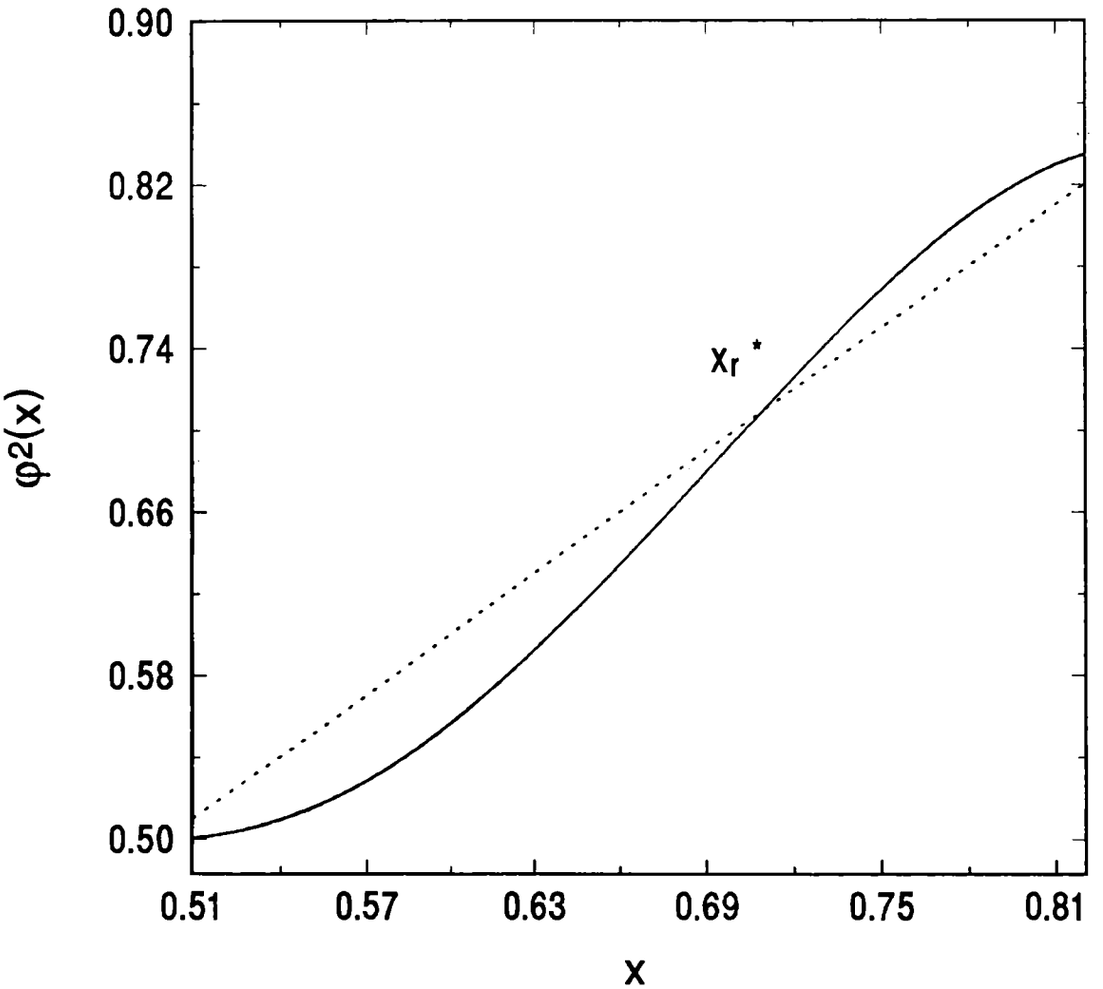

Fig 4.2 A plot of $\phi^2(x)$ vs x. The value of C is taken as 0.1 and that of $\mu \simeq \mu_r$.

Figure 4.3. Schematic representation of the

iterates for $\mu = \mu_r$

Case (a). $x_2 > x_r^*$

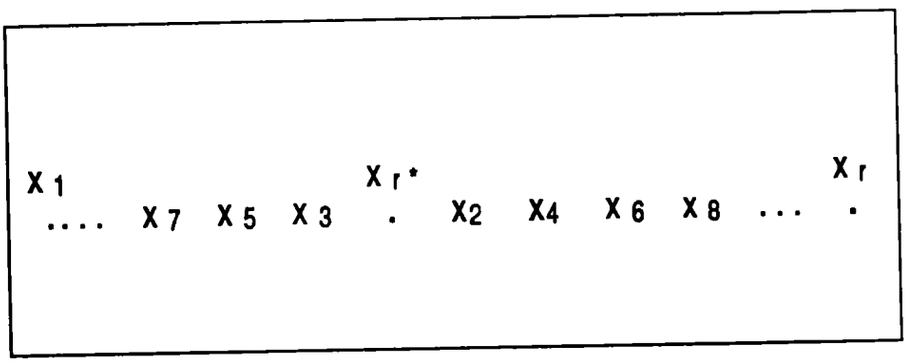

Case (b). $x_2 < x_r^*$

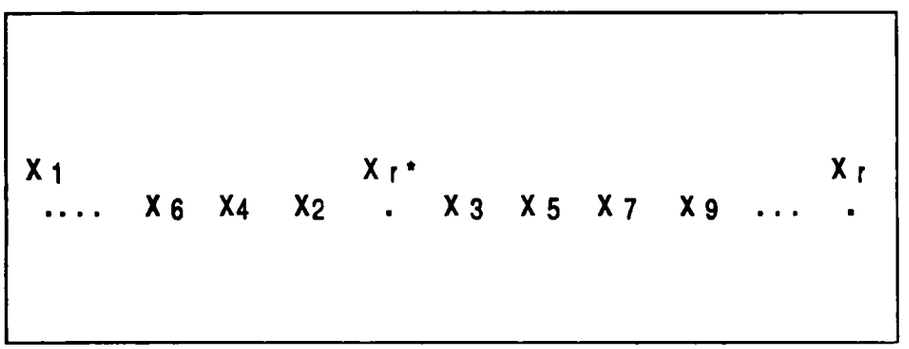

Fig 4.3 Schematic representation of the iterates of the discontinuous logistic map .

Since $\phi(x)$ is a decreasing function of x for any $x \in (1/2, 1)$, it is clear that $\phi^{\,2}(x)$ is an increasing function of x for all x for which $\phi(x)$ is greater than $1/2$. Thus $\phi^{\,2}(x)$ is an increasing function of x for all x in $(1/2, x_r)$. The behavior of $\phi^{\,2}(x)$ on either side of x_r^* is shown in figure 4.2. It is obvious that, $\phi^{\,2}(x) > x$ for $x > x_r^*$; $\phi^{\,2}(x) < x$ for $x < x_r^*$ and $\phi^{\,2}(x) = x$ for $x = x_r^*$. Thus since $x_2 > x_r^*$, we have $\phi^{\,2}(x_2) > x_2$). i.e.,$\phi^2(x_2) > x_2 > x_r^*$. Again, since $\phi^{\,2}(x_2) > x_r^*$, $\phi^{\,4}(x_2) > \phi^{\,2}(x_2)$. Similarly, $\phi^{\,6}(x_2) > \phi^{\,4}(x_2)$ and so on. Likewise, since $\phi(x_2) < x_r^*$, $\phi^{\,3}(x_2) < \phi(x_2); \phi^{\,5}(x_2) < \phi^{\,3}(x_2)$ and so on. A schematic representation of the iterates on either side of x_r^* is presented in figure 4.3. We thus, have an ordering for the iterates as,

$$x_r^* < x_2 < \phi^2(x_2) < \phi^4(x_2) < \phi^6(x_2) < \ldots \text{and}$$

$$x_r^* > \phi(x_2) > \phi^3(x_2) > \phi^5(x_2) > \phi^7(x_2) > \ldots$$

Thus it is clear that the even iterates of x_2 tend to x_r and the odd iterates of x_2 tend to $(1/2)_+$. Thus at some stage of iteration, $\phi^{2r}(x_2)$ becomes infinitesimally close to x_r. This iterate will be considered as x_r itself by the computer and the sequence of iterates will be repeated. The value of r depends on the precision used for the computation. Thus we have a cycle of periodicity $n = 2r + 2$.

Case 2. Second iterate of x_2 is less than the unstable fixed point x_r^*.

Based upon similar reasons as for case (1), we find that the successive iterates of x_r satisfy the inequalities:

$$x_r^* > x_2 > \phi^2(x_2) > \phi^4(x_2) > \phi^6(x_2) > \ldots \text{and}$$

$$x_r^* < \phi(x_2) < \phi^3(x_2) < \phi^5(x_2) < \phi^7(x_2) < \ldots$$

Thus the odd iterates of x_2 move towards x_r and even iterates approach $(1/2)_+$. Hence, after some stage of iteration, we have $\phi^{2r+1}(x_2)$ almost $= x_r$, leading to a periodicity $n = 2r + 3$.

The outward spiralling of the iterates to an n-periodic attractor at the parameter value $\mu = \mu_r$ is shown in figures 4.4 and 4.5 for two typical cases of $C = 0.1$ and $C = 0.2$ corresponding to even and odd periods respectively. It is to be emphasized that the true period at $\mu = \mu_r$ is infinity. But in numerical computations, a finite period is obtained; The period in this case is,in fact, equal to the number of iterations required by x_r to come back to a value 'almost' equal to itself; the degree of closeness being pre fixed by the precision of the computer. The map thus belongs to the class of maps with precision dependent periods [69]. If the map function were $\phi(x)$ throughout the interval (0,1), the role of C would be that of an additive constant applied to the logistic map [82] and the system would still have a stable 2-periodic behavior. The bifurcation of a 2-cycle to an n-cycle, in the case of the discontinuous logistic map, as the cycle elements touch the basin boundary is a discontinuous bifurcation. It is because of the discontinuity in the second iterate $T^2(x)$ near $x = 1/2$ and $x = x_r$. Note that $T^2(x) = \phi^2(x)$ for $x = (x_r - \epsilon)$ and $T^2(x) = f\{\phi(x)\}$, for $x = (x_r + \epsilon)$.

When μ is slightly greater than μ_r, the 'virtual' 2-cycle (x_1^*, x_2^*) falls outside the interval $[1/2, x_r]$. In this case, the successive iterates of any initial

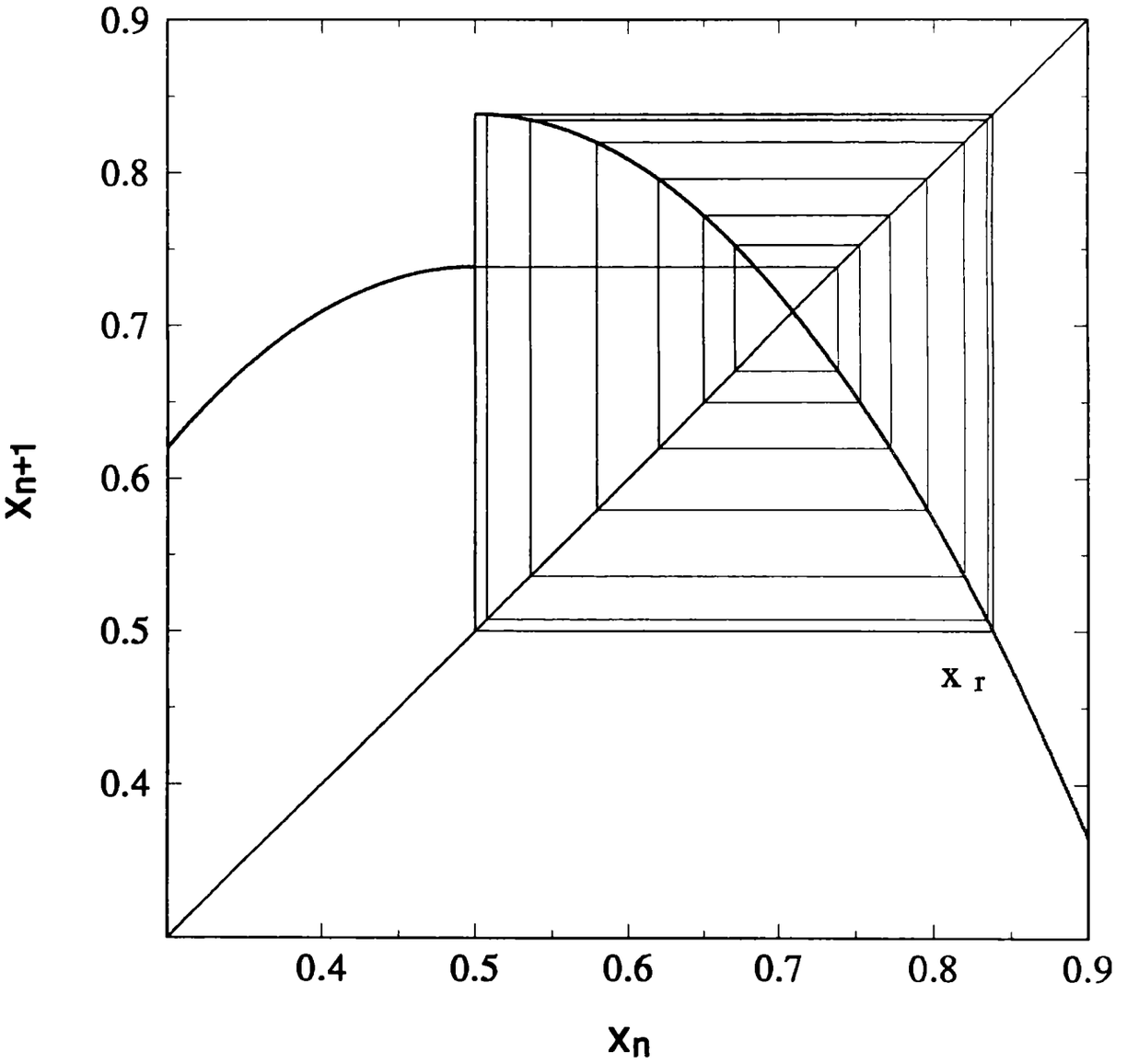

Fig 4.4 Graphical representation of the outward spiralling of the iterates to an attractor of large periodicity at the parameter value $\mu = \mu_r$, for $C = 0.1$.

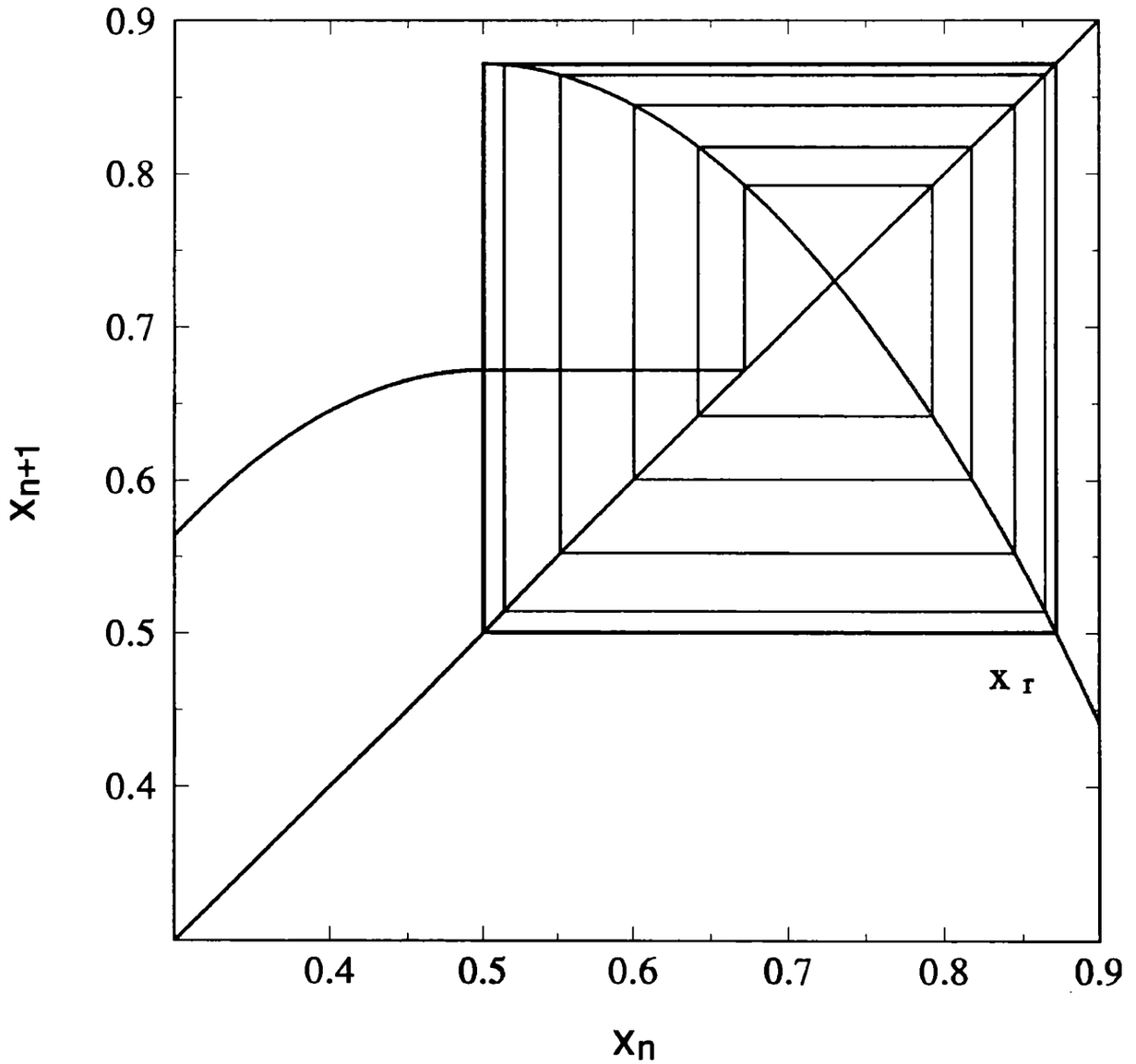

Fig 4.5 Graphical representation of the outward spiralling of the iterates to an attractor of large periodicity at the parameter value $\mu = \mu_r$, for $C = 0.2$

value $x_0 \in (1/2, x_r)$ form a sequence which shows a tendency to settle down at the 2-cycle. (Also, any initial value outside $(1/2, x_r)$ will come to this interval, after a few iterations, since the system has no other stable periodic solutions). In this process, an iterate slightly greater than x_r is obtained. This point is mapped by $\phi(x)$ into the domain of $f(x)$. The next iteration by the mapping $f(x)$ takes it to the interval $[1/2, x_r]$. This point, under repeated iterations by $\phi(x)$ comes outside this range and the whole process is continued again and again. The periodicity (n) will be even or odd depending on whether $x_2 = f\{\phi(x_r)\}$ is $> x_r^*$ or $< x_r^*$, where x_r^* is the fixed point (unstable) of $\phi(x)$. The behavior of the iterates of the map for values of μ immediately below and above μ_r can be understood from figures 4.6 and 4.7, in which the value of the iterates are plotted against the iteration number.

The mechanism of the bifurcation in which a 2-cycle directly gives birth to an n-cycle is quite different from the usual period doubling bifurcations and it is a characteristic feature of discontinuous maps. In the period doubling process, the slope (that determines the stability of the cycles) at the bifurcation point becomes equal to -1. But in the case of bifurcation of the 2-cycle to an n-cycle, the slope of $\phi^{\,2}(x) = 0$ at the bifurcation point. The elements of the n-cycle are $\{x_0 = x_r, x_1 = 1/2, x_2 = \mu_r, x_3, x_4, x_5, x_6, ...x_{n-1} = x_r\}$. These elements are equilibrium points of $T^n(x)$, for $\mu = \mu_r$. With increase of μ, the cycle elements move out until at some value of μ, the interval boundary x_r is reached after $(n-2)$ iterations. This should be so, since only alternate

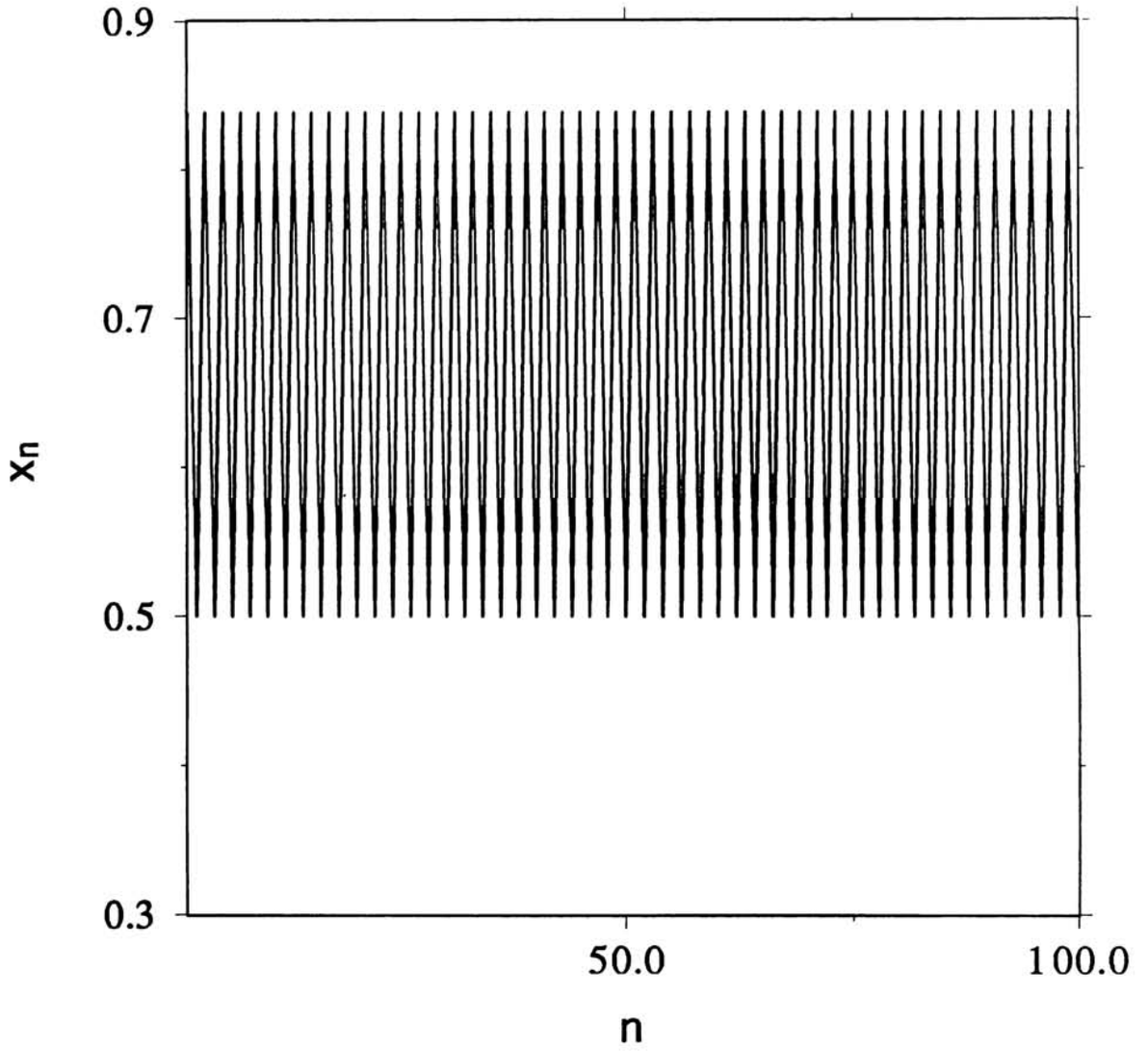

Fig 4.6 The time plot of the system in eqn 4.1 . The value of $C = 0.1$ and μ is slightly less than μ_r

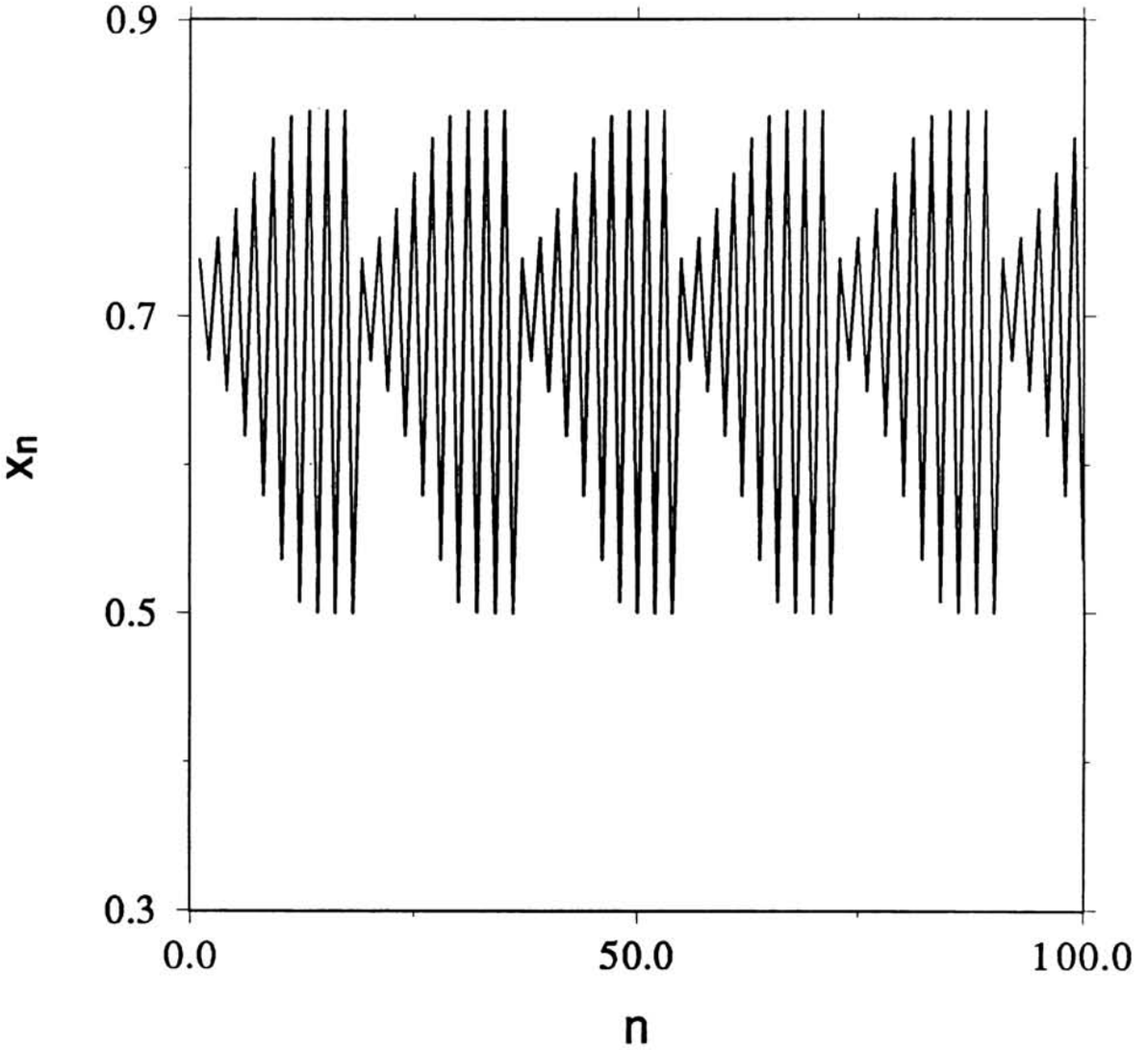

Fig 4.7 The time plot of the system in eqn 4.1 . The value of $C = 0.1$ and μ is slightly greater than μ_r.

iterates move towards x_r. The periodicity of the system is thus lowered by 2. Note that x_r also increases (very slowly) with μ and that one set of alternate iterates are repelled by the unstable fixed point x_r^* towards one side and the other set of alternate iterates to the other side. With further increase of μ, the outermost element (x_0) increases beyond the corresponding value of x_r and the cycle element nearest to x_r within $(1/2, x_r)$ moves towards x_r until at some stage, the basin boundary x_r is attained after $(n-4)$ iterations. Hence the period is again decreased by 2. Proceeding like this, we infer that as μ increases beyond μ_r, there exist different ranges of the parameter μ, for which cycles of periods decreasing by 2 exist. In a numerical computation, the periods decrease in an arithmetic progression. The common difference of the progression will be even numbers, since only alternate iterates move towards one boundary of $[1/2, x_r]$. The common difference also depends on the step size with which μ is increased as well as on the precision used for the computation. Again, the bifurcations within an inverse cascade occur whenever one of the cycle elements approaches the discontinuity of $T(x)$ at $x = 1/2$ and another element approaches x_r. [In this case, all the cycle elements approach the discontinuities of the n^{th} iterate of the map where n is the period of the cycle]. A given cycle of period n can exhibit the usual period-doubling bifurcation, if the slope of the n^{th} iterate becomes equal to -1 and the cycle loses stability before any of its elements gets a chance to collide with the discontinuity. The bifurcation process continues until the iterates become aperiodic at a parameter value (μ_∞) and the system enters the chaotic region.

A parameter space plot (C, μ) for the system is presented in figure 4.8. The fixed point x_r^* arising from the right part of the map exists only for points above the straight line, KLM, that represents $\mu + C = 1/2$. The straight line PQRS, given by the equation $\mu + C = 1$, determines the limiting values of the parameters upto which the iterates are confined in the unit interval. The straight line NLRN′ represents $\mu = 1/4$. The left part of the map function has only zero as the stable attractor for values of $\mu < 1/4$. i.e., for all parameter points inside the trapezium, ONRS. The line KQK′, represents $\mu = 1/2$. The fixed point of the logistic part (x_l^*) exists for the region of parameter space formed by the trapezium KQRN. The trapezium PKMS represents the region in which x_r^* exists. Thus the attractors x_l^* and x_r^* co-exist within the parallelogram KLRQ. Similarly, the attractor x_r^* and the zero fixed point co-exist for the parameter region represented by the parallelogram LMSR. The triangular region PKQ represents the set of (C, μ) points for which only x_r^* is present and the triangle KNL denotes the space in which the only attractor for the system is x_l^*. Within the parameter region bounded by the trapezium ONLM, the zero attractor alone is present. Obviously, for the co-existence of x_r^* and the zero attractor, the value of C should be $> 1/4$. The curves EFN′ and GQG′ represent μ_1 and μ_r respectively, as given by eqns.4.8 and 4.9. All the discontinuous cascades of bifurcations occur within the region PGQ. Note that both μ_1 and μ_r are decreasing functions of C. Hence, by taking negative values for C, one can have a 1-cycle behavior for the map for values of μ corresponding to the 2-cycle region of the logistic map.

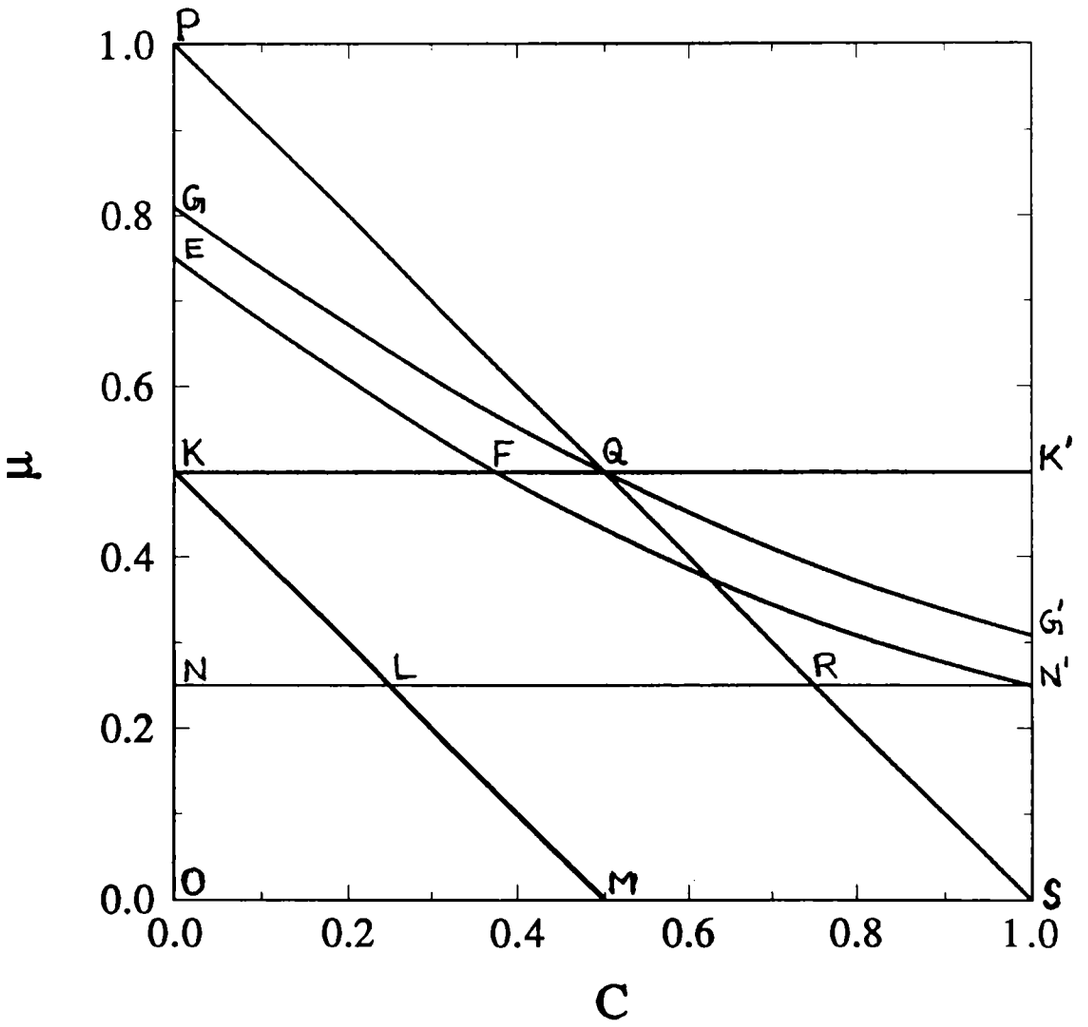

Fig 4.8 A parameter space plot (C, μ) for the discontinuous logistic map. The lines GQG′ and EFN′ represent μ_r and μ_1 respectively.

From the parameter space plot, one can select suitable (C, μ) points to have a desired dynamics for the system. It is possible to have a control over the dynamics of the system by proper choice of C for each μ, as in the case of the combination maps [80-82].

4.3 Numerical Results

The analytical studies presented above have been well substantiated by numerical computations. This section deals with the numerical investigations carried out to check the validity of the results obtained in the previous section. The discontinuity parameter C is kept at various fixed values. For each value of C, the bifurcation structure of the map is determined, by varying the parameter μ in small steps. A series of bifurcation diagrams are drawn, for different initial values (x_0). Figure 4.9 shows a bifurcation diagram for the system. It is obvious that the map has got multiple attractors. Initial value dependent behavior is seen in the bifurcation diagrams. In the case of $C = 0.2$, for example, we observe the following facts. For μ varying from 0 to 0.25, the only attracting fixed point is zero and all initial points $x_0 \in (0, 1)$ converge asymptotically to this attractor. When μ increases beyond 0.25, the system stabilizes to a non zero fixed point (x_l^*) which remains stable upto $\mu = 0.5$ and after that it vanishes. For values of $\mu > 0.3$, another fixed point (x_r^*) is observed. The two fixed points x_l^* and x_r^* co-exist for values of μ varying from 0.3 to 0.5. Initial values like 0.1,0.2,0.3, etc. converge to the fixed point x_l^*. But, seed values like 0.6 converge asymptotically to the other fixed point.

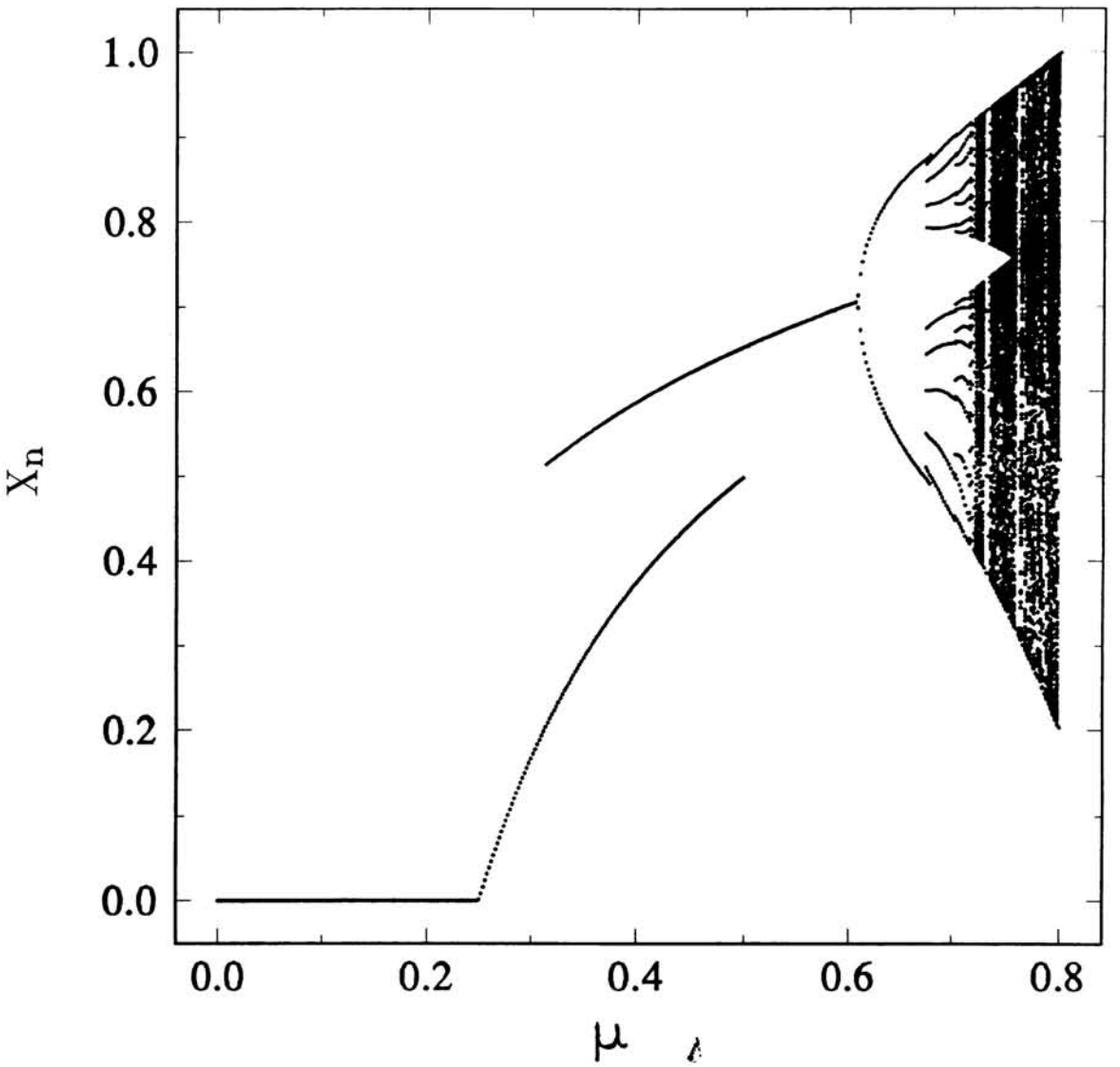

Fig 4.9 A Bifurcation diagram of the discontinuous logistic map for various initial points in (0,1). The value of $C = 0.1$ and μ is varied from 0 to 0.8. Note that the 2-cycle suddenly bifurcates to an n-cycle when $\mu = \mu_r$

The fixed point x_r^* undergoes the standard pitchfork bifurcation to a 2-cycle at a value $\mu = 0.608222$. The two cycle behavior continues upto the parameter value $\mu = 0.672055$. These values of μ_1 and μ_r are obtained accurately, by taking further and further blow ups of the bifurcation diagrams. When μ increases beyond 0.672055, a sudden bifurcation takes place and the iterates form a cycle of large periodicity. The period depends on the precision of the computer. The zero fixed point does not co-exist with x_l^* for values of $C < 0.25$. The parameter values μ_1 and μ_r obtained numerically and analytically for various values of C are presented in table 4.1. The close agreement between the numerical and analytical values give a strong support to the theory developed in the previous section. A check for any evidence of chaos was performed, based on the criterion of the positivity of the L.C.E (λ) given by [14]:

$$\lambda = \lim_{n\to\infty} \frac{1}{n} \sum_{t=0}^{n-1} \ln \mid \frac{dT(x)}{dx} \mid_{x=x_t} \tag{4.10}$$

Accordingly, the values of λ are computed for various values of μ in the neighborhood of μ_r. No trace of chaos is seen at these points; We have observed cycles of periodicities decreasing by 2 for μ values greater than μ_r. Two typical cases of $C = 0.1$ and $C = 0.2$ are analyzed in detail. Figs. 4.10 and 4.11 shows the bifurcation diagrams for these cases. In the case of $C = 0.1$, cycles of even periods $(14, 12, 10, 8, 6, \ldots)$ are observed when μ is increased beyond μ_r; For $C = 0.2$, we observe cycles of odd periods for values of μ greater than μ_r. The usual period-doubling process is also observed. For certain values of the parameters, different initial points converge to cycles of different periods.

Table 4.1

Parameter values for period doubling and period n-tupling of the discontinuous logistic map for different values of C.

Discontinuity parameter C	Control parameter (μ) for			
	period doubling (μ_1)		period n-tupling (μ_r)	
	Analytical	Numerical	Analytical	Numerical
0.05	0.71298053240	0.712945	0.77329280499	0.7732925
0.10	0.67696960071	0.676985	0.73851648071	0.7385165
0.15	0.64203854231	0.642015	0.70474050251	0.7047450
0.20	0.60825756950	0.608222	0.67201532545	0.6720155
0.25	0.57569390943	0.575664	0.64038820320	0.6403885
0.30	0.54440972087	0.544410	0.60990195136	0.6099020
0.35	0.51445989578	0.514447	0.58059371040	0.5805935
0.40	0.48588989435	0.485876	0.55249378106	0.5524935
0.45	0.45873378932	0.458677	0.52562460986	0.5256245
0.50	0.43301270189	0.432997	0.5	———

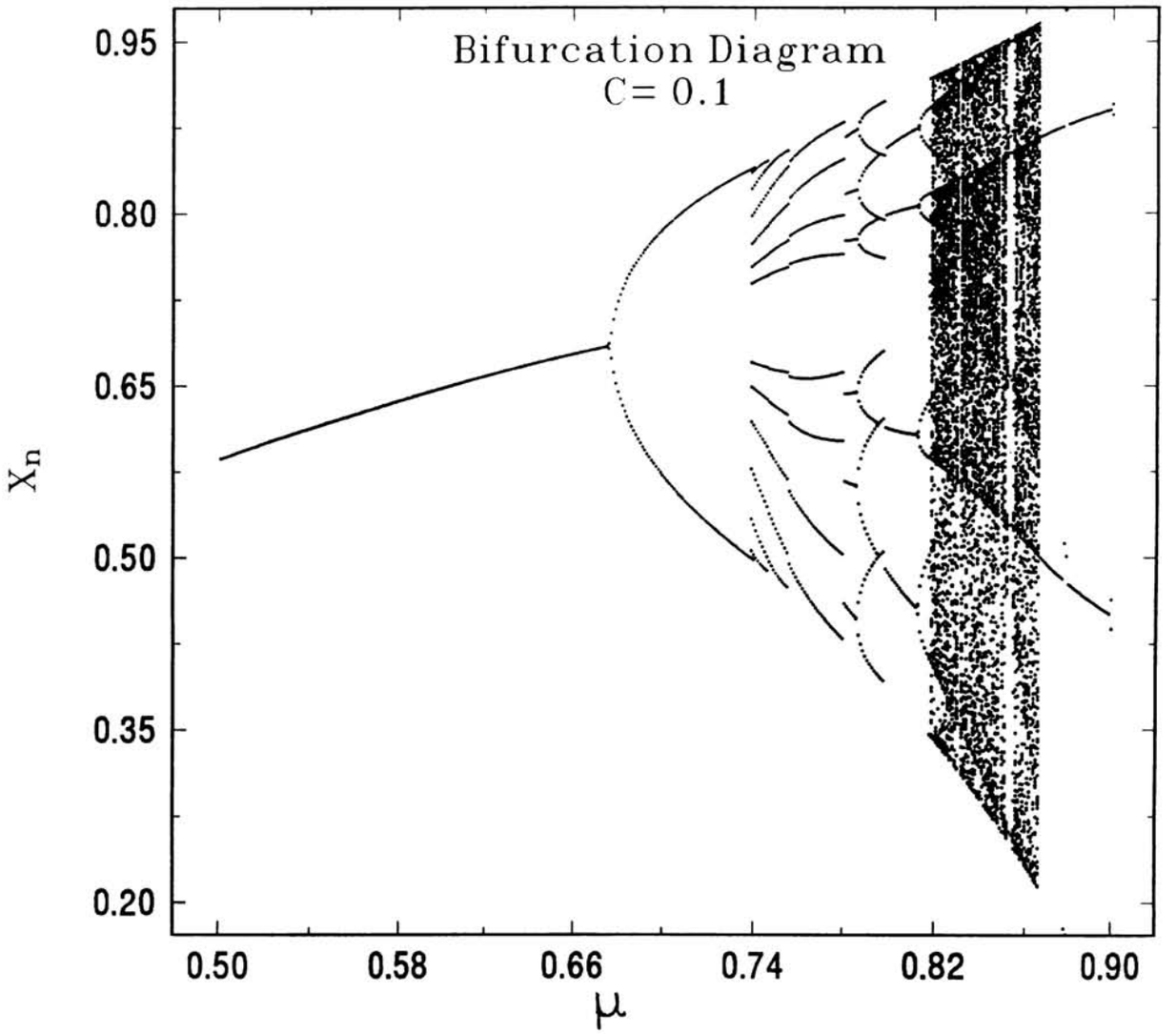

Fig 4.10 A bifurcation diagram of the discontinuous logistic map for $C = 0.1$

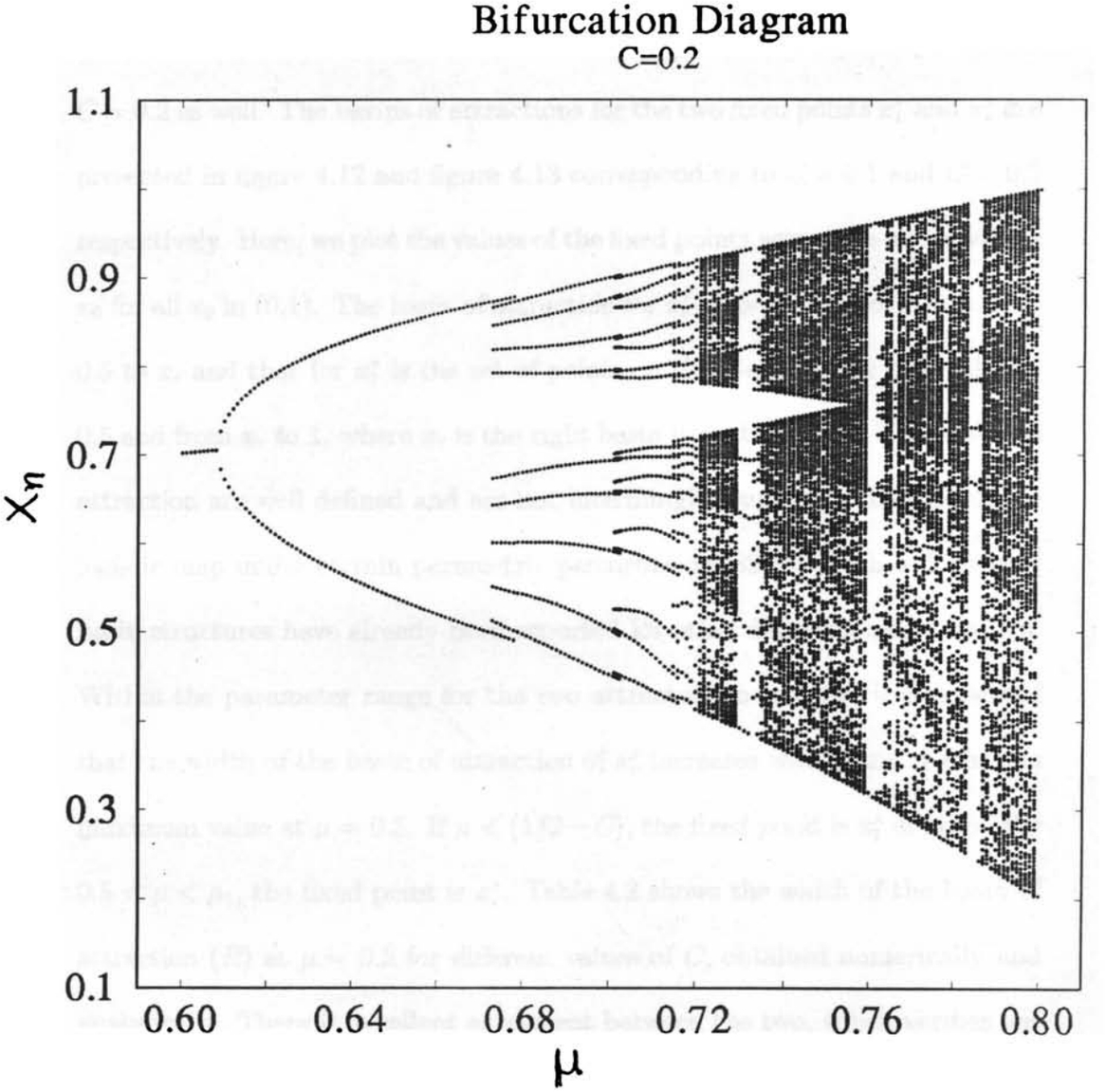

Fig 4.11 A bifurcation diagram of the discontinuous logistic map for $C = 0.2$

Keeping the value of $C = 0.1$ and μ at various fixed values in the interval $(1/2 - C)$, the asymptotic value of the iterate $\{x_n\}$ generated from a seed value x_0 is determined. This is repeated for various values of x_0. In this way, the basin of attraction is determined. This procedure is then repeated for $C = 0.2$ as well. The basins of attractions for the two fixed points x_l^* and x_r^* are presented in figure 4.12 and figure 4.13 corresponding to $C = 0.1$ and $C = 0.2$ respectively. Here, we plot the values of the fixed points versus the initial values x_0 for all x_0 in (0,1). The basin of attraction for x_r^* is the portion of x-axis from 0.5 to x_r and that for x_l^* is the set of points on the x-axis in the interval 0 to 0.5 and from x_r to 1, where x_r is the right basin boundary of x_r^*. The basins of attraction are well defined and are not intermingled, unlike in the case of the logistic map under certain parametric perturbations[83,84]. Such well defined basin structures have already been reported for other discontinuous maps[85]. Within the parameter range for the two attractors to co-exist, it is observed that the width of the basin of attraction of x_r^* increases with μ and reaches its maximum value at $\mu = 0.5$. If $\mu < (1/2 - C)$, the fixed point is x_l^* or zero. For $0.5 < \mu < \mu_1$, the fixed point is x_r^*. Table 4.2 shows the width of the basin of attraction (R) at $\mu = 0.5$ for different values of C, obtained numerically and analytically. There is excellent agreement between the two, which verifies our theoretical analysis.

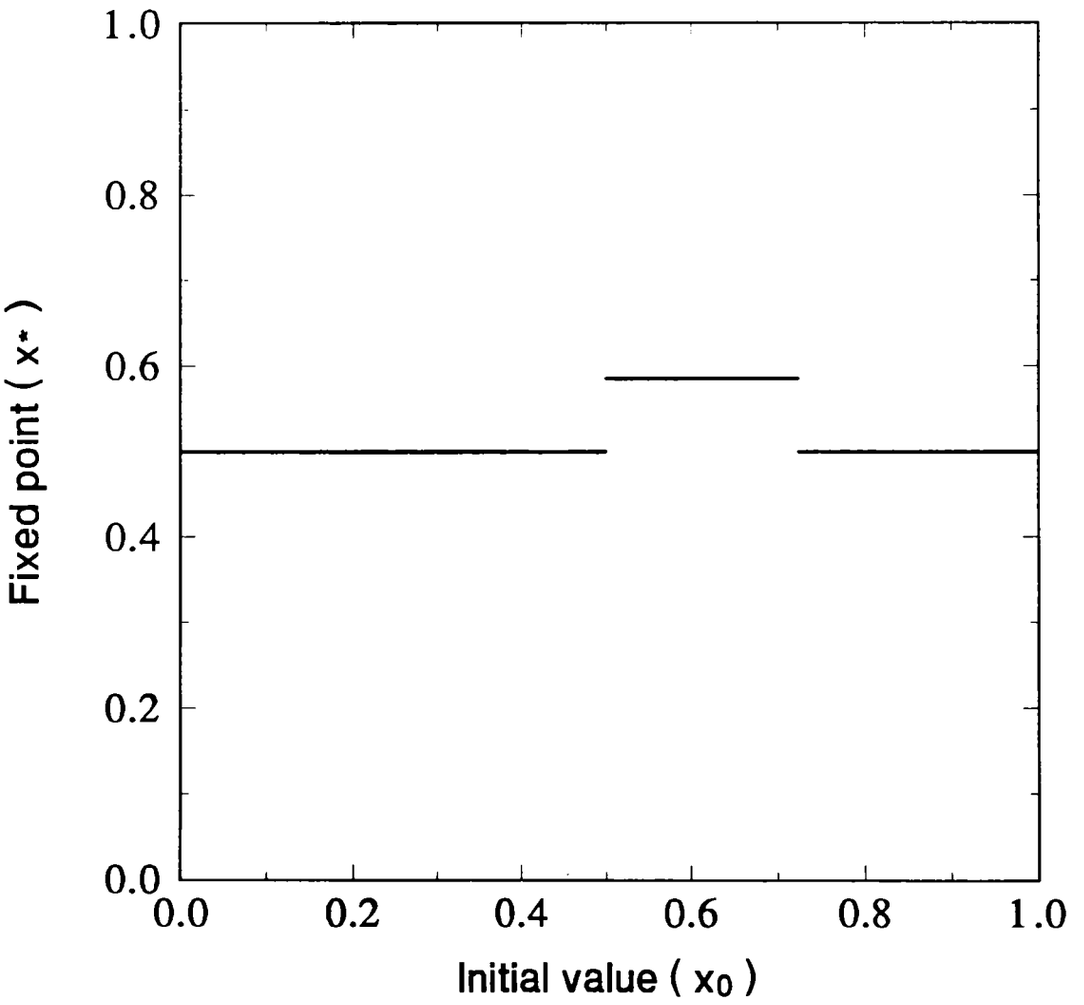

Fig 4.12 The basins of attraction of the discontinuous logistic map with $C = 0.1$. The asymptotic state is plotted against the seed values. The value of μ is taken as 0.5

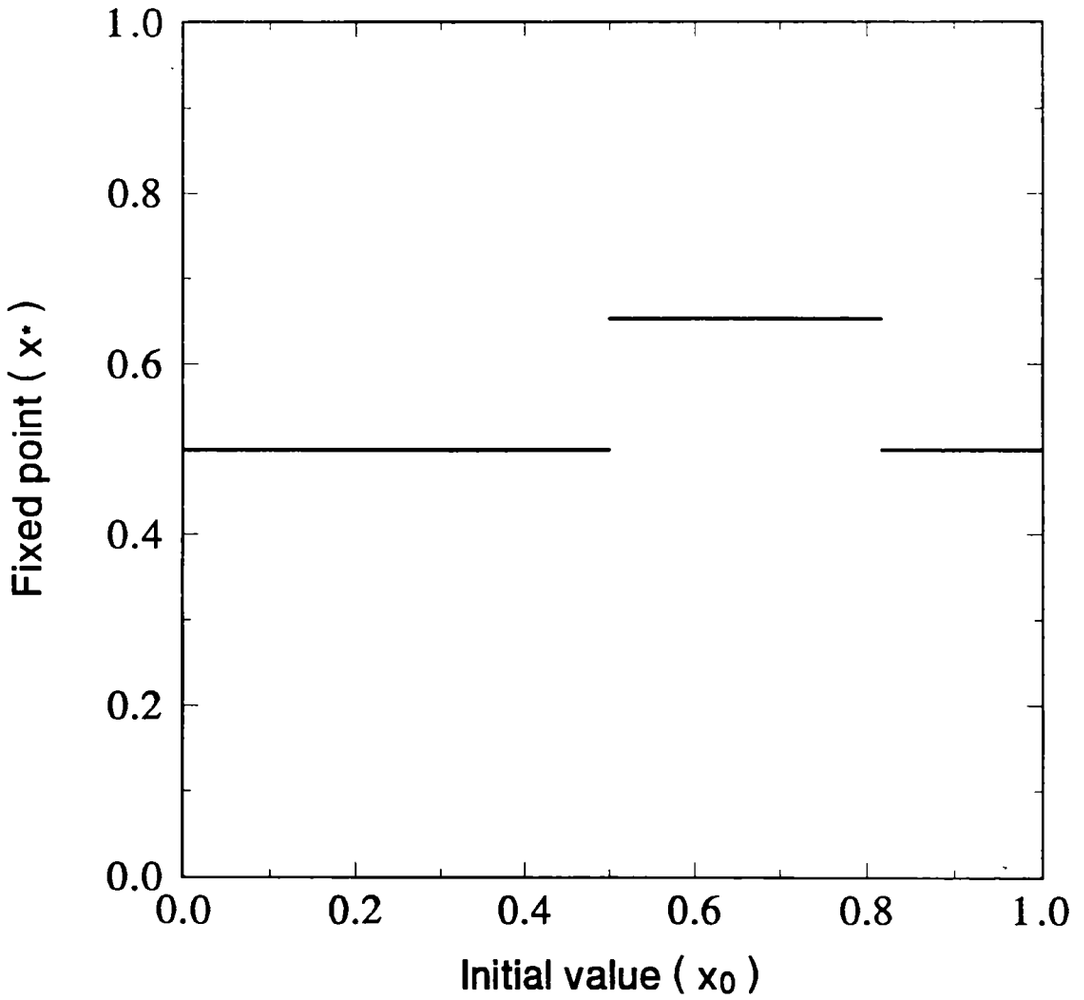

Fig 4.13 The basins of attraction of the discontinuous logistic map with $C = 0.2$. The asymptotic state is plotted against the seed values. The value of μ is taken as 0.5

Table 4.2

Width of the basin of attraction of the right fixed point for various values of C. The control parameter μ is kept at 0.5.

Discontinuity parameter (C)	Width of the basin of attraction of x_r^*	
	Analytical	Numerical
0.05	0.1581139	0.1581101
0.10	0.2236068	0.2236059
0.15	0.2738613	0.2738593
0.20	0.3162278	0.316227
0.25	0.3535534	0.3535532
0.30	0.3872984	0.3872979
0.35	0.4183300	0.4183283

4.4 Conclusion

The work presented above gives a theoretical understanding of the route to chaos in discontinuous systems. A detailed analysis of the dynamics of a discontinuous logistic map is carried out, both analytically and numerically, to understand the route it follows to chaos. We have shown analytically that the discontinuous logistic map has got multiple attractors with different basins of attraction. We also give expressions for the basin boundaries and a theory for the bifurcation phenomenon of the map is developed. In contrast to the standard pitchfork bifurcation in which the slope of a cycle becomes -1, the border collision bifurcation occurs whenever a cycle element touches the discontinuity of the map; For the map with a discontinuity at the extremum, the slope of the cycle becomes 0 at this point. Our results are verified by numerical investigations of the map. We have presented a parameter space plot for the map so that one can have a desired dynamics for the system, by suitable choice of the discontinuity parameter (C) for every value of the control parameter (μ). However, the present analysis deals only with the case of the discontinuity parameter applied to the right half of the interval of mapping. A detailed analysis for the n-furcations of various periodicities can be made and a more general theory for the map with discontinuities applied at different positions can be formulated on a similar footing.

5. SUMMARY

This chapter provides a summary of the work presented in the preceding chapters. The thesis focuses on the results obtained by our investigations on combination maps, scaling behaviour of he Lyapunov characteristic exponents of one dimensional maps and the nature of bifurcations in a discontinuous logistic map. Chapter 1 gives a general introduction to chaos in deterministic systems. Various qualitative and quantitative measures adopted to detect and characterize chaotic motion are briefly described. Some simple one dimensional maps exhibiting chaotic behavior are also discussed. This chapter gives a review of the major routes to chaos in dissipative systems, namely, Period-doubling, Intermittency and Crises. The dynamics of one dimensional iterative maps are discussed, taking the logistic map as a specific example. The Feigenbaum's universality theory for the period doubling route to chaos are described in some detail. The relevance of the scaling relations of the Lyapunov characteristic exponents in the context of control of chaos is explained. This is essential for understanding the contents of the subsequent chapters.

The dynamics of combination maps form the content of chapter 2. By a combination map, we mean a map obtained by combining two one dimensional maps. The constituent maps may or may not belong to the same universality class. The bifurcation scenario for both these types of combinations are analyzed. In the first case, the logistic map is combined with the

sinusoidal map, both belonging to the quadratic family. This combination map is a two parameter one dimensional map possessing an interesting property that it goes over from one humped to two humped state by continuously varying one of the parameters. Keeping the parameter (μ) of the logistic part at various fixed values, the bifurcation structure of the system is analyzed by varying the parameter (A) of the sine part. It is observed that the system retraces the entire period doubling route to chaos in the reverse order, as this parameter is increased. A parameter space plot for the system is also obtained. The bifurcation lines in the parameter space are parallel straight lines, indicating that the Feigenbaum's convergence rate (δ) computed in terms of A for fixed values of μ is the same as the value of δ calculated in terms of μ for any fixed value for A. It is possible to have any desired periodicity or chaos in the system, by proper choice of the parameters. Again, the parameter μ can be increased beyond $\mu = 4$ by taking suitable high values for A. Even though the periodic region of the system is exactly similar to the periodic regime of the logistic map, the chaotic regime is very much different in structure. For the logistic like family, the chaotic band undergoes an infinite sequence of band bifurcations in a mirror sequence of the cascade of bifurcations in the periodic region. But in the case of the combination map, these band bifurcations do not take place ad infinitum. What we observe is a series of band splittings and recombinations in the chaotic regime of the combination map. This incomplete nature of the cascade of band bifurcations results in a different scaling behaviour for the characteristic constants of the combination map. The studies

of this combination map for certain high values of μ like $\mu = 32, 36$ etc., have revealed some fascinating results. In this case, the combination map is always two humped in nature. The bifurcation structure for the two humped case is considerably different from that for the one humped state. With increase of the parameter A, the iterates switch over from one hump to the other. The system thus exhibits an inverse period doubling for some range of A and the a forward period doubling for the remaining range of A. The formation of a bubble structure is a distinct possibility for certain high values of μ. We then consider the case of a combination of two maps chosen from two different universality classes. For this, the Hemmer's map is combined with the logistic map. The bifurcation structure of the system is analyzed by varying the parameter a of the Hemmer's part, for various fixed values of the parameter μ of the logistic part. The presence of a cusp at the extremum point of this combination map produces severe differences to the bifurcation pattern. In this case, both the chaotic and the periodic region of the combination map are different from those of the constituent maps. It is observed that the system exhibits a transition from chaos to order and then from order to chaos. The transition from chaos to order occurs by inverse period doubling while the transition from order to chaos takes place by tangent bifurcations and intermittency. We have also obtained a parameter space representation for the system. The bifurcation lines in this case are smooth curves, in contrast to the parallel straight lines obtained for the first case.

The results of the numerical computations of the Lyapunov characteristic exponents of one dimensional maps are presented in chapter 3. The Lyapunov characteristic exponent (λ) serves as an order parameter in the transition from order to chaos. A scaling law for λ for maps undergoing the Feigenbaum scenario of pitchfork bifurcations have been theoretically worked out by Huberman and Rudnick. They have shown that the envelope of positive λ follows the relation, $\lambda \sim (a - a_\infty)^\nu$ where a_∞ is the value of the control parameter a at the period doubling accumulation point and $\nu = \frac{\ln 2}{\ln \delta}$, δ being the Feigenbaum constant. We have established numerically that this relation is valid not only for the quadratic maps, but also for all one dimensional one humped maps exhibiting the period doubling route to chaos. A necessary requirement for the validity of this law is that the chaotic bands should display an infinite cascade of band splittings. The Lyapunov exponents of combination maps follow a different scaling relation. The scaling index ν is found to be almost unity for the combination map formed by combining the logistic map with the sine map. The incomplete nature of the band bifurcations is the reason for the violation of the Huberman- Rudnick scaling law by the combination map.

An analytical explanation for the bifurcations of a discontinuous logistic map is given in the fourth chapter. Numerical results in support of theory are included. We have established that a discontinuous bifurcation takes place whenever the elements of an $n-$ cycle collides with the discontinuities of the

n^{th} iterate of the map. The periods of the cycles are shown to be precision dependent. Also the periods decrease in an arithmetic progression, as the control parameter is increased. The common difference of the progression will always be even numbers. A parameter space plot for the system is also obtained. The usual period doubling phenomenon is also possible, if the slope of the n^{th} iterate at its cycle elements becomes equal to -1, before any of the cycle elements gets a chance to collide with a discontinuity.

The work presented in this thesis opens up some possibilities for future research. A number of different combination maps can be formed and the dynamics of such systems can be analyzed by the techniques presented in this thesis. The idea of combination maps can be used advantageously for the control of chaos in discrete systems. The scaling relations of the Lyapunov characteristic exponents are very useful in developing suitable control algorithms. Extension to higher dimensional systems can also be tried out. The mechanism for bubble formation can be studied in detail by analyzing suitable combination maps. The phenomenon of border collision bifurcations for a number of discontinuous systems can be analyzed by the methods presented for the discontinuous logistic map. Similar studies can be carried out for continuous systems as well. Detailed investigations on one dimensional maps can provide valuable informations in understanding the onset of chaos in many practical systems. Developments in the field of chaotic dynamics can lead to a satisfactory explanation for the unsolved problem of turbulence.

References

[1]. H.G.Schuster, *Deterministic Chaos* (Physik Verlag, Weinhem, 1984).

[2]. P.A. Miloni, Ackerhalt *et al.*, *Chaos in Laser Matter Interactions* (World Scientific, Singapore).

[3]. Ray Brown and Leon O. Chua, *Int. J. Bifurcations and Chaos* **3(5)**, 1235 (1993)

[4]. Guckenheimer J., *Comm. Math. Phys.* **70**, 133 (1979)

[5]. Young, L.S., *IEEE Trans.* CAS- **30**, 599 (1983)

[6]. P. Fredrickson, J.L. Kaplan, E.D.Yorke and J.A. Yorke, *J. Differential equations*, **49** , 185 (1983)

[7]. Farmer J.D and Sidorowich J.J, *Phys. Rev. Lett.* **59** , 845 (1987)

[8] Thomas J. Taylor, *Nonlinearity* **6**, 369 (1993)

[9]. J.P Eckman and D. Ruelle, *Reviws of Modern physics* **57(3)**, 617 (1985)

[10]. R. M. May, *Nature* **261**, 459 (1976)

[11]. Hao Bai-lin, *Elementary symbolic Dynamics and Chaos in Dissipative Systems*, (World Scientific, Singapore)

[12]. E. Ott, *Rev. Mod. Phys.***53**, 655 (1981)

[13]. Devaney R. L., *An Introduction to Chaotic Dynamical systems*, (Addison-Wesley, 1984)

[14]. Collet, P and Eckman, J.P., " Iterated maps on the interval as dynamical systems" in *Progress in Physics*, (Birkhauser, Basel-Boston-Stuttgart, 1980)

[15]. M.J. Feigenbaum, *J. Stat. Phys.* **21**, 665 (1979)

[16]. Manneville, P. and Pomeau, Y., *Physica* **1 D**, 219 (1980)

[17]. Grebogi, C., Ott. E. and Yorke, J.A., *Physica* **7 D**, 181 (1983)

[18]. M. J. Feigenbaum, *Los Alamos reprint* (1980)

[19]. A. Libchaber, C. Lanouche and S. Faueve, *J. Phys. Lett.* **43**, L 211 (1982)

[20]. V. Franceschini and C. Tebaldi, *J. Phys.* **21**, 707 (1979)

[21]. D. Rand, S. Ostlund, J. Sethna and E. Siggia, *Physica* **6 D**, 303 (1984)

[22]. Bambi Hu and J. Rudnick, *Phys. Rev.* **A 34**, 2453 (1986)

[23]. P. Berge, M. Dubois, P. Manneville and Y. Pomeau, *J. Phys. Lett.* **41**, L 344 (1980)

[24]. M. Dubois, M. A. rubio, and P. Berge, *Phys. Rev. Lett.* **51**, 1446 (1983)

[25]. C. Jefferies and J. Perez, *Phys. Rev.* **A 26**, 2117 (1982)

[26]. W. J. Yeh and Y. H. Kao, *Appl. Phys. Lett.* **42**, 299 (1983)

[27]. Y. Pomeau, J. C. Roux, A. rossi, S. Bachelart and C. Vidal, *J. Phys. Lett.* **42**, L 271 (1981)

[28]. J. C. Roux, P. Kepper and H. L. Swinney, *Physica* **D 7**, 57 (1983)

[29]. E. Ott, C. Grebogi and J. A. Yorke, *Phys. Rev. Lett.* **64**, 1196 (1990)

[30]. S. Rajasekhar and M. Lakshmanan, *Int. J. Bifurcation and Chaos* (1992)

[31]. J. Singer, Y. Z. Wang and H. H. Bau, *Phys. Rev. Lett.* **66**, 1123 (1991)

[32]. L. Fronzoni, M. Giocondo and M. Pettini, *Phys. Rev.* **A 43**, 6483 (1991)

[33]. B. A. Hubermann and E. Lummer, *Proc. IEEE* **37**, 547 (1990)

[34]. S. Sinha, R. Ramaswamy and J. Subba Rao, *Physica* **D 43**, 118 (1990)

[35]. R. Lima and M. Pettini, *Phys. Rev.* **A 41**, 726 (1990)

[36]. Y. Braiman and I. Goldhirsch, *Phys. Rev. Lett.* **66**, 2545 (1991)

[37]. T. Kapitaniak, *Int. J. Bifurcation and Chaos* **1**, 357 (1991)

[38]. Q. Zhilin and G. Hu, *Phys. Lett.* **A 178**, 265 (1993)

[39]. B. A. Huberman and J. Rudnick, *Phys. Rev. Lett.* **45**, 154 (1980)

[40]. S. Parthasarathy and S. Sinha, *Phys. Rev.* **E 51**, 6239 (1995)

[41]. S. Sinha and S. Parthasarathy, *Proc. Natl. Acad. Sci., U S A* **93**, 1504 (1996)

[42]. Shay Gueron, *Phys. rev.* **E 57**, 3645 (1998)

[43]. Kloeden P.E and Mees A.I, *Bulletin of Mathematical Biology* **47(6)**, 637 (1985)

[44]. C. L. Pando L, R. Meucci, M. Ciofini and F. T. Arechi, *Chaos* **3(3)**, 279 (1993)

[45]. C. Leppers, J. Legrand, and P. Glorieux, *Phys. Rev* **A 43**, 2573 (1991)

[46]. J. M. T. Thompson and H. B. Steward, *Nonlinear Dynamics and Chaos* (Wiley, N. York, 1986)

[47]. E. Knobloch and N. O. Weiss, *Physica* **D 9**, 379 (1983)

[48]. G. Ambika and K. Babu Joseph,*Pramana- J. Phys.* **39**, 193 (1992)

[49]. J. Crutchfield, D. Farmer *et al., Phys. Lett.* **76 A**, 1 (1980)

[50]. S. C. Johnstone and R. C. Hilborne, *Phys. Rev.* **A 37**, 2680 (1988)

[51]. B. Shraiman, E. wayne and P. C. Martin, *Phys. Rev. Lett* **46**, 935 (1981)

[52]. J. C. Earnshaw and D. Haughey, *Am. J. Phys.* **61**, 5 (1993)

[53]. Mira. C., *Chaotic dynamics* (World Scientific, Singapore, 1987)

[54]. Laura Gardini, Ralph Abraham, Ronald. J. Record and D. Fournier Prunaret, *Int. J. Bifurcation and Chaos* **4(1)**, 145, (1994)

[55]. J. P. Crutchfield, J. D. Farmer and B. A. Huberman, *Phys. Rep.* **92**, 45 (1982)

[56]. B. Hu and I. I. Satija, *Phys. Lett* **A 98**, 143 (1983)

[57]. Jean Coste and Nelly Peyraud, *Physica* **5 D**, 415 (1982)

[58]. K. P. Harikrishnan and V. M. Nandakumaran, *Pramana- J. Phys.* **29**, 533 (1987)

[59]. K. P. Harikrishnan and V. M. Nandakumaran, *Phys. Lett.* **A 125**, 465 (1987)

[60]. K. P. Harikrishnan and V. M. Nandakumaran, *Phys. Lett.* **A 133**, 305 (1988)

[61]. K. P. Harikrishnan and V. M. Nandakumaran, *Phys. Lett.* **A 142**, 483 (1989)

[62]. Sangeeta Batra and V. S. Varma, *Pramana- J. Phys.* **37**, 83 (1991)

[63]. V. M. Nandakumaran, *Pramana- J. Phys.* **48**, 99 (1997)

[64]. Sanju and Varma V. S., *Phys. Rev* **E 48**, 1670 (1993)

[65]. De Sousa Vieira M. C., Lazo. E and Tsallis C., *Phys. Rev* **A 35**, 945 (1987)

[66]. De Sousa Vieira M. C., and Tsallis C., *Europhys. Lett.* **9(2)**, 119 (1989)

[67]. Chia T. T. and Tan B. L, *Phys. Rev* **A 45**, 8441 (1992)

[68]. Tan B. L and Chia T.T, *Phys. Rev* **E 47**, 3087 (1993)

[69]. Chia T. T. and Tan B. L, *Phys. Rev* **A 44**, 2231 (1991)

[70]. Nusse H. E, Ott E. and Yorke J. A, *Phys. Rev* **E 49**, 1073 (1994)

[71]. Nusse H. E and Yorke J. A, *Int. J. Bifurcation and Chaos* **5(1)**, 189 (1995)

[72]. Gutman M. and Gontar V., *Int. J. Bifurcation and Chaos* **5(1)**, 123 (1995)

[73]. Real Vallee and Claude Delisle, *Phys. Rev.* **A 31**, 2390 (1985)

[74]. Firdaus E. Udwadia and Ramesh S. Guttalu, *Phys. Rev.* **A 40**, 4032 (1989)

[75]. Wung-Hong Huang, *Phys. Lett.* **A 194**, 57 (1994)

[76]. Fournier-Prunaret, D., *Int. J. Bifurcation and Chaos* **1(4)**, 828 (1991)

[77]. Vignoles G. L., *Int. J. Bifurcation and Chaos* **3(5)**, 1177 (1993)

[78]. G. Conto Poulos, *Lett. Nuovo Cimento* **37**, 149 (1983)

[79]. Hnilo A. A., *Opt. Commun* **53**, 194 (1985)

[80]. P. R. Krishnan Nair, V. M. Nandakumaran and G. Ambika, in *Computational Aspects in Chaos and Nonlinear Dynamics* eds. G. Ambika and V. M. Nandakumaran (Wiley Eastern, N. Delhi), 144 (1994)

[81]. P. R. Krishnan Nair, V. M. Nandakumaran and G. Ambika, in *Pramana-J. Phys.* , **43**, 421 (1994)

[82]. Somadatta Sinha and Parichay K. Das, *Pramana-J. Phys.* **48**, 87 (1997)

[83]. Sarathchandran P. P., V. M. Nandakumaran and G. Ambika, *Pramana-J. Phys.* **47**, 339 (1996)

[84]. John C. Sommerer and Edward Ott, *Phys. Lett.* **A 214**, 243 (1996)

[85]. Lima A. S, Moreira I. C and Serra A. M, *Phys. Lett.* **A 190**, 403 (1994)